ISSN 1590-8844
Vol. 16 No 02
2015

International Journal of Mechanics and Control

Editor: Andrea Manuello Bertetto

Scopus Indexed Journal

Reference Journal of IFToMM Italy
International Federation for the Promotion of Mechanism and Machine Science

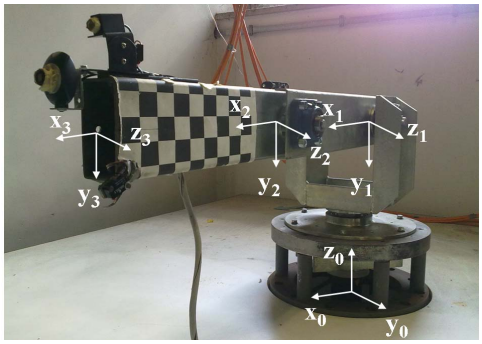

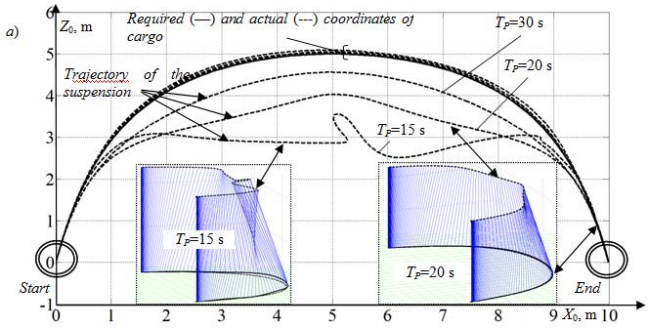

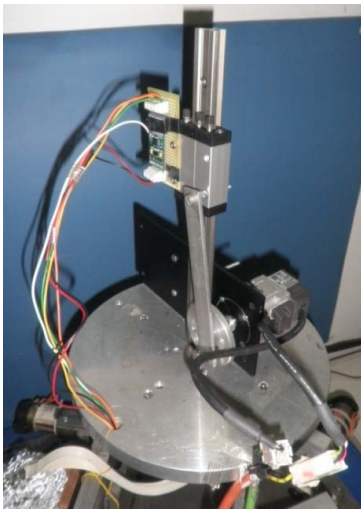

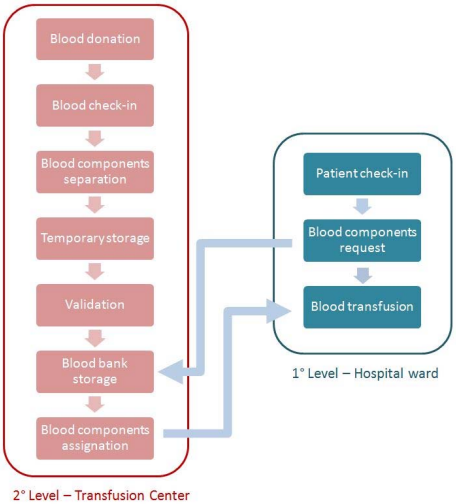

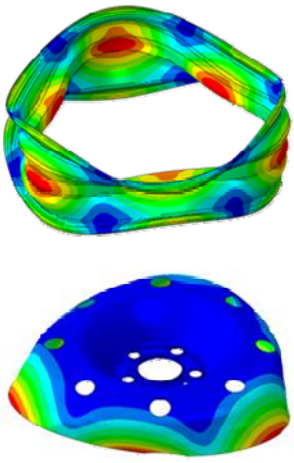

LIBRERIA EDITRICE UNIVERSITARIA
LEVROTTO & BELLA
TORINO

Official Torino Italy Court Registration
n.5390, 5th May 2000

Deposito presso il Tribunale di Torino
numero 5390 del 5 maggio 2000
Direttore responsabile:
Andrea Manuello Bertetto

International Journal of Mechanics and Control

The Journal is addressed to scientists and engineers who work in the fields of mechanics (mechanics, machines, systems, control, structures). It is edited in Turin (Northern Italy) by Levrotto&Bella Co., with an international board of editors. It will have not advertising.

Turin has a great and long tradition in mechanics and automation of mechanical systems. The journal would will to satisfy the needs of young research workers of having their work published on a qualified paper in a short time, and of the public need to read the results of researches as fast as possible.

Interested parties will be University Departments, Private or Public Research Centres, Innovative Industries.

Aims and scope

The *International Journal of Mechanics and Control* publishes as rapidly as possible manuscripts of high standards. It aims at providing a fast means of exchange of ideas among workers in Mechanics, at offering an effective method of bringing new results quickly to the public and at establishing an informal vehicle for the discussion of ideas that may still in the formative stages.

Language: English

International Journal of Mechanics and Control will publish both scientific and applied contributions. The scope of the journal includes theoretical and computational methods, their applications and experimental procedures used to validate the theoretical foundations. The research reported in the journal will address the issues of new formulations, solution, algorithms, computational efficiency, analytical and computational kinematics synthesis, system dynamics, structures, flexibility effects, control, optimisation, real-time simulation, reliability and durability. Fields such as vehicle dynamics, aerospace technology, robotics and mechatronics, machine dynamics, crashworthiness, biomechanics, computer graphics, or system identification are also covered by the journal.

Please address contributions to

Prof. Guido Belforte
Prof. Andrea Manuello Bertetto
PhD Eng. Elvio Bonisoli

Dept. of Mechanics
Technical University - Politecnico di Torino
C.so Duca degli Abruzzi, 24.
10129 - Torino - Italy - E.C.

www.jomac.it
e_mail: jomac@polito.it

Subscription information

Subscription order must be sent to
the publisher:

Libreria Editrice Universitaria
Levrotto&Bella
C.so Luigi Einaudi 57/c – 10129 Torino – Italy

www.levrotto-bella.net
e_mail: info@levrotto-bella.net
ph.: +39 011 4275423
mob.: +39 328 5369063
fax: +39 011 4275425

ISSN 1590-8844
International Journal of Mechanics and Control, Vol. 16, No. 02, 2015

IMPACT SIGMOIDAL CARGO MOVEMENT PATHS ON THE EFFICIENCY OF BRIDGE CRANES

Mikhail S. Korytov Vitaly S. Shcherbakov Elena O. Volf

Siberian State Automobile and Highway Academy (SibADI)

ABSTRACT

The article dwells upon the results of study influence of movements time at traversing single obstacle arcwise with suppression of load's oscillation on the indices of assessing working process of a bridge crane. Simulation of movements was implemented using an imitating model with proportional-integral-differential control. The required trajectories of load transfer were set using sigmoid functions.

Keywords: bridge crane, PID regulator, sigmoidal

1 INTRODUCTION

The characteristic problems for the bridge crane (BC) with flexible suspension are uncontrolled load oscillations at movement, which significantly reduce the accuracy and performance of implementing works. Optimization of the trajectory of transferring point of load suspension located on the baggage cart (trolley) BC, i.e. optimization of the process controlling the bridge and cart's drive mechanisms is one of the perspective ways to solve this problem [1, 2]. There was proposed to use proportional-integral-differential (PID) control independently by two controlled coordinates of the bridge and baggage cart [3].

2 PROBLEM SOLUTION

According to the proposed functional diagram (Fig. 1), with using packet burst SimMechanics Second Generation of the system MATLAB, Simulink model of the BC mechanical system with PID-control was developed. Simulink-model allows us to study the bridge crane's operating modes on the engineering stage [4, 5, 6, 7, 8].

The conducted studies have shown that using sigmoid functions for setting required time dependencies of the horizontal coordinates of a cargo at traversing (load bypass) single obstacle, can significantly reduce, and in some cases even eliminate high-frequency oscillations of coordinates of load and suspension.

Contact author: Vitaly S. Shcherbakov**,** Mikhail S. Korytov

644080, Omsk, prospect Mira 5, Russian Federation
E-mail: kms142@mail.ru

In addition, there are removed the oscillations of velocities and accelerations of the suspension point in comparison with other methods of setting required trajectory of load movement (for example, using trigonometric sinusoidal time or coordinate functions or using consistent integration of graded jerk's functions). Also, there is a reduction of the absolute values of acceleration of the suspension point, they become comparable (i.e. values of the same order) with accelerations of load at the required ideal sigmoidal trajectory.

A series of computational experiments on a simulation model was conducted for study BC dynamic system's performance with PID regulators. As an example, which has wide practical application, there was modeled load bypass of a single obstacle of a "wall" type on a levelled trajectory assigned by horizontal coordinates X_0, Z_0 space in a fixed Cartesian system $O_0X_0Y_0Z_0$ by sigmoid (logistic) time functions of the form [9]

$$X_{TP}(t,a,c) = l_x / \left(1 + e^{-a\cdot(t-c)}\right); \quad (1)$$

$$Z_{TR}(t,a_1,c_1,a_2,c_2) = \left(s_x \cdot k_{sx}\right) / \left(\left(1 + e^{-a_1\cdot(t-c_1)}\right)\cdot\left(1 + e^{-a_2\cdot(t-c_2)}\right)\right), \quad (2)$$

where t - time; X_{TR}, Z_{TR} - the required coordinates of cargo in the horizontal plane at time moment t; a, c, a_1, c_1, a_2, c_2 - parameters of sigmoidal functions; l_x - the length of the displacement along the axis X_0 between starting and ending points of the required load trajectory (this points have zero coordinate Z = 0); s_x - value of maximum arc's displacement of the required trajectory of load along the axis Z_0 (laterally to avoid obstacles); k_{sx} - the correction coefficient of maximum value of the lateral displacement

$$k_{sx} = \left(1 + e^{-a_1 \cdot (c - c_1)}\right) \cdot \left(1 + e^{-a_2 \cdot (c - c_2)}\right). \quad (3)$$

Function (2) is the product of two sigmoid functions of the type (1) - increasing and decreasing with different time of inflection's points. The parameters c, c_1, c_2 set the time of inflection's points of sigmoid functions, and parameters a, a_1, a_2 - the rate of change (the rate of growth or decline is determined by the sign) of functions.

During a series of considered experiments, there was varied the conditional time of moving suspension point of the load T_P , which, according to the results of the research, is entered in the limits T_P = 1,33333 T_{GR}, where T_{GR} - conditional time of the load's movement.

By-turn, at using threshold value of the sigmoid function P = 0,999, at achievement of which a given load's movement was considered complete, the parameters of the sigmoid function (1) were determined by:

$$a = \ln(1/P - 1)/(-T_{GR}/2);\ c = 2 \cdot T_{GR}/2\,, \quad (4)$$

where $T_{GR} = 0{,}75 \cdot T_P$.

Parameters sigmoid function (2) were determined by:

$$a_1 = a;\ a_2 = -a;\ c_1 = c - k_{ud} \cdot T_{GR};\ c_2 = c + k_{ud} \cdot T_{GR}, \quad (5)$$

where k_{ud} = 0,15 - accepted coefficient of relative distance from each other of two multiplied (2) simple sigmoid functions.

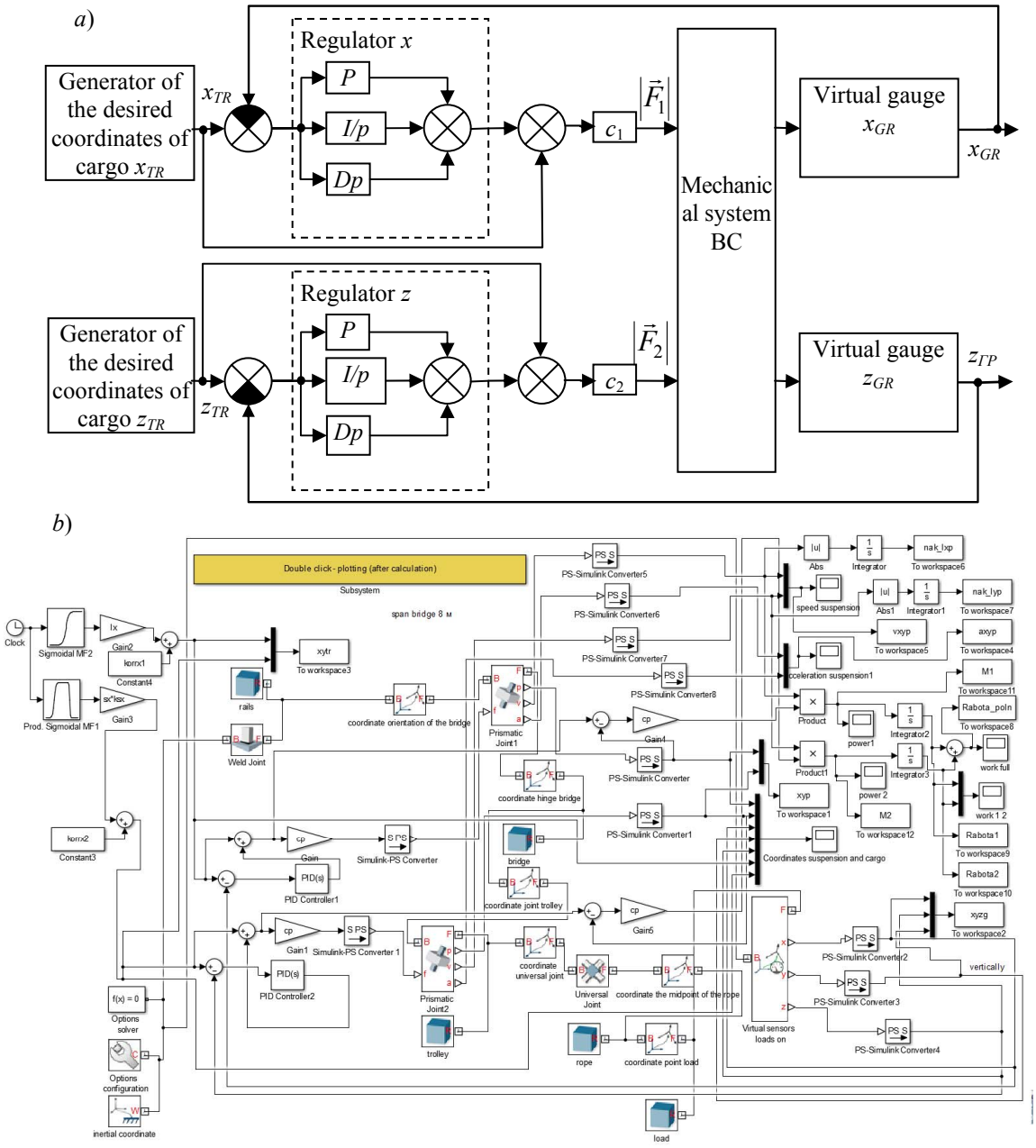

Figure 1 Functional diagram of connections for building model of mechanical subsystems of the bridge crane with PID-controller (a) and its corresponding model in the notations SimMechanics Second Generation and Simulink (b).

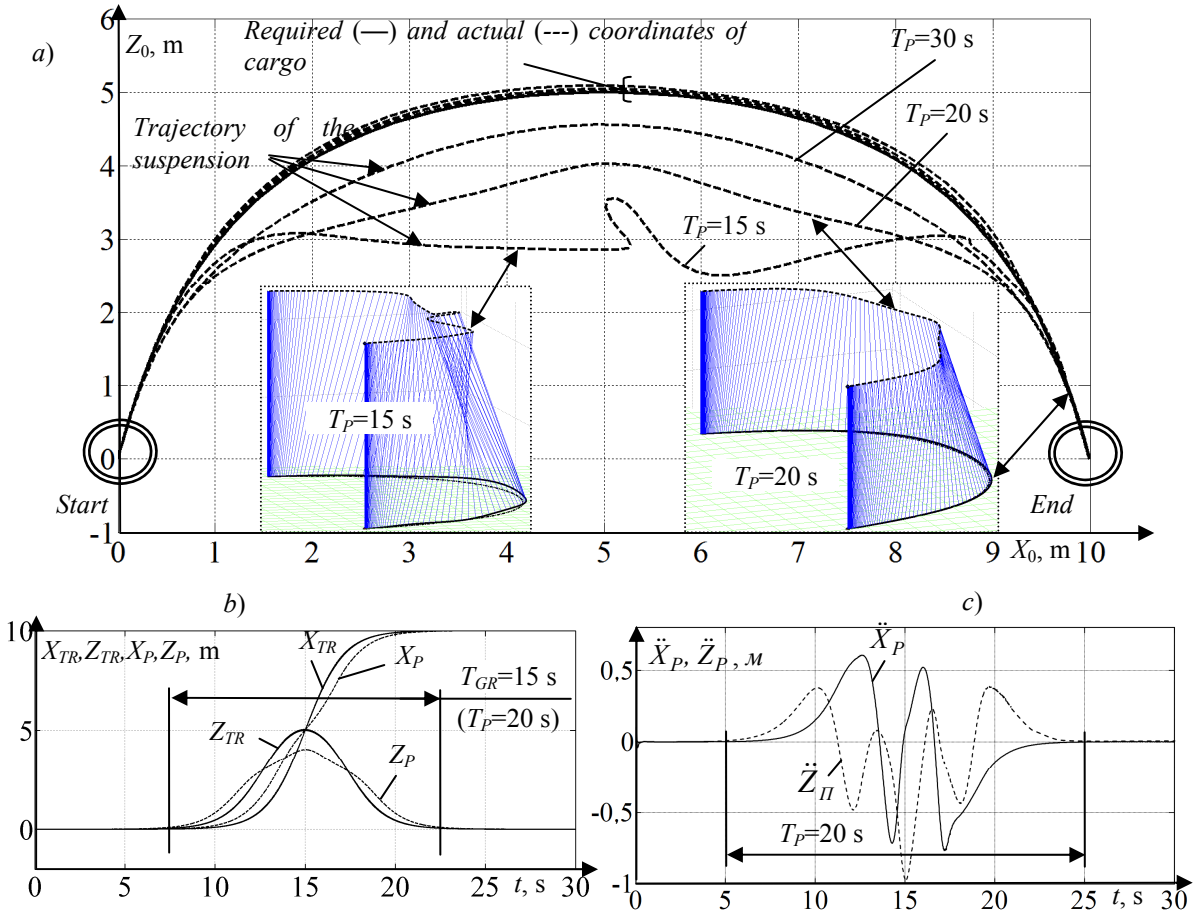

Figure 2 Diagrams of Cartesian coordinates of the load center's point and the suspension point (a, b) and acceleration of the suspension point (c) at realization of traversing single obstacle with the use of PID-control (example).

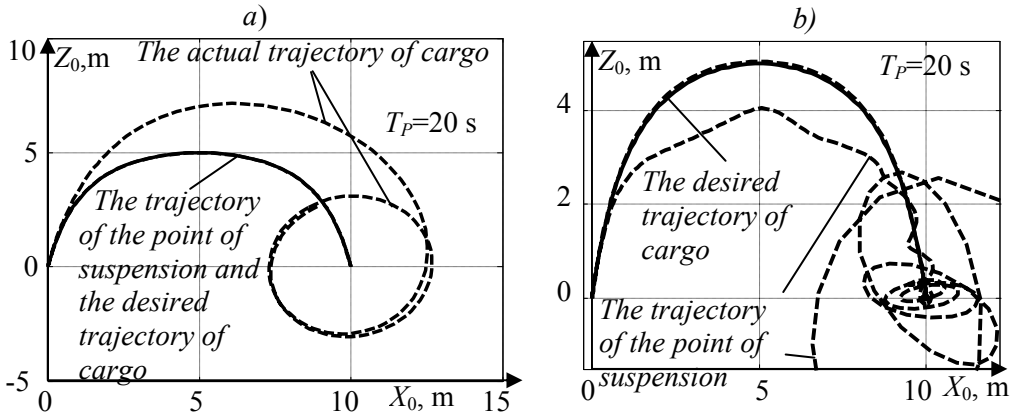

Figure 3 The examples of diagrams of Cartesian coordinates of the load's center point and the suspension point in the absence of correction of load's deviations (a) and proportional control (b).

Coordinate and time dependences of the synthesized, with the use of PID-regulators, coordinates of the load suspension's point (baggage cart) X_P, Z_P required X_{TR}, Z_{TR}, and actual X_{GR}, Z_{GR} coordinates of the load, and the time dependence of the acceleration of the suspension point are shown in the Fig. 2, as an example, for the conventional time for movement of cargo suspension point T_P = 15, 20 and 30 s.

The proportional, integral and differential coefficients of PID-regulators of controlling drives of the cart and bridge's movement in this task were possessed the values: P = 20; I = 5; D = 5.

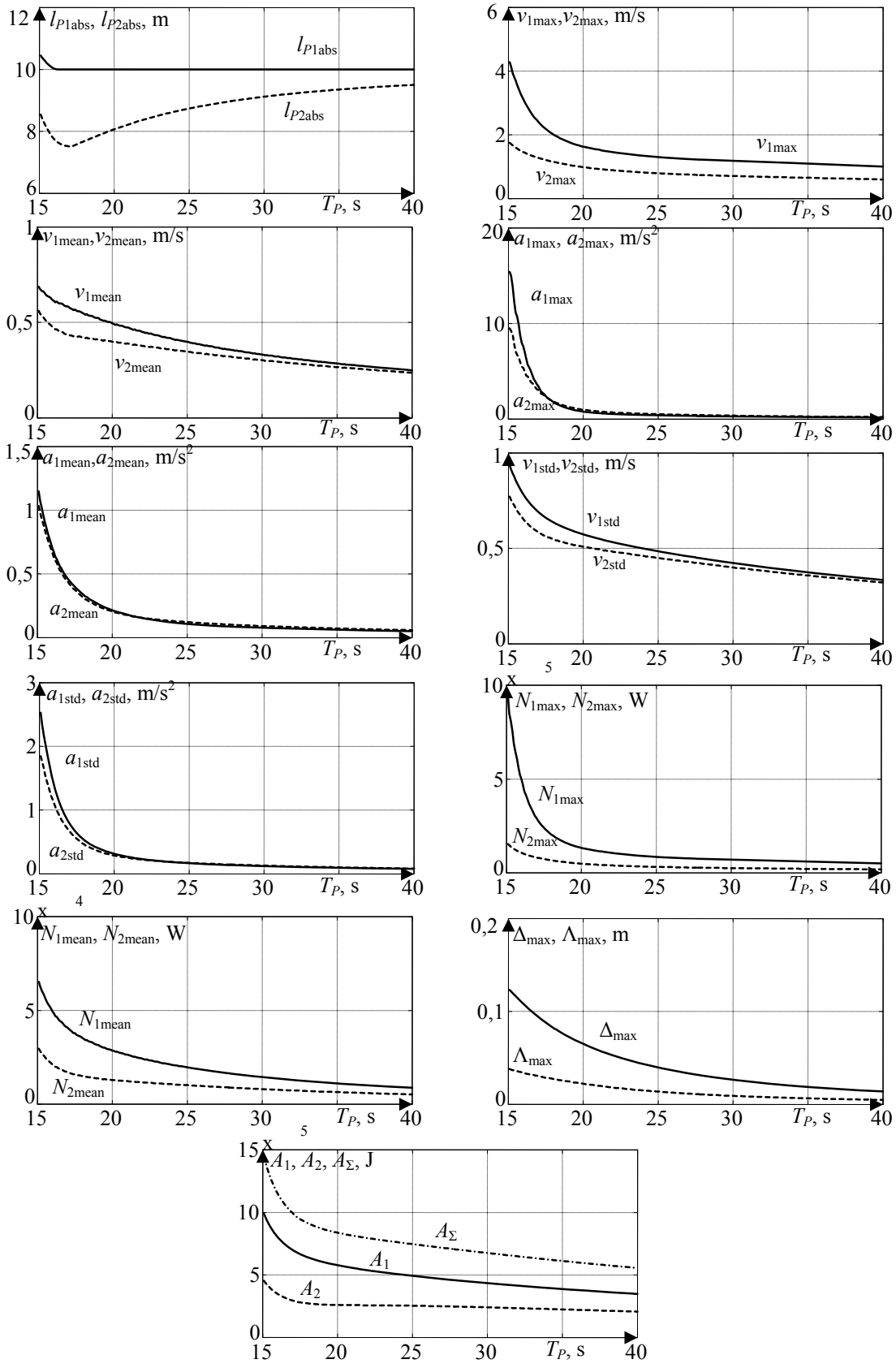

Figure 4 Performance of evaluation of the operation overhead crane depending on the travel time suspension point of cargo TA (example).

On the Fig. 3 for the illustration of the working efficiency and effectiveness of using the PID-regulators of controlling drives of the bridge and BC cart's movement, there are presented diagrams of Cartesian coordinates of the load's center and the point of suspension for a specified trajectory of the load movement, that shown in Fig. 2 with T_P = 20, with the values of the regulators' coefficients P = 0; I = 0; D = 0 (Fig. 3, and corresponds to the absence of correcting load deviations, i.e. drives move the point of suspension along the required trajectory of load movement) and P = 20; I = 0; D = 0 (Fig. 3*b*, proportional regulation). In the absence of corrective influences, the load, after a soft stop of the suspension point, begins to oscillate around the end point of equilibrium. At proportional regulation the specified trajectory of the load's movement is realized sufficiently precisely, but at approaching the end point the process becomes unstable and the suspension's point begins to oscillate with increasing amplitude around the end point of equilibrium.

The other parameters of the working process have the following values: the load cable length 12 m; the magnitude of the required movement of the load along the axis O_0X_0 - 10 m; the magnitude of lateral displacement for obstacles' bypass along the axis O_0Y_0 - 5 m; the mass of the bridge - 3500 kg; the mass of the baggage cart - 1250 kg; load weight - 100 kg; the presented coefficients of decrement by the angular coordinates of deviations of the load cable from the vertical in two mutually perpendicular planes - 100 N·m·s/rad.

The total time of the suspension's movement was varied from 15 to 40 s with interval of 0,1 s.

The working process of the bridge crane can be assessed by various parameters. On the Fig. 4, as an example, there are presented some of them, obtained during the described series of computational experiments: the absolute movements of the bridge and baggage cart correspondingly (at the realization of the specified trajectory) l_{P1abs}, l_{P2abs}, m; the maximum velocities of the bridge and baggage cart's movements v_{1max}, v_{2max}, m/s; the average velocities of the bridge and baggage cart's movements v_{1mean}, v_{2mean}, m/s; the maximum accelerations of the bridge and baggage cart's movements a_{1max}, a_{2max}, m/s^2; the average accelerations of the bridge and baggage cart's movements a_{1mean}, a_{2mean}, m/s^2; the standard deviations of the speeds of the bridge and baggage cart's movements v_{1std}, v_{2std}, m/s; the standard deviations of the accelerations of the bridge and baggage cart's movements a_{1std}, a_{2std}, m/s^2; the maximum instantaneous values of powers, spent by the bridge and baggage cart's drives N_{1max}, N_{2max}, W; the average values of powers, spent by the bridge and baggage cart's drives N_{1mean}, N_{2mean}, W; the maximum absolute error of the trajectory's realization Δ_{max}; the average absolute error of realization of the trajectory Λ_{max}, m; the work, implemented by the drive of the bridge A_1, J; the work, implemented by the drive of the baggage cart A_2, J; the total work of the drives A_Σ, J.

The virtual measuring sensors, embedded in blocks of mechanical joints SimMechanics Second Generation, measuring movements and velocities by the degrees of joints' freedom were used during the working process for measuring and calculating the values of the above parameters.

The developed model allows solving the problems of the BC dynamics, analysis and synthesis of structural and technological parameters of the BC and their control systems. There is possible the study of large movements of the links. The results of the conducted studies lead to a conclusion that realization of the leveled trajectory of the movement of a certain type's load without high-frequency oscillations (rocking) of both the load and the suspension's point is possible at relatively low values of accelerations, developed by the suspension's point.

3 CONCLUSION

Analysis of the obtained dependences allows us to conclude that increasing the specified time of movement for the same test trajectory enables to reduce the requirements to the bridge and baggage cart's drives in terms of maximum and average values of velocities, accelerations, powers, works fulfilled by the drives, during simultaneous increasing the accuracy of load's movements.

Thus, the requirement to increase of the BC's operating efficiency (decreasing movements' time) is associated with the need of applying more powerful and fast-acting drives, increasing energy consumption and decreasing movements' accuracy.

The receiving of the mentioned dependences for an arbitrary specified trajectory creates the possibility to optimize the BC's working process by the criteria of accuracy, efficiency and energy consumption, including multi-criterion optimization taking into account various limitations.

REFERENCES

[1] Blackburn D., Singhose W., Kitchen J., Patrangenaru V., Lawrence J., Command Shaping for Nonlinear Crane Dynamics, *Journal of Vibration and Control*, No. 16. 2010, pp. 477-501.

[2] Tolochko O.I., Bazhutin D.V., Comparative analysis of methods of damping oscillations of cargo suspended to the mechanism of translational motion of overhead crane, *Electrical machinery and electrical equipment*, No. 75, 2010, pp. 22-28.

[3] Denisenko V.V., Varieties of PID-regulators, *Automation in the industry*. No.6, 2007, pp. 45-50.

[4] Korytov M.S., Glushets V.A., Zyryanova S.A., Simulation of workers' movements of mobile crane using SimMechanics and Virtual Reality Toolbox, *Exponenta Pro. Math applications*, No. 3-4, 2004, pp. 94-102.

[5] Korytov M.S., Zyryanova S.A., Simulation of the mobile crane dynamic system with aid of blocks of package «SIMMECHANICS» system MATLAB, *Omsk Scientific Gazette*, No. 4, 2004, pp. 88-90.

[6] Shcherbakov V.S., Korytov M.S., Kotkin S.V., Automation *System simulation of jib cargo cranes: monograph*, SibADI, Omsk, 2012.

[7] Shcherbakov V.S., Korytov M.S., Volf E.O., A method for improving the accuracy of the trajectory of moving an object of crane by compensating its unmanaged spatial oscillations, *Mechanization construction*, No. 2, 2014, pp. 21-25.

[8] Shcherbakov V., Korytov M., Sukharev R., Volf E., Mathematical modeling of process moving cargo by overhead crane, *Applied Mechanics and Materials*, Vols. 701-702, 2015, pp. 715-720.

[9] Mitchell, Tom M, *Machine Learning*, WCB/McGraw-Hill, 1997, 414 p.

ISSN 1590-8844
International Journal of Mechanics and Control, Vol. 16, No. 02, 2015

A CONTACTLESS ROBOT KINEMATIC CALIBRATION METHOD BY DIGITAL PHOTOGRAMMETRY

Massimo Martorelli Cesare Rossi Sergio Savino Gabriele Staiano

Department of Industrial Engineering
University of Naples – "Federico II", Italy

ABSTRACT

A technique to obtain the kinematic calibration of multilink systems is presented. The technique that is based on a digital photogrammetry vision system and the D-H based kinematic equations, can be considered as a reverse engineering aspect. The most important aspects of this technique consist in that no information on the kinematics chain is needed, it is fast, low cost, non invasive and also friendly for the operator. Tests of the technique on a revolute robot are also reported, showing a good reliability of the technique itself.

Keywords: Kinematic calibration; digital photogrammetry; Robot mechanics; Reverse engineering

1 INTRODUCTION

Kinematic Calibration

Because of the manufacturing and assembly tolerance, the actual kinematic parameters of a robot differ from their design values; these differences represent the kinematic errors. Because of these kinematic errors the robot end-effector will reach a position that is different from the one that was expected if the nominal kinematic parameters were considered. Especially when the lowering of the costs is required, the kinematic calibration is an effective way to improve the absolute accuracy of robots without the need of a high accurate tooling during the link manufacturing. The kinematic calibration process of an articulated mechanism has different implications in all areas where they are present. This often implies that the presence of such a procedure is also required in applications where the need of the procedure is not so evident. An example can be represented by all the devices that are used as simulators [1].

A relatively recent trend is to use optical equipment based on artificial vision techniques for the measurement instrumentation that is necessary to measure the data used in the calibration of the kinematic chain. Studies were implemented on the use of stereoscopic vision system to obtain the tri-dimensional data necessary to a kinematic calibration procedure [2, 3].

Contact author: Cesare Rossi

Via Claudio, 21 80125 Naples, Italy.
E-mail: cesare.rossi@unina.it

It must be also said that nowadays, calibration tasks need a lot of measurement techniques [4].

The need for an increasingly automated techniques for kinematic calibration of robots, has always pushed toward greater use of vision as a measure of the environment. Different visual feedback motion control methods of the robots was studied in the last few years, to achieve accurate measurement in the industrial robot [5]. At the same time, many algorithms have been developed for the environmental recognition and the motion detection in robot applications, with the aim to promote the integration of vision systems in robotics, especially in mobile and autonomous robots, and to promote and to improve the possibilities of control in robotic applications [6].

The applications based on main sensor with one camera installed in the robot hand, are always more and more numerous, and by means of them the positions of the end effector are related to the positions of the robot joints, and so it is possible to implement a kinematic calibration of the robot, using a kinematic model based on the Denavit-Hartenberg parameters [7, 8].

In this paper is presented a kinematic calibration technique based on a vision system measurement, in particular the position data of some points of the robot are detected by means of digital photogrammetry. The technique uses a kinematic model of the robot based on the Denavit-Hartenberg convention, and the relative displacements between the points "observed" with the vision system.

The main purpose of this work was to develop a kinematics calibration procedure that could be applied without knowing any information on the kinematic chain under investigation and therefore without having to do any measure on it.
The main goals were also represented by the possibility of obtaining a fast, low cost, non-invasive and also friendly for the operator technique

Digital Photogrammetry

Today Reverse Engineering (RE) systems make it possible to solve the problem of the digital reconstruction of objects, even of complex shapes, through principles codified in complete sets of procedures, specific to various applications.
Among the RE systems, the digital photogrammetry – low cost non-contact passive technique – was chosen for this research.
Photogrammetrical methods are as old as photography and can be dated to the Mid-nineteenth century.
Photogrammetry was used for the first time in 1851 by the French officer Aimé Laussedat, referred to as the "Father of Photogrammetry", who developed the first photogrammetrical devices and methods, using terrestrial photographs for topographic map compilation.
The process was called iconometry (from the Greek words icon meaning image and –metry measurement) [9].
Digital Photogrammetry instead was born in the 80's, having as a great innovation the use of digital images as a primary data source.
The extraction of 3D information from digital images is a complex task requiring a mathematical formulation between the images (at least two) and the object. It uses methods from many disciplines, including optics and projective geometry, in particular, the fundamental principle is that of triangulation (Fig. 1): taking photos from at least two different locations, so-called "lines of sight" can be developed from each camera to points on the object. These lines of sight, the viewing ray (i.e. a ray from the optical centre of the camera through the projection of the feature on the image plane), are mathematically intersected to produce the 3-dimensional coordinates of the points of interest. It is what our brain does all the time in conjunction with our eyes' retinas. Algorithms for photogrammetry typically express the problem as that of minimizing the sum of the squares of a set of errors, known as bundle adjustment [10].
Due to the fact that the 3D reconstruction is performed through the identification of common natural features in the image set, the accuracy of the reconstruction depends on the quality of images and textures.
Digital photogrammetry is characterized by the following main phases:

- analysis of the shape of the object and planning of the photos to be taken;
- calibration of the camera;
- processing of the photos with specific software to generate a point cloud;
- transfer of the point cloud to CAD software to create a 3D CAD model.

The advances in computing speed, parallel processing, high camera resolution and the availability of several photogrammetry software packages, that work in ordinary computers without any specialized hardware systems that were required in the past, has made photogrammetry much more feasible and affordable in many applications [11-14].
Currently, photogrammetry is used in several applications such as: Topography (e.g. GIS, Map production), Civil Engineering & Historical Preservation (e.g. 3D CAD reconstruction of buildings or historic objects for preservation or restoration purposes [15]), Quality Control (e.g. quality control tool for piping manufacturers), Aerospace (e.g. tooling inspection, Reverse Engineering of parts by aftermarket fabricators), Automotive (e.g. measuring the effect of crash-tests), Shipbuilding & Repair (it represents the main industrial application [16]. Most shipyards have adopted an advanced measurement technology in an effort to contain costs and further cut down the production cycle) and also Medicine (e.g. in Dentistry to record the location and orientation of multiple implants [17]).

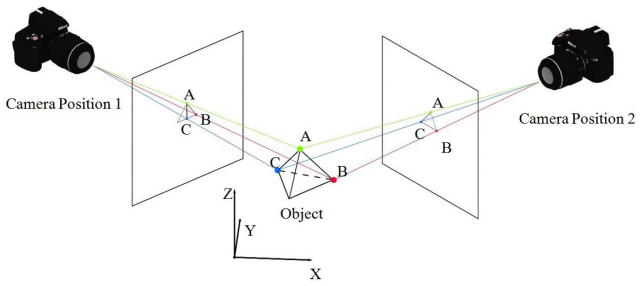

Figure 1 Triangulation Principle used to produce 3-dimensional point measurements.

By mathematically intersecting converging lines in space, the precise location of the point can be determined. It is the two-dimensional (x, y) location of the point on the image that is measured to produce this line. By taking pictures from at least two different locations and measuring the same point in each picture a line of sight is developed from each camera location to the point.

2 THE CALIBRATION TECHNIQUE

If the coordinates in the working space and the joint parameters are known, it is possible to write the direct kinematics equations by means of the Denavit-Hartenberg convention. With this method, each degree of freedom of the robot is characterized by four parameters that describe also the type of joint. As shown in Figure 2, the four

parameters are sufficient to describe any geometric transformation associated to a generic kinematic joint.
A matrix transformation (homogeneous coordinates), associated to a generic geometric transformation between the coordinates in the frame "i" and the coordinates in the frame "i-1",can be obtained as the product of the four basic transformations described by four parameters:

$$ {}^{i-1}A_i = \begin{bmatrix} \cos(\vartheta_i) & -\cos(\alpha_i)\cdot\sin(\vartheta_i) & \sin(\alpha_i)\cdot\sin(\vartheta_i) & a_i\cdot\cos(\vartheta_i) \\ \sin(\vartheta_i) & \cos(\alpha_i)\cdot\cos(\vartheta_i) & -\sin(\alpha_i)\cdot\cos(\vartheta_i) & a_i\cdot\sin(\vartheta_i) \\ 0 & \sin(\alpha_i) & \cos(\alpha_i) & d_i \\ 0 & 0 & 0 & 1 \end{bmatrix} \quad (1) $$

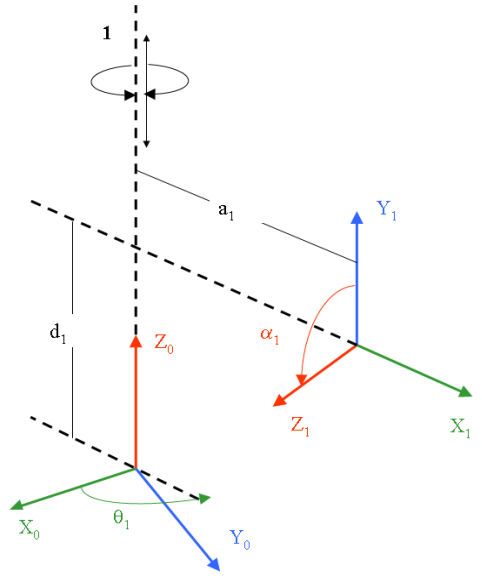

Figure 2 Denavit-Hartenberg parameters of a generic kinematic joint transformation.

The four parameters θ_i, d_i, a_i and α_i of matrix (1), describe the type of joint, so if the joint is rotational the joint variable is θ_i, while if the joint is translational the joint variable is d_i.
By means of such matrixes it is possible to calculate the transform matrix that allows to obtain the coordinates in the frame 0 (the fixed one) of the robot, from those in frame n, that is the one of the last link of the robot: ${}^0T_n = {}^0A_1 \cdot {}^1A_2 \cdot \ldots \cdot {}^{n-1}A_n$.

$$ \{P_0\} = {}^0T_n \cdot \{P_n\} \quad (2) $$

The equation (2) contains all Denavit-Hartenberg parameters, which describe the kinematic chain of the robot, among these there are the joint variables that describe the configurations of the robot.
The kinematic calibration consists of an inversion of the equation (2), by means of whose it is possible to calculate the Denavit-Hartenberg parameters, other than the variables of the joints.
To do this it is necessary to know $\{P_0\}$, $\{P_n\}$ and the joint variables, but in general it is not possible to calculate more unknowns with only one equation, so (2) must be estimate for a sufficient number of robot configurations.
The developed procedure, consists of measuring the position of the robot with a photogrammetric technology. In particular, by means of this technique it is possible to know the position of some targets, that are placed on a revolute robot with three rotational joints, figure 3.
The photogrammetric measure allows to calculate the position of the targets in its reference system, $\{P_v\}_i$.
In order to use the equation (2) to estimate the Denavit-Hartenberg parameters, it is necessary to know the positions of the target in the reference of the robot. This operation is possible if the relation between the reference of the robot and the reference of the photogrammetric system is known, but this relationship is not easy to know or to measure.
This proposed and developed calibration procedure is based on the measures of distances, instead of the absolute positions of the target points, so it is not necessary to know the relation between the robot and the photogrammetric system.

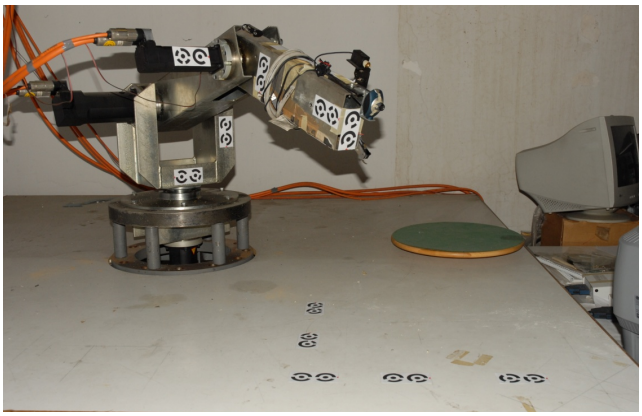

Figure 3 Robot and target.

If $[d_{ij}]_{kt}$ is the distance between the target point "i" in the robot configuration "k" and the target point "j" in the robot configuration "t", it is possible to write the following relation:

$$ \left[d_{ij}\right]_{kt} = \left\| \left[\{P_0\}_i\right]_k - \left[\{P_0\}_j\right]_t \right\| = \left\| \left[\{P_v\}_i\right]_k - \left[\{P_v\}_j\right]_t \right\| = \left\| \left[{}^0T_n\right]_k \cdot \{P_n\}_i - \left[{}^0T_n\right]_t \cdot \{P_n\}_j \right\| \quad (3) $$

where:
i, j = target points;
k,t = robot configurations;

$[\{P_0\}_i]_k$ = position of target "i" in the robot base system and for the robot configuration "k";
$[\{P_0\}_j]_t$ = position of target "j" in the robot base system and for the robot configuration "t";
$[\{P_v\}_i]_k$ = position of target "i" in the photogrammetric reference system and for the robot configuration "k";
$[\{P_v\}_j]_t$ = position of target "j" in the photogrammetric reference system and for the robot configuration "t";
$[{}^0T_n]_k$ = robot transform matrix between frame "n" and frame "0" and for robot configuration "k";
$[{}^0T_n]_t$ = robot transform matrix between frame "n" and frame "0" and for robot configuration "t"
$\{P_n\}_i, \{P_n\}_j$ = coordinates of the target points "i" and "j" in the reference system "n" of the robot.
In equation (3) there is no dependency from the relationship between the reference of the robot and the reference of the photogrammetric system, and the unknown are the Denavit-Hartenberg parameters, other than the coordinates of the target point in the reference "n" of the robot, while the variables of the joints and the distance d_{ij} are known.
The kinematic calibration problem can be expressed as following:

$$d_{ij} = F\left(\{\Theta\}_k, \{\Theta\}_t, \pi_{DH}, \{P_n\}_i, \{P_n\}_j\right) \quad (4)$$

where:
$\{\Theta\}_k$ = vector of the variables of the joints in the robot configuration "k";
$\{\Theta\}_t$ = vector of the variables of the joints in the robot configuration "t";
π_{DH} = vector of unknown parameters of the Denavit-Hartenberg convention;
$\{P_n\}_i, \{P_n\}_j$ = coordinates of the target points in the reference system "n" of the robot.
The problem described by equation (4), obviously, can not be resolved to find the unknown Θ, $\{P_n\}_i$ and $\{P_n\}_j$ with only one distance $d_{ij,}$ so it is necessary to write it for a sufficient number of times, and then it is possible to invert the equations (4) to estimate the unknowns.
The proposed procedure estimates the equation (4) for some target points, applied on the last link of the robot and for some different configurations of the robot. In this way it is possible to write a lot of equations (4) because it is possible to compute the distances between each target point and the others in all the different configurations of the robot.
If N_T is the number of target point and N_C is the number of robot configurations, all the possible distances, N'_d, that it is possible to compute is the number of combinations of N_TxN_C points taken two at a time.

$$N'_d = (N_T \cdot N_C)! \,/\, ((N_T \cdot N_C - 2)! \cdot 2!) \quad (5)$$

In addition to these distances, it is possible to calculate the mutual distances between the target points, also in the coordinate reference system "n" of the robot. The number of these last distances N''_d, is the number of combinations of N_T points taken two at a time. In the calculation of these distances the parameters of Denavit-Hartenberg convention and the vector of the variables of the joints, but only the coordinates of the target points in the reference system "n" of the robot.

$$N''_d = (N_T)! \,/\, ((N_T - 2)! \cdot 2!) \quad (6)$$

In conclusion the total number of distances that is to possible to evaluate and so the number of equation (4) that is possible to compute, N_d, is the following:

$$N_d = N'_d + N''_d \quad (7)$$

3 THE EXPERIMENTAL PROCEDURE

The proposed procedure was applied to a revolute robot with three degree of freedom, figure 4.
The reference systems hypothesized according the convention of Denavit-Hartenberg are shown in Figure 4.
In particular the photogrammetric analysis, was performed using 50 targets to define the three-dimensional coordinates. Some of these were fixed and identified the reference system, the others were attached to the robot and were moved with it.

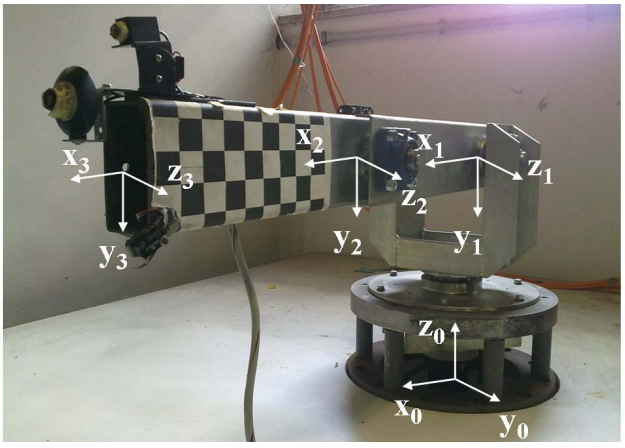

Figure 4 Revolute robot and the Denavit-Hartemberg reference system.

3.1 3D POINT ACQUISITION

A photogrammetry software package, RhinoPhoto by Qualup SAS (France) and a Nikon D200 camera were used for 3D points acquisition.
The following two main phases were performed:

- calibration of the camera;
- processing of the images.

3.2 CAMERA CALIBRATION

Camera calibration plays a fundamental role in Photogrammetry, in order to obtain accurate digitizing, as confirmed in literature [18, 19].
During the process of camera calibration, that is obtained by RhinoPhoto with 4 photos taken with the camera rotated 90°of a calibration grid (Fig. 5) fixed on a perfectly flat area, the metric characteristics of the camera are determined.
This phase is essential for determining:

- the real focal length of the camera, not exactly the same as the focal length indicated by the manufacturer;
- the real position of the Principal Point of the CDD sensor essential in order to calculate the exact 3D positions of the camera;
- the Lens Distortion in order to compensate for this error.

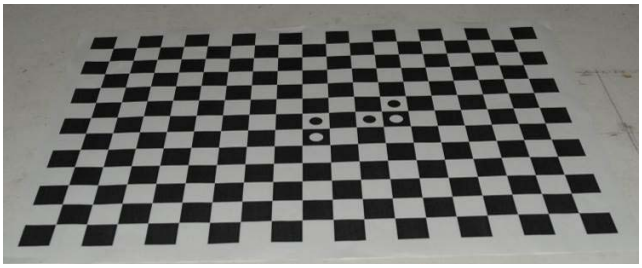

Figure 5 Camera calibration grid.

3.3 IMAGE PROCESSING

After the camera calibration phase, coded targets, similar to circular barcodes were defined and positioned on the points to acquire and various photos were taken at different angles (Fig. 6).
To each one of the target corresponds a number (Fig. 7a). These numbers are automatically read from the images and 2D points on the images are created at the center of the target (Fig. 7b).
The 3D positions of the camera, not known when the photos were taken, then were computed from 2D points on each image (the centers of targets) and finally, the 3D points were created (Fig. 8).

4 EXPERIMENTAL RESULTS: ROBOT PARAMETERS IDENTIFICATION

To perceive all the robot degree of freedom, three coded markers were placed on the end of the third link, like it is shown in Figure 9. Each of these markers is composed of two calibrated target points and of a third target on the side of the marker.
The tests were carried out by analyzing five configurations of the robot and seven target points, shown in Figure 9.

For each of the five configurations of the robot there is a vector of the variables of the joints Θ, as reported in Table I.
In this case $N_T = 7$ and $N_C = 5$, so all the possible distances, N'_d, that are possible to compute with (5), are 595, while the distances N''_d, that it is possible to compute with (6) are 21. So, the total number of equations that can be used to the identification of unknown parameters, is 616.

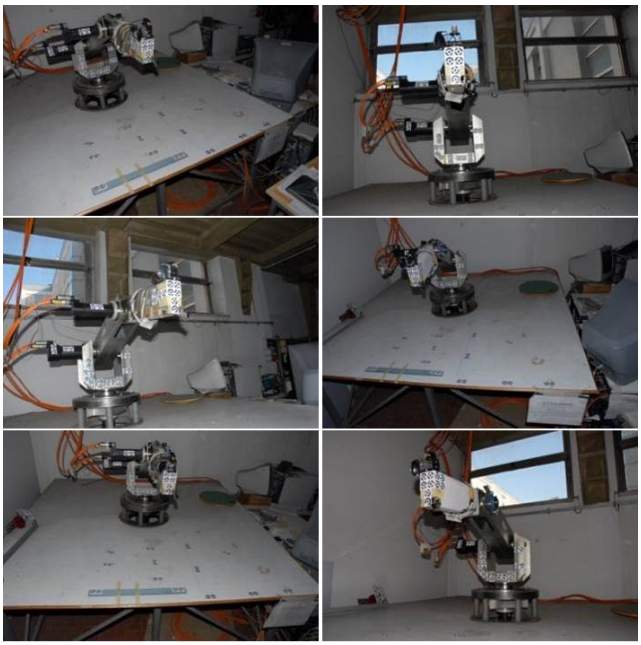

Figure 6 Photos of the points to be acquired taken at different angles.

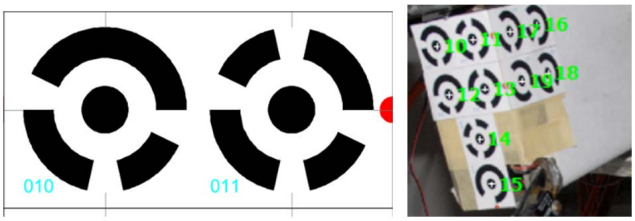

a) b)

Figure 7 Coded targets.

The kinematic calibration problem (4) has been inverted with an optimization procedure, as said, it is possible to evaluate the parameters of the Denavit-Hartenberg convention and the coordinates of the seven target points in the reference system “3” of the robot.
In particular the problem (4) is written as a scalar function of several variables, and constrained nonlinear optimization attempts to find a constrained minimum of this function starting at an initial estimate.

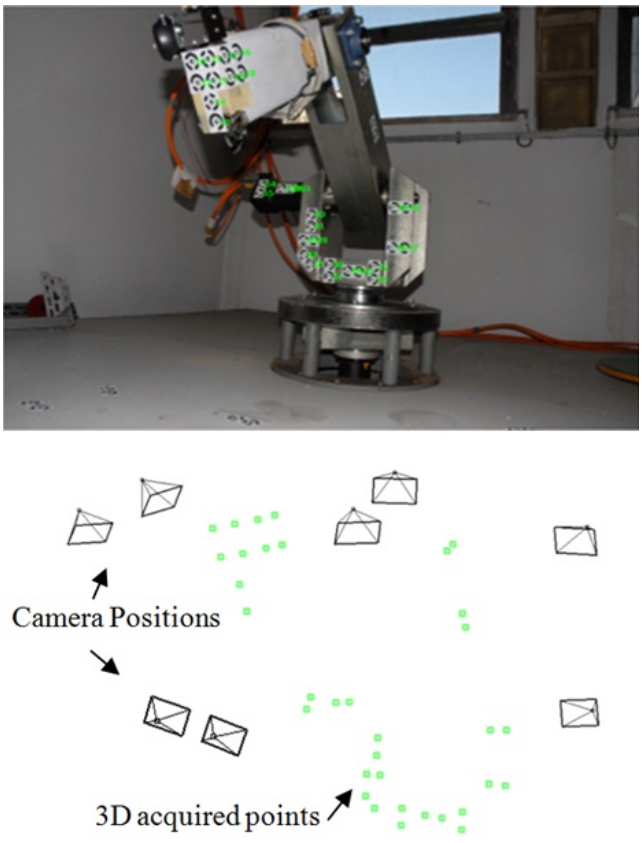

Figure 8 3D acquired points in a CAD environment.

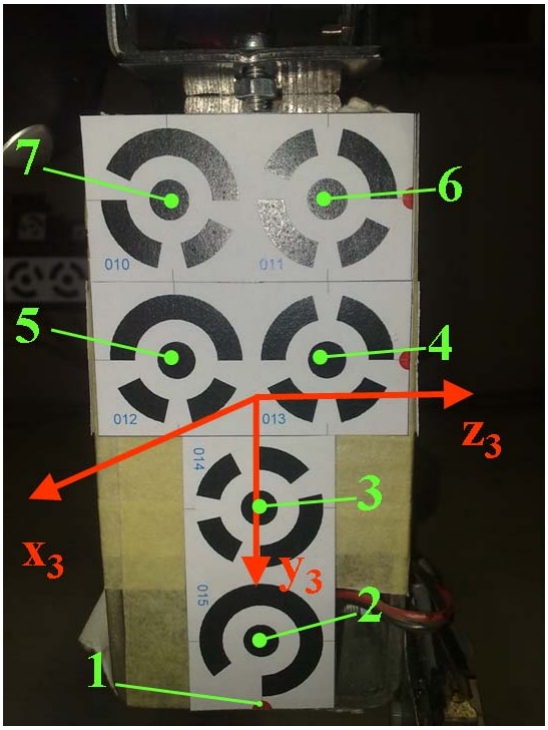

Figure 9 Target points used
for robot parameters identification.

Table I – Value of variables of joint
in five robot configuration

Robot configuration	θ_1 (rad)	θ_2 (rad)	θ_3 (rad)
1	0	-0,4443	1,1709
2	0	-0,6487	1,5995
3	0	-0,2674	1,0974
4	0,1419	-0,4265	1,1342
5	0,0082	-0,4389	1,1430

The vector of unknown parameters of the Denavit-Hartenberg convention, π_{DH}, consists of 9 elements, while the coordinates of the target points in the reference system "3" of the robot, are 3x7=21.
In Table II the identified parameters of problem (4) are reported.

Table II – Identified parameters

	Identified value (mm)		Identified value (mm)
a_1	-1,41	X_3	1,01
a_2	398,76	Y_3	15,40
a_3	404,06	Z_3	0,83
d_1	449,00	X_4	0,3
d_2	4,2	Y_4	-14,35
d_3	4,33	Z_4	14,31
α_1	-1,56	X_5	0,84
α_2	0,00	Y_5	-14,52
α_3	0,00	Z_5	-14,44
X_1	1,07	X_6	0,32
Y_1	59,95	Y_6	-44,37
Z_1	0,64	Z_6	14,44
X_2	1,01	X_7	0,66
Y_2	44,35	Y_7	-44,48
Z_2	0,73	Z_7	-14,36

In Figure 10, the residual values of the distances calculated with the identified parameters, compared to those measured with the photogrammetric system, are shown. It is possible to see that the mean value of the residual is 0.32 mm with the identified parameters and target points coordinates, while the same value is 1.68 mm with the nominal parameters and the measured coordinates of the target points.
A verification of the results is obtained by measuring the displacement of point 1 with photogrammetric system, planning the robot motion with nominal and identified parameters of the Denavit-Hartenberg convention.
Three sets of coordinates, in the reference system 0 of the robot, are taken in to account for point 1 and these are shown in Table III.

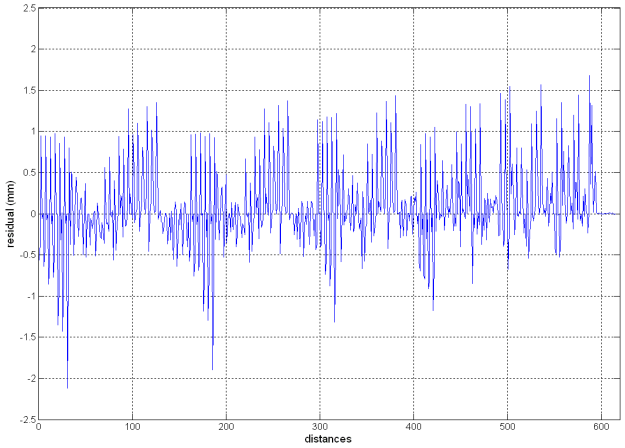

Figure 10 Residual values in mm of the distances calculated with the identified parameters.

The motion of the robot is planned to move point 1 of the reference system 3 of the robot, indicated in Table II, in the three positions indicated by the Table III. The inverse kinematics was applied with the nominal parameters of the Denavit-Hartenberg convention and with those identified with the kinematic calibration.

Table III – Sets of coordinates for point 1.

Point 1 pos.	x mm	y mm	z mm	Distance	d (mm)
1	700	0	450	$d_{1,2}$	100
2	600	0	450	$d_{1,3}$	100
3	700+100/e3	100/e3	450+100/e3	$d_{2,3}$	177,6148

The photogrammetric system made it possible to measure the distances between the positions, whose nominal values are shown in the last column of the Table III.
In Table IV the obtained results are shown:

Table IV – Measured distances with nominal and identified robot parameters.

Distances	NOMINAL PARAMETERS			
	d (mm)	error		
		(mm)	%	% mean
$d_{1,2}$	99,7678	0,2322	0,2322	1,1551
$d_{1,3}$	101,9261	1,9261	1,9261	
$d_{2,3}$	179,9363	2,3215	1,307	

Table IV – cont.

Distances	IDENTIFIED PARAMETERS			
	d (mm)	error		
		(mm)	%	% mean
$d_{1,2}$	100,6948	0,6948	0,6948	0,878
$d_{1,3}$	98,6149	1,3851	1,3851	
$d_{2,3}$	176,6305	0,9843	0.5541	

The data reported in Table IV show the measurements of movements performed by the robot planned with the two sets of D-H parameters, and the relative percentage errors with respect to the nominal displacements. With the identified parameters a lower average percentage error is obtained.

5 CONCLUSIONS

A method for the kinematic calibration of almost any multilink system was presented. The method was then experimentally tested on a low cost revolute robot prototype that was designed and built in our laboratory.
Mainly the technique presents the following peculiarities:

- the technique is non-invasive for the mechanism;
- no measures from an operator are required; this drastically reduces the possibility of errors and, hence it is friendly for the operator;
- the procedure is simple and requires a very short time to obtain the full calibration data;
- the computational efforts are very low;
- once the test rig is acquired, the procedure is a very low cost one. Hence it can be used for a mass production;
- no information is necessary on the kinematics chain.

The presented test results clearly show that the technique permits to obtain accurate values of the kinematic parameters.
Further developments will concern deeper investigations on the error sources in order to obtain a further increase in the accuracy of the calibration proposed technique.

REFERENCES

[1] D. Yu, H. Li, W. Chen, Kinematic Calibration of Parallel Robots for Docking Mechanism Motion Simulation, International Journal of Advanced Robotic Systems, 2011, Vol. 8, No. 4, pp. 158-165.
[2] V. Niola, C. Rossi, S. Savino, A Robot Arms Kinematic Calibration Method, Published on International review: *WSEAS TRANSACTIONS ON SYSTEMS*, Iusse 4, Vol.5, April 2006, pp. 833-838, ISSN: 1109-2777.
[3] V. Niola, E. Pollasto, C. Rossi, S. Savino, An Algorithm for Kinematics Calibration of Robot Arm, Proc. of *15th int. Workshop RAAD 2006* - Balatonfured, Hungary, June 15-17, 2006.
[4] M. Vannocci, V. Colla, Kinematic Calibration Procedure for Anthropomorphic Robots, In book: Introduction To Modern Robotics II, Chapter: 17, Publisher: iConcept press, 01/2011.
[5] A. Watanabe, S. Sakakibara, K. Ban, M. Yamada, G. Shen, T. Arai, A Kinematic Calibration Method for Industrial Robots Using Autonomous Visual Measurement, CIRP Annals - Manufacturing Technology, Volume 55, Issue 1, 2006, pp. 1-6.
[6] S. Savino, An algorithm for robot motion detection by means of a stereoscopic vision system, Advanced Robotics, 2013, vol. 27, issue 13, pp. 981-991
[7] A. Traslosheros, J. M. Sebastián, J. Torrijos, R. Carelli, E. Castillo, An Inexpensive Method for Kinematic Calibration of a Parallel Robot by Using One Hand-Held Camera as Main Sensor, Sensors, Vol. 13, August 2013, pp. 9941-9965, ISSN 1424-8220.
[8] K. English, M. J. D. Hayes, M. Leitner, C. Sallinger, Kinematic Calibration of Six-Axis Robots.
[9] R. Burtch, History of Photogrammetry. Technical report, The Center for Photogrammetric Training, Ferris State University, 2008, pp. 1-36.
[10] B. Triggs, P. McLauchlan, R. Hartley, A. Fitzgibbon, Bundle Adjustment - A Modern Synthesis. ICCV '99: Proceedings of the International Workshop on Vision Algorithms, Springer-Verlag, 1999, pp. 298-372, ISBN 3-540-67973-1.
[11] K. Kraus, Photogrammetry: Geometry from Images and Laser Scans. Second Edition. Walter de Gruyter, 2008, pp. 459.
[12] E.M. Mikhail, J.S. Bethel, J.C. McGlone, Introduction to Modern Photogrammetry, John Wiley & Sons, Inc., New York, 2001.
[13] K. Atkinson, Close Range Photogrammetry and Machine Vision, Whittles Publishing, 2001.
[14] Y. Egels, M. Kasser, Digital Photogrammetry., CRC Press, 2001.
[15] Martorelli M., Pensa C., Speranza D., Digital Photogrammetry for Documentation of Maritime Heritage, Journal of Maritime Archaeology, 2014, pp. 1-13, doi: 10.1007/s11457-014-9124-x.
[16] Y.M. Ahmed, A.B. Jamail, O.B. Yaakob, Boat survey using photogrammetry method, International Review of Mechanical Engineering, Volume 6, Issue 7, 2012, pp. 1643-1647.
[17] J.M. Bergin, J.E. Rubenstein, L. Mancl, J.S. Brudvik, A.J. Raigrodski, An in vitro comparison of photogrammetric and conventional complete-arch implant impression techniques, J. Prosthet. Dent., 2013, 110 (4), pp. 243-251.
[18] F. Remondino, C. Fraser, Digital Camera Calibration Methods: Considerations and Comparisons, Proceedings of the ISPRS Commission V SymposiumImage Engineering and Vision Metrology, 2006, pp. 266-272.
[19] L. Barazzetti, L. Mussio, F. Remondino, M. Scaioni, Targetless Camera Calibration, International Archives of the Photogrammetry, Remote Sensing and Spatial Information Sciences, Volume XXXVIII-5/W16, 2011, pp. 335-342.

ISSN 1590-8844
International Journal of Mechanics and Control, Vol. 16, No. 02, 2015

STOCHASTIC MODELLING AND EXPERIMENTAL OUTCOMES OF MODAL ANALYSIS ON AUTOMOTIVE WHEELS

Elvio Bonisoli Marco Brino Matteo Scapolan Domenico Lisitano

Politecnico di Torino, Dept. of Management and Production Engineering, Torino, Italy

ABSTRACT

An experimental investigation of the effects of the fitting procedure of disk and rim in automotive wheels on their dynamic behaviour is reported. Due to the variation of mass and fitting diameters of the two components, the goodness of the process is evaluated through the assembled wheel dynamics. The geometrical data of an experimental measuring campaign on a large sample of each sub-component are provided and critically analysed with statistical methods, while the results of an experimental modal analysis supply the modal properties of each component. The potential of this method lies in the possibility of being able to deduct the residual stress due to the fit, difficult to quantify in other way, directly from the correlation of the experimental measurements of the natural frequencies of the sub-components and of the wheel after the fitting. Finally, an indirect measure of the fitting procedure can be detected.

Keywords: experimental modal analysis, interference fit, automotive wheel

1 INTRODUCTION

The search for more and more performing and safe vehicles has led, in recent years, to an increasing optimization of all automotive components.
Components designed are safer at the same time lighter to comply with emissions standards become progressively ever more restrictive.
Nowadays the dynamic behaviour of automotive wheels has become particularly important for the overall performance of the vehicle. The design of these components must be accurate enough because they have a particular importance and on their dynamic depend driving stability, safety and most of the vibrational and acoustic comfort of the vehicle. In order to satisfy these aims, the study of the wheel should include analytical and numerical models to take into account the quasi-random variations in the real components due to the production process.

Contact author: Elvio Bonisoli

Politecnico di Torino
Dept. of Management and Production Engineering
Corso Duca degli Abruzzi, 24 – 10129 Torino, Italy
E-mail: elvio.bonisoli@polito.it

The stochastic changes of the main variables involved, owing to the dimensional and geometric tolerances, assume a major role. A large part of the automotive wheels are obtained by fitting the disk in the rim: this process produces stress on the component, in addition to the residual production process residual stress, that is very difficult to estimate due to variability in the production process and due the geometric and dimensional tolerances of the components.
Several studies have been done on the wheels classical fatigue tests: in [1] a simulation of the cornering fatigue test is provided, in [2] the radial fatigue test of the wheels is presented, but in both cases the effects of the fitting are not considered.
The determination of the service stress of a wheel, due to the vertical and horizontal loads and production process is reported in [3], but also in this case the residual stresses are not considered.
In [4] the authors also investigated the effect of residual stresses due to production process and the fit of the disk in the rim, considering a large sample of disks, rims and wheels.
The stress causes variations in the frequencies of the components, stress stiffening or softening effect: in [5] is shown as the stress affecting the dynamic behaviour of the

component, while in [6] an analytical formulation is obtained for the fundamental frequency for a clamped plate increasing stress.
The fitting of the disk in the rim produces plastic deformation of the components. Therefore it is not possible to deal the wheel with linear elastic equations; recent works show the limitations of the classical thick-wall theory when dealing with complex geometry components and with plastic deformations [7].
It is well known that any measure made on nominally equal components has some variability [4, 8, 9, 10], so it is not possible to estimate in advance the stress due to fitting because it is influenced by a large number factors, and because the stress on the wheel depends on the two particular component assembled.
The basic idea of this work is that of being able to estimate the tension due to the fitting of disk and rim, just starting from the measurement of the natural frequencies of the components and subsequently of the assembled wheel: in effect, at each modeshape of the wheel is possible to associate a component modeshape [4].
A statistical approach is needed to study the influence of the components properties on their natural frequencies, this paper in particular focuses on the effects of mass and fitting diameter. To correlate fitting diameter and mass to the natural frequencies, an experimental modal analysis campaign has been conducted on a sample of 40 disks, 40 rims to detect which of the modeshapes is useful to the aim.

2 MEASURED DIAMETERS AND MASSES

The subject of the study is a spare wheel of a common car, with the disk and rim shapes and cross section shown in Figure 1.
The fitting diameter considered is the minimum in case of the rim, and the maximum in case of the disk, thus the ideal interference value is the difference of the two.
While the 40 disks come from the same component specifications and thus they only differ one another for production tolerance ranges, the 40 rims are divided into 3 families:

- standard rims (20 samples);
- increased diameter rims (10 samples);
- decreased diameter rims (10 samples).

With those families in addition to the standard interference fit range, two extreme ranges can be taken into account, one with very low and the other with very high interference fit. The residual stresses caused by the interference conditions after the fitting process are presented in Figure 2.
The masses and the diameters for the samples of disks and rims are subject of a first statistical check using Normal Probability Plots (NPP) to evaluate the normality of the distributions.
Figure 3 shows the distributions of rims and disks diameters, where in the top plot the three rim families are

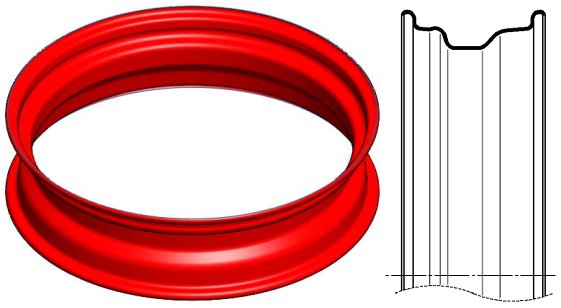

(a)

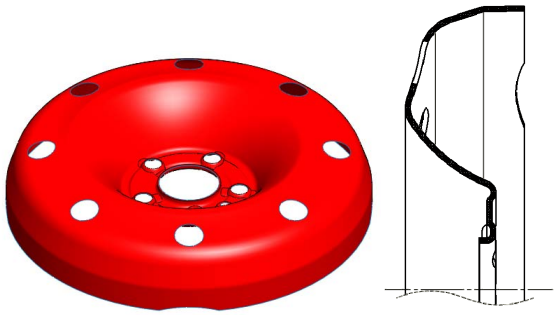

(b)

Figure 1 Isometric view (left) and cross section (right) of the rim (a) and disk (b) considered.

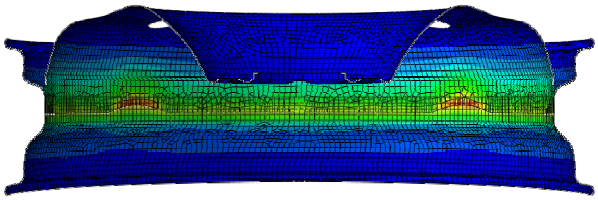

Figure 2 Contour plot of the residual stresses due to the fitting process, from numerical simulation.

clearly distinct, and in the bottom plot the disks have an unexpected trend in the central zone, raising the possibility of a bi-normal distribution.
One of the possible causes of this distribution might be due to different sheet metal coils.
The same plots are shown in Figure 4, considering the mass property. Each component was measured four times and randomised with other samples, and in this plots all the single measurements are represented.
In both plots a gap is present, dividing the range into two separate distributions. In both cases the trends are hypo-normal, with several samples located at the tails of the distribution, and considering the left portion the trend is more normal with respect to the right portion for both rim and disk cases.

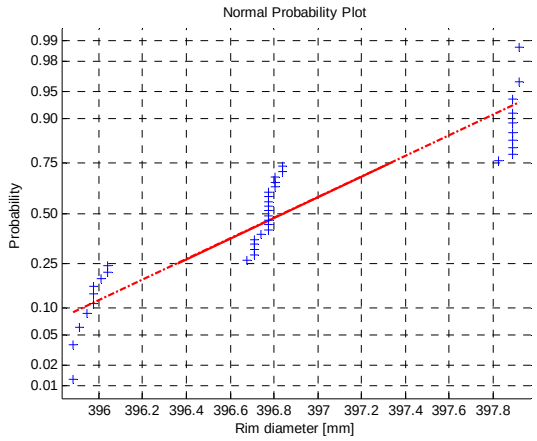

(a)

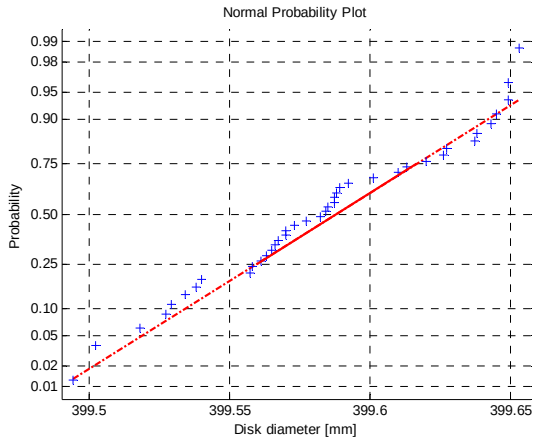

(b)

Figure 3 NPP for rims (a) and disks (b) diameter.

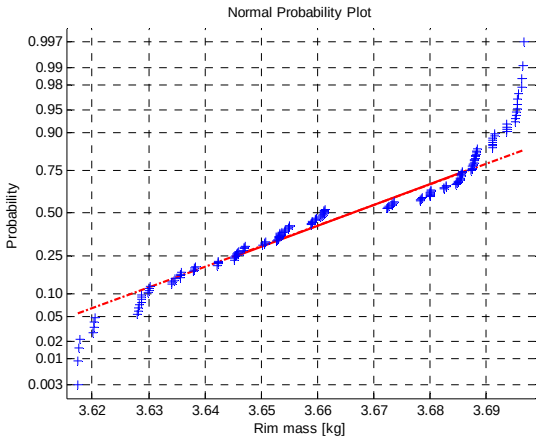

(a)

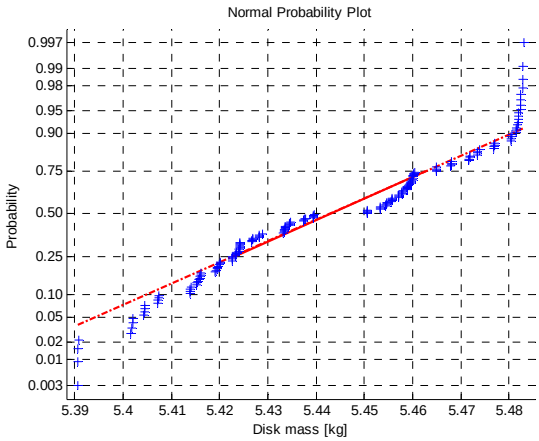

(b)

Figure 4 NPP for rims (a) and disks (b) mass.

Analysing the rims, the mass NPP can be arranged considering the averages of the four measurements of each component, and colouring differently the three diameter families, as shown in Figure 5. It is interesting to notice that while standard and bigger rims distribution are mixed, with bigger rims slightly heavier, the smaller rims are more concentrated and located on higher values. This says that smaller rims are heavier.

Considering the sheet metal thickness as one of the most relevant parameter which influences the mass, the heavier smaller rims could be due to the non-standard production process of the component, which could induce a lower influence on the thickness.

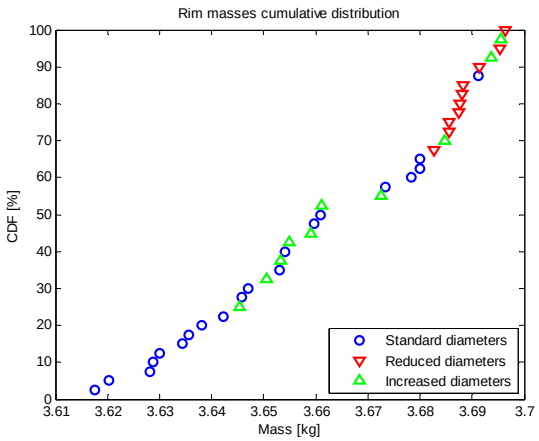

Figure 5 NPP for rims mass in separated families.

3 EXPERIMENTAL MODAL ANALYSIS

For the correlation analysis, Experimental Modal Analysis (EMA) has been performed on each sample of disk and rim, in free-free boundary conditions simulated using low stiffness springs. The data are acquired using two monoaxial accelerometers, placed in three different configurations on the rims and two configurations on the disks, and the excitation chosen is impact hit with force detection hammer.

The aim is not to perform a full modal identification but only the Frequency Response Function (FRF) in order to identify the natural frequencies of each component, not considering the whole modeshapes.

Figure 4 and Figure 5 show the acquired FRFs for one sample of rim and one sample of disk respectively, where the different configurations for disk and rim are clear.

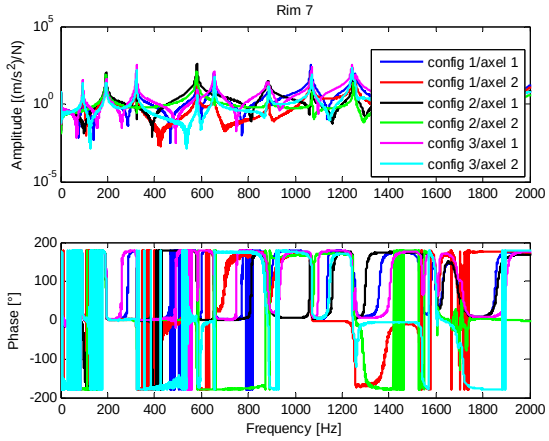

Figure 6 FRFs for rim #7.

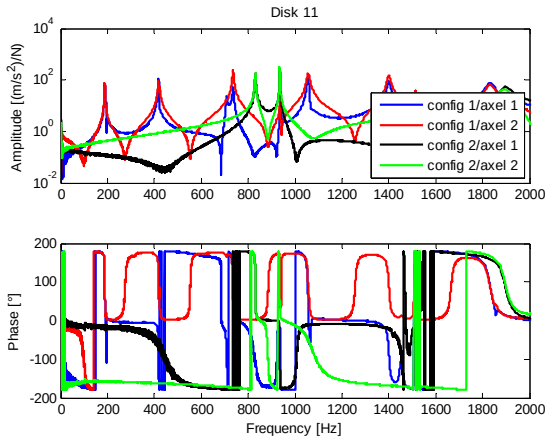

Figure 7 FRFs for disk #11.

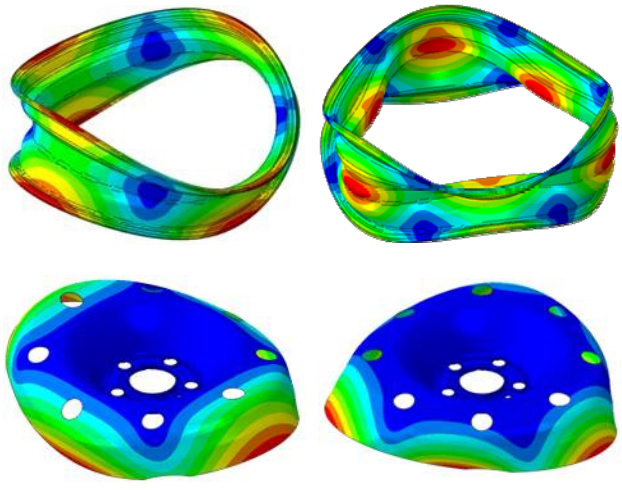

Figure 8 Numerical modeshapes of rim (upper) and disk (bottom) for the 1st mode (left) and the 4th mode (right).

Knowing the location of the accelerometers, it is possible to determine the modeshape, known the modeshapes sequence from a numerical simulation. Figure 8 shows the 1st and the 4th numerical modeshapes of disk and rim.

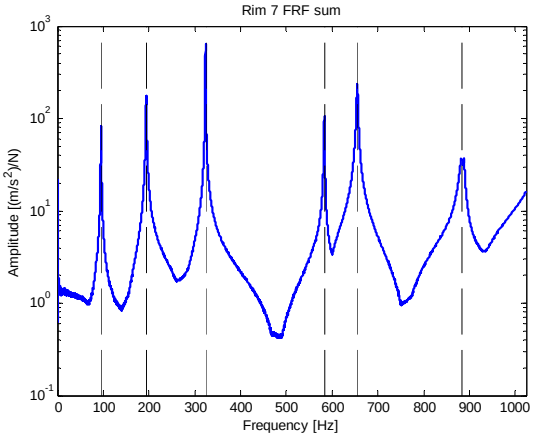

Figure 9 FRFs sum and frequencies for rim #7.

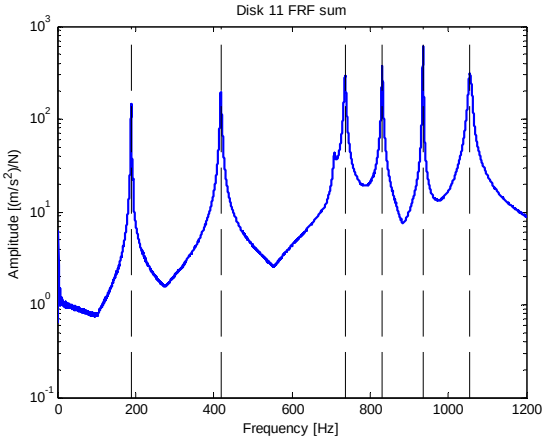

Figure 10 FRFs sum and frequencies for disk #11.

The single FRFs allow evaluating the zones where structural nodes apply by curve comparison, and helping recognising the modal shape.

In the rim case, the accelerometers for the second configuration were located in the central zone. The central zone is less relevant and it is subject to several structural nodes, thus for all the rims it has not been considered.

All the remaining FRFs have been subject to a sum, in order of obtaining a single curve FRF sum which could represent the component.

This sum was then subject of automatic peak detection for the identification of the natural frequencies, which are then assigned to each disk and rim.

Figure 9 and Figure 10 show the sum of the samples related to the single FRFs, with vertical dashed lines which represent the location of the natural frequencies identified though the automatic routine.

Due to the difficulty of automatically separate in the experimental identification the different modes when they have very similar frequency (common feature of axisymmetric objects), they are considered as single modes, thus with the same mode number.

4 FREQUENCY CORRELATIONS

The automatically identified natural frequencies for rims and disks can then be correlated to diameters and masses through qualitative evaluations on simple plots.
In the rim case, it is possible to analytically predict the dependency of natural frequencies with respect to the geometrical parameters by taking into account the dynamic bending behaviour of a generic *r*-mode, with the assumption of an equivalent curved beam with rectangular cross-section. With modal coordinates the related frequency would be

$$f_r = \frac{1}{2\pi}\sqrt{\frac{k_r}{m_r}} \tag{1}$$

and by making explicit the stiffness *k* and mass *m* terms of the related geometry

$$f_r \propto \frac{1}{2\pi}\sqrt{\frac{12\,E\,I}{\rho\,A\,l^3}} \tag{2}$$

it is possible to show the dependency with respect to thickness *s* and diameter *d*

$$f_r \propto \frac{1}{2\pi}\frac{s}{\pi^2 d^2}\sqrt{\frac{E}{\rho}} \tag{3}$$

with linear direct effect of the thickness and inverse quadratic effect of the diameter. For the thickness in particular the behaviour is the opposite of what one would expect: an increase of thickness would increase the mass thus lower the frequency, but in this case the stiffness contribution is predominant, providing a direct dependency between natural frequencies and mass. Similar dependency can be detected for disks, considering equivalent bending modes of a circular plate.
Figure 11 shows the correlation between the first and fourth mode of the rims, with respect to the diameters. The rim families are clearly separated and represented with different colours.

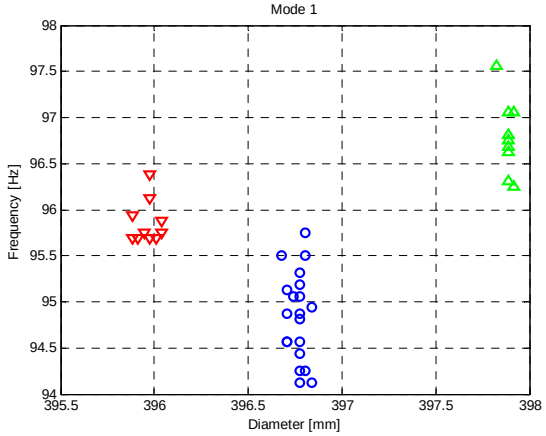

(a)

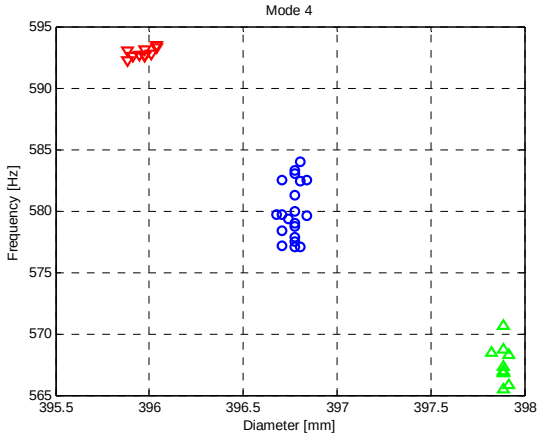

(b)

Figure 11 Frequency vs. diameter plot of rims for mode #1 (a) and mode #4 (b).

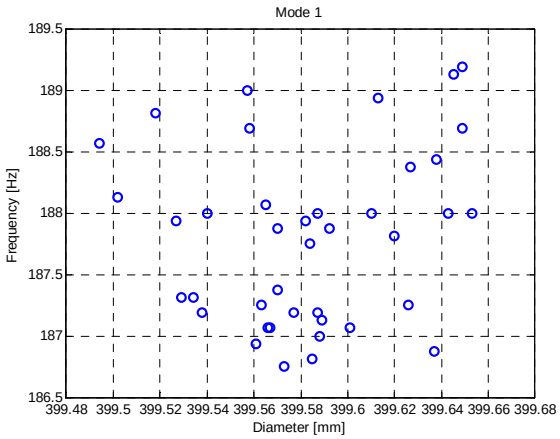

(a)

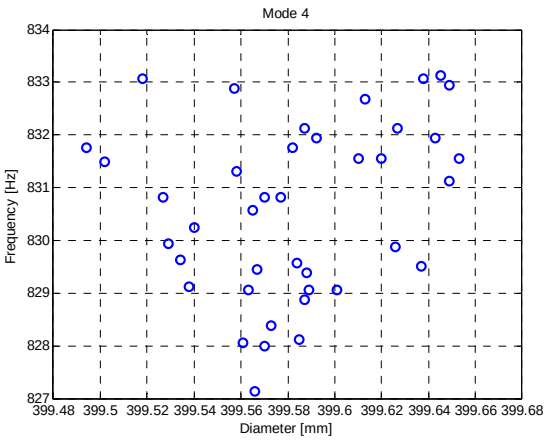

(b)

Figure 12 Frequency vs. diameter plot of disks for mode #1 (a) and mode #4 (b).

There is a general tendency, considering the difference of the families, while inside the families there is no tendency evidenced. In particular, for mode #4, the trend is a decreasing frequency on increasing diameter, as predicted in (3). Not evident tendency are detected inside each families, most probably because other parameters have the same influence on the frequency with respect to the diameter and mask the trend.

On the other hand Figure 13 and Figure 14 show the dependency of the frequencies with respect to the mass for both rims and disks respectively.

In this case the mass has particular influence on the resonance frequency and with a linear positive trend.

Figure 12 then shows the same plot but considering the disks. Having only a single standard family the plotted point are randomly scattered, it is clearer that there is no particular trend considering just the tolerance range for the diameter, as happen in each family of the rims.

Considering the rims, the trend is increasing frequency on increasing mass, and this can be counterintuitive. There are visible three different linear correlation, one for each family, depending on the diameter, as obtained before.

This time is also visible a trend inside the families, with much less dispersion in case of mode #4.

In the disks case, where a single family is present, the trend is still clear, and also in this case mode #4 shows a clear trend with much less dispersion. These trends tend to confirm the hypothesis of the relevant influence of the sheet metal thickness on the mass of the component, as in (3) for both rims and disks.

5 CONCLUSIONS

In this paper large samples of rims and disks for automotive wheels are been analysed. The fitting diameters and the masses of rims and disks are been measured. From statistical analysis of the diameters the three known families of rims appears clearly, but also the disks seems divided into two families probably because of different sheet metal coil. The statistical analysis on the masses evidence a strange behaviour in the rims, indeed the smaller rims results to be heavier, while the masses of standard and large rims are mixed respect the diameters.

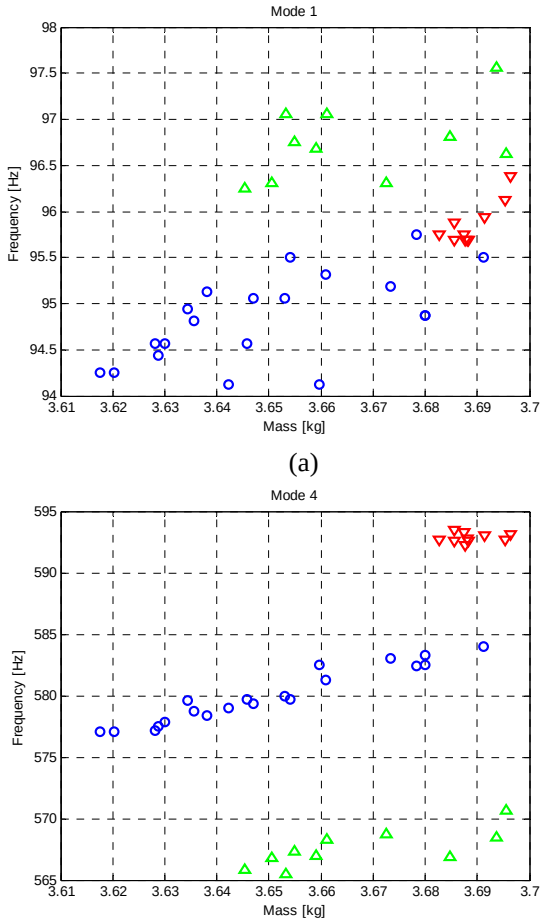

(a)

(b)

Figure 13 Frequency vs. mass plot of rims for mode #1 (a) and mode #4 (b).

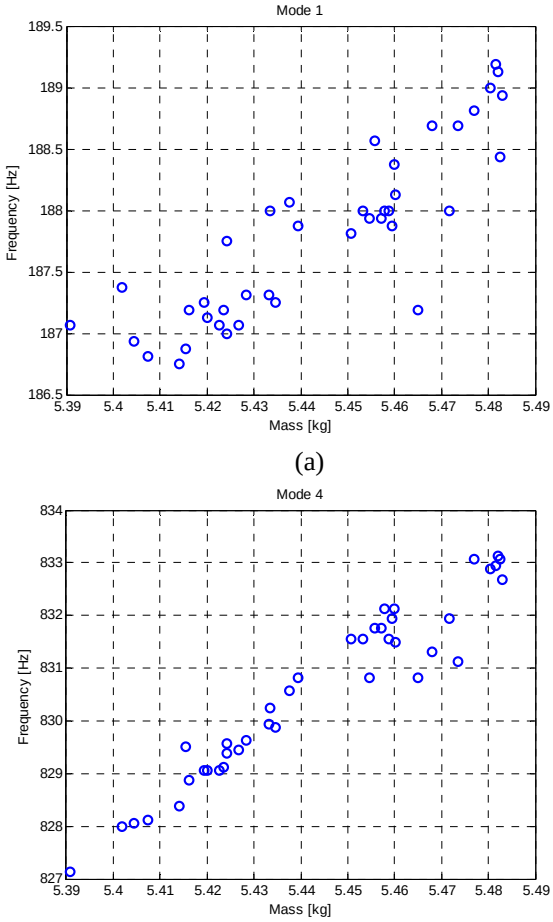

(a)

(b)

Figure 14 Frequency vs. mass plot of disks for mode #1 (a) and mode #4 (b).

After the detection of the natural frequencies of each sample of rims and disks the relationship between natural frequencies and mass or fitting diameters has been researched.

The correlation between diameters and resonance frequency of the rims evidence a trend among the families but not inside each one, while the same correlation on the disks does not show any particular relationship.

On the other hand the correlation between masses and natural frequencies is clearly visible both for rims, also inside the three families, and disks. The aim is to find a modeshape for which there is a relationship between fitting diameters and its natural frequency, both for disks and rims. The fourth mode of rims and disks can be a valid candidate. The study of the corresponded system modeshape, correlated to the chosen component modeshape, can give very useful information of the stress due to the interference level.

The natural continuation of this work will be the fitting of rims and disks, in order to have as much as possible different level of interference, and studying the changes in the dynamic behaviour of the system to find the correlation with the residual stress.

ACKNOWLEDGMENTS

The authors thank D. Rovarino, R. Majocchi and G. Gallio of MW Italia for providing the technical material, suggestions and supporting the research in this study. The authors would like to thank the MW Italia S.p.A. for permission to publish this work. Special thanks go to all of those who have contributed to the result achievement of this project.

REFERENCES

[1] Wang X., Zhang X., Simulation of dynamic cornering fatigue test of a steel passenger car wheel. *International Journal of Fatigue*, 32, 2010, pp. 434–442.

[2] Firat M., Kozan R., Ozsoy M., Mete O.M., Numerical modeling and simulation of wheel radial fatigue tests. *Engineering Failure Analysis*, 16, 2009, pp. 1533–1541.

[3] Grubisic V., Fischer G., Procedure for optimal lightweight design and durability testing of wheels. *International Journal of Vehicle design*, 5(6), 1984, pp. 659–671.

[4] Bonisoli E., Marcuccio G., Tornincasa S., Vibration-based stress stiffening effect detection on automotive wheels through PCE meta-model. Manuscript sumbitted for publication, 2015.

[5] Lieven N.A.J., Greening P., Effect of experimental pre-stress and residual stress on modal behaviour. *Philosophical Transaction of the Royal Society Lond.*, 359, 2001, pp. 97–111.

[6] Weinstein A., Chen W.Z., On the vibration of a clamped plate under tension. *Quarterly of Applied Mathematics*, 1, 1943, pp. 61–68.

[7] Zhang Y., McClain B., Fang X.D., Design of interference fits via finite element method. *International Journal of Mechanical Sciences*, 42, 2000, pp. 1835–1850.

[8] Kompella R.S., Bernhard R.J., Variation of structural-acoustic characteristics of automotive vehicles. *Noise Control Engineering Journal*, 44(2), 1996, pp. 93–99.

[9] Hasselman T., Chrostowski J.D., Effects of product and experimental variability on model verification of automobile structures. *Proceedings of IMAC, International Modal Analysis Conference XVI*, 1, pp. 612–620, 1997.

[10] Cafeo J.A., Doggett S.J., Feldmaier D.A., Lust R.V., Nefske D.J., Shung H.S., A design-of -experiments approach to quantifying test-to-test variability for a modal test. *Proceedings of IMAC, International Modal Analysis Conference XVI*, 1, pp. 598–604, 1997.

ISSN 1590-8844
International Journal of Mechanics and Control, Vol. 16, No. 02, 2015

EFFECTS OF EARTHQUAKE MOTION ON MECHANISM OPERATION: AN EXPERIMENTAL APPROACH

Özgün Selvi[1] Marco Ceccarelli[2] Erman B. Aytar[3]

[1] Cankaya University, Ankara, Turkey

[2] LARM, Laboratory of Robotics and Mechatronics, University of Cassino and South Latium, Italy

[3] Izmir Institute of Technology, Izmir, Turkey

ABSTRACT

This paper presents an experimental characterization of the effects of earthquakes on the operation of mechanical systems with the help of CaPaMan (Cassino Parallel Manipulator), which is a 3 DOF robot that can fairly well simulate 3D earthquake motion. The sensitivity of operation characteristics of machinery to earthquake disturbance is identified and characterized through experimental tests. Experimental tests have been carried out by using a slider-crank linkage, a small car model, and LARM Hand as test-bed mechanisms that have been sensored with proper acceleration or force sensors. Results are reported and discussed to describe the effects of earthquake motion on the characteristics of mechanism operation as a service application of the robotic CaPaMan system.

Keywords: Experimental mechanics; Simulation; Mechanisms; Earthquake effects

1 INTRODUCTION

For investigating the earthquake characteristics and earthquake-resistant constructions, earthquake simulators are commonly used for experimental tests in the field of Civil Engineering. For dynamic testing of structures subjected to earthquake accelerations and for experimenting effects on structures small scale uni-axial servo-hydraulic seismic simulators have become popular, [1, 2]. A number of new large-scale seismic simulator facilities have recently been presented as in [3, 4, 5], and some exceptional simulators, like for example in [6], are also made for outdoor. The case of 6 DoF motion simulator is also presented for shaking tables in [7]. It is important to have earthquake simulators that can reproduce earthquakes with main real characteristics. Generally, most of the earthquake simulators are shaking tables, which are actuated by hydraulic actuators that are fixed on the base. High payload capacity, high motion speeds, and high accelerations are the main characteristics of shaking tables, but they refer to seismic translational motions only.

A new earthquake simulator is a suitable service application of CaPaMan which can simulate not only translational motion but also 3-D waving motions of earthquakes. Performances and suitable formulation for the operation of CaPaMan as earthquake simulator have been presented by theoretical investigations and experimental validations in [8-11]. In fact, CaPaMan can be operated fairly easily by giving suitable input motion to obtain any kind of earthquake in terms of magnitude, frequency and duration.

A novel field of interest can be recognized in investigating the effects of earthquake motion on the operation of machinery. Although vibrations are well known as affecting the machinery operation, the specific effects of earthquake actions on machinery characteristics are not yet fully explored. In previous works [12] the effects of earthquakes on mechanism operation are shown with first experiments on a slider-crank mechanism and a robotic hand.

In this paper the effects of earthquake on the operation of mechanical systems have been investigated experimentally by an analysis and reproduction of an earthquake motion

Contact author: Özgün Selvi[1], Marco Ceccarelli[2]

[1] Cankaya University, Ankara, Turkey.
E-mail: ozgunselvi@cankaya.edu.tr

[2] LARM, Laboratory of Robotics and Mechatronics, University of Cassino and South Latium, Italy
E-mail: ceccarelli@unicas.it

disturbing machine operation. This paper illustrates a specific activity that has been focused in determining experimentally the effects of earthquake motion on mechanism operation by looking at the changes in the motion (acceleration) or force outputs of the mechanisms. Experimental tests have been carried out by using a slider-crank linkage with servo motor, a small car model, and LARM Hand as test-bed mechanisms with acceleration or force sensors in a service application of CaPaMan system.

2 MOTION CHARACTERISTICS OF EARTHQUAKES

A sudden and sometimes catastrophic movement of a part of the surface of the Earth is called an earthquake when it results from a dynamic release of elastic strain energy with seismic waves. Large earthquakes can cause serious destruction and massive loss of life through a variety of damages such as fault rupture, vibratory ground motion, inundation, permanent ground failures, and fire or a release of hazardous materials, and even buildings/constructions collapses and vehicles/machinery operation crashes. Ground motion is the dominant and most widespread cause of damages, as stressed in [13].

In general an earthquake has three phases, namely an initial phase, which corresponds to the beginning of the seismic motion, an intermediate phase where maximum acceleration peaks and displacements occur, and a final phase representing the end of the earthquake. Main characteristics of an earthquake are frequency, amplitude, and acceleration magnitude, because the resonance of a system is determined by frequency value, duration of the stress action due to a seismic motion, amplitude and acceleration magnitude of an earthquake excitation.

A seismic motion is characterized by the period of a seismic cycle and characteristic length for each seismic wave. As shown in Fig.1 [13], main types of seismic waves can be considered the compression expansion waves P, transversal waves S, and superficial waves M, when referring to the spread speed and terrain movements. S waves are transversal waves and their usual period is between 0.5 and 1 second. The P waves spread through a spring-like-motion with a typical period between 0.1 and 0.2 second. Both P and S waves occur close to the epicenter. Unlike P and S waves, M waves occur on the surface of the terrain at a considerable distance from the epicenter of the earthquake and usually they have a period from 20 second to 1 minute.

In Figure 1.c) main differences among the seismic waves are represented in terms of acceleration magnitude and characteristic period of oscillating motion, which is responsible of a periodical excitation of structures that can be damaged when resonance situation occurs.

Usually, critical resonant motion is analyzed in terms of translational seismic components, but even angular motion can strongly contribute to the resonant excitation. Thus, unlike most of the simulators that do not consider the 3D motion of the terrain due to earthquake, in this paper 3D motion capability of CaPaMan parallel manipulator has been used to simulate earthquake motion with its full motion effects. Thus, an earthquake simulator has been arranged with CaPaMan as service system for experiencing the variety of seismic motions and their effect on mechanism operation.

3 OPERATION OF MECHANISMS

As mentioned in terminology of IFToMM [14] a machine is a "mechanical system that performs a specific task, such as the forming of material, and the transference and transformation of motion and force". Similarly a mechanism is defined as a "constrained system of bodies designed to convert motions of, and forces on, one or several bodies into motions of, and forces on, the remaining bodies". Mechanisms, which can be considered the core parts for machines, are combination of gears, cams, linkages, springs, and other mechanical parts [15, 16].

Properties of mechanisms operation can be characterized by input-output relationships, motion performance of task unit, energy efficiency, and so on. In a design process a task goal of the can be classified as function generation, point guidance, and body guidance [15, 16]. Function generation is the coordination of positions of the input and output links, in which the output members need to rotate, oscillate or reciprocate according to a specified function of time or input motion. Path generation is the design of mechanism for guiding a coupler point along a described path. Rigid body guidance is the problem of translation and/or orientation of a rigid body from one position to another.

Machinery operations are usually worked out to perform motions and actions with the task performance that are related to the machinery aim and also interaction with users and environments.

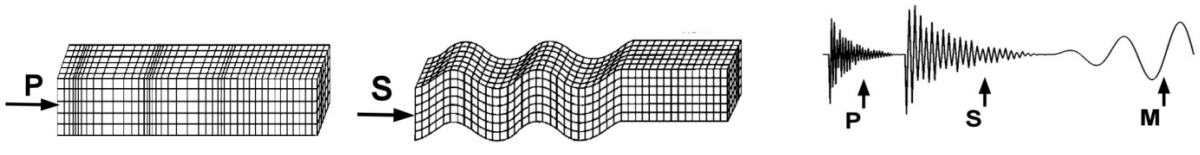

a) b) c)

Figure 1 Basic characteristics of seismic waves [13]:
a) compression and expansion waves; b) transversal waves; c) types of seismograms.

A machinery aim can be in general described by mechanical properties whose performance merits can be expressed in term of motion characteristics and transmission actions with efficiency features both from kinematical and energy viewpoints. Machinery interactions can be understood as related to the effects toward the surrounding environment and mainly as from the viewpoint of human-machine interactions. Those last features will include issues on comfort and safety that can make strong constraints to machinery operations with limited range of operation feasible characteristics. Thus, machinery operations can be described and characterized by performance indices which can be formulated for general but specific aspects that permit both design procedures towards optimal solutions and experimental control/monitoring of successful operation. Special attention is today addressed to safety as interaction with human users, even when using a machine under critical risky situations which can be characterized by impact, high accelerations or changed operation outputs. Even efficiency in force transmission and energy consumption are of great importance in modern machinery.

In general the effects of earthquakes are neglected during machine design. The difficulty to determine the effects of earthquakes is due to different types of totally random waves caused by them, as mentioned in section 2. An illustrative example of earthquake influence on machinery operation can be given as referring to the running of a train. Input for trains is the action of actuators for wheel motion, task for the train is the body guidance of the train, and the output is a stable motion with the features of comfort, safety, efficiency and reliability. A general disturbance of train operation is related to vibrations which effect also comfort of passengers. Comfort in train task is felt by human users mainly in terms of acceleration of the train cars. This task efficiency of cars motion is a result from the transmission of motions and forces from the mechanism for the wheel actuation and car guidance during train run. Those characteristics are demanded in more robust outputs in faster trains. Motion disturbances can produce not only uncomfortable operation, but even risks of disasters in train run, as it can occur in the case of earthquakes.

In order to define a motion of a mechanism it is essential for the mechanism to have a fixed frame which is usually ground. In the event of an earthquake the fixed frame starts to move and apply unexpected random forces to the mechanism so that it may produce changes in the mechanisms outputs. These unexpected changes should be investigated to give useful feedbacks for the design and operation of machines that can work properly even under earthquake disturbances.

3.1 AN EXAMPLE WITH A SLIDER CRANK MECHANISM

For converting rotary motion into alternating linear motion the mostly used mechanism is the slider-crank mechanism shown in Figure 2.a). A slider-crank mechanism consists of four bodies that are linked with three revolute joints and one prismatic joint. Four different mechanisms or inversions of this kinematic chain are possible as depending on which body is grounded, namely the crank, connecting link, sliding link or slot link. One of the inversions of slider crank mechanism is used in internal combustion engines (automobiles, trucks, and small engines). A wide use of these machines makes the slider-crank mechanism the most used mechanism in the world.

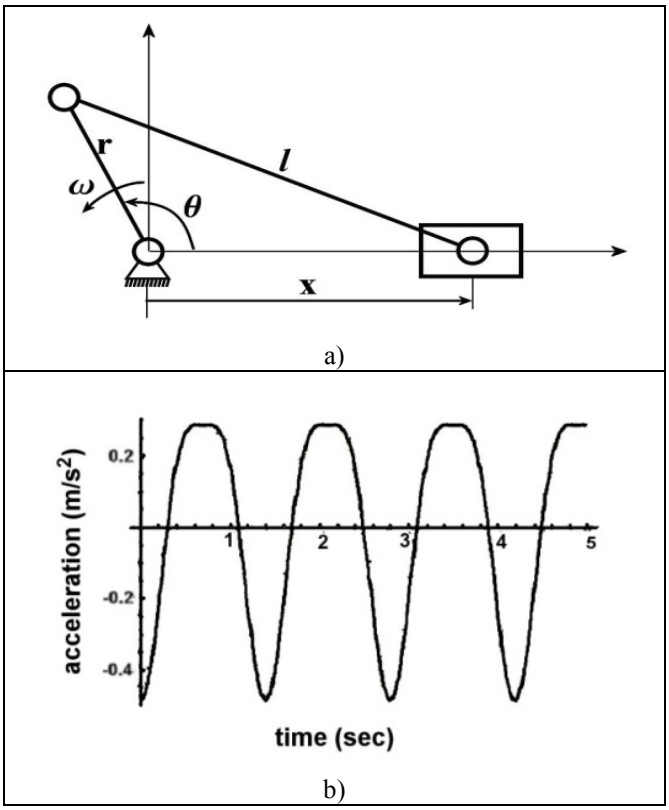

Figure 2 A test-bed slider-crank mechanism:
a) kinematic parameters; b) slider accelerations with stationary frame and input motion at 43 rpm.

In Figure 2.a) kinematic parameters of slider crank are shown, acceleration equation as output of the slider can be calculated from the acceleration equation of the slider with respect to input rotation as,

$$\ddot{x}=-r\alpha\left(\sin\theta+\frac{r\sin 2\theta}{2l}\right)-r\omega^2\left(\cos\theta+\frac{r\cos 2\theta}{l}\right) \qquad (1)$$

A numerical computation is shown in Figure 2.b) which shows a nearly harmonic motion for slider acceleration.

Expected influence during a seismic disturbance can give changes in the shape and magnitude of the slider acceleration with significant alteration of the task motion behaviour. But Eq.(1) gives indication of which parameter can be affected or can be used for limiting this effects.

4 EXPERIMENTAL SETUP WITH CAPAMAN AS EARTHQUAKE SIMULATOR

The here-in test-bed prototype for earthquake simulator shown in Figure 3 consists of a service application of CaPaMan (Cassino Parallel Manipulator) when equipped with acceleration sensors, a controller for seismic motion reproduction, and an acquisition board that is connected to a computer. Data acquisition is used to monitor accelerations that occur along the axes of a reference system that is fixed on the mobile platform [8, 9].

Since the minimum number of accelerometers that are needed to describe velocity and acceleration of a 3D motion of a rigid body is twelve when properly located [17], CaPaMan has been equipped with four of three-axis accelerometers are installed with a symmetrical distribution. The four three-axis accelerometers are located on the below surface of the CaPaMan platform with positions that are indicated in Figure 4. The control system scheme layout for CaPaMan manipulator is shown in Figure 5. Motors signals for simulating an earthquake are sent from a servo motor controller (Scorbot-ER V) by using the ACL programming language for the formulated closed-form direct kinematics of CaPaMan. The motors move the mobile platform as a seismic testing frame and the acceleration information of the mobile platform is processed through the NI-DAQ 6210 and then visualized with the LabView software.

A suitable Virtual Instrument has been developed in LabView environment to manage the signals coming from sensors. The measured acceleration data from the accelerometers are used to compute the acceleration of the center point H of the moving plate and plate angular velocity, beside monitoring the acceleration of the simulated seismic motion.

Figure 3 An experimental setup of CaPaMan as earthquake simulator at LARM with a slider-crank mechanism.

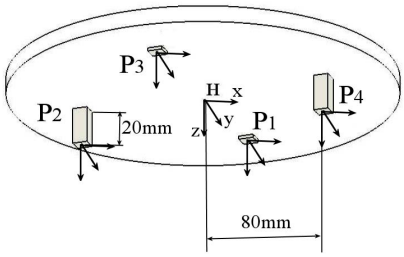

a)

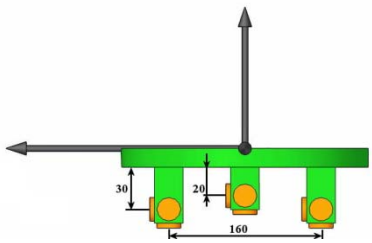

b)

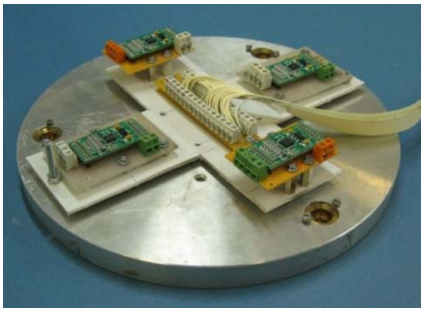

c)

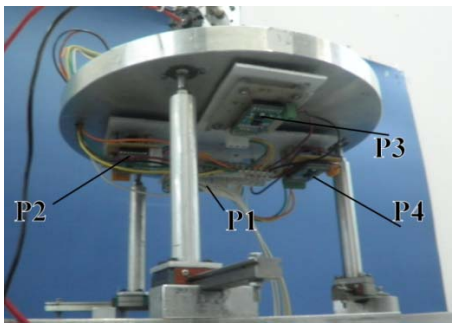

d)

Figure 4 Sensored CaPaMan platform with accelerometers:
a) a scheme, b) sensor locations, c) sensor installation, d) test lay-out.

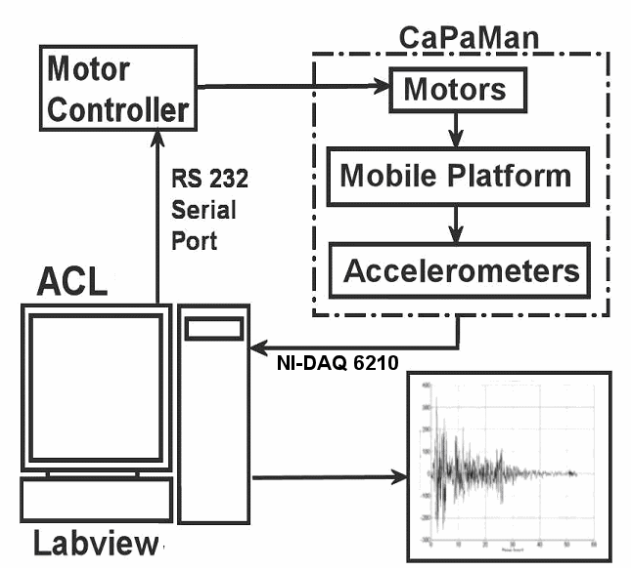

Figure 5 Control system layout for CaPaMan as earthquake simulator.

Two types of earthquakes are simulated for a characterization of earthquake effects on mechanism operation. Characteristic phases of the simulated earthquakes are given in Table I and a reference earthquake that is shown in Figure 6 is used for defining parameters of earthquake characteristics. Type 1 and 2 in Table I refer to typical earthquakes with different time parameters and frequency of motion excitation, as from the mort recurrent events.

Typical values of measured accelerations in simulated earthquake of type 1 are shown in Figure 7.

In order to calculate accelerations and velocities characterizing the seismic effects in an experimental set up an analysis of rigid body motion must be properly formulated as we may suggest in the following. The acceleration of a point P in a rigid body in a position with **r** with respect to a reference frame can be expressed by [17],

$$\mathbf{a}_P = \mathbf{a}_B + \boldsymbol{\alpha}_B \times \mathbf{r} + \boldsymbol{\omega}_B \times (\boldsymbol{\omega}_B \times \mathbf{r}) \tag{2}$$

where acceleration $\mathbf{a}_B$, angular velocity $\boldsymbol{\omega}_B$ and angular acceleration $\boldsymbol{\alpha}_B$ refer to the relative movement of the rigid body frame O_B with respect to the fixed frame O_F. The term $\boldsymbol{\alpha}_B$ x **r** can be described as tangential acceleration and $\boldsymbol{\omega}_B$x($\boldsymbol{\omega}_B$x**r**) is the centripetal acceleration in a rigid node motion.

Table I - The characteristics of simulated earthquakes.

	Total Time (sec)	**ΔT_{max} (sec)**	**ΔT_{min} (sec)**	**Number of oscillations**	**Maximum Frequency (Hz)**
Earthquake Type 1	45	2.0	0.8	30	1.2
Earthquake Type 2	50	2.0	1.5	30	0.8

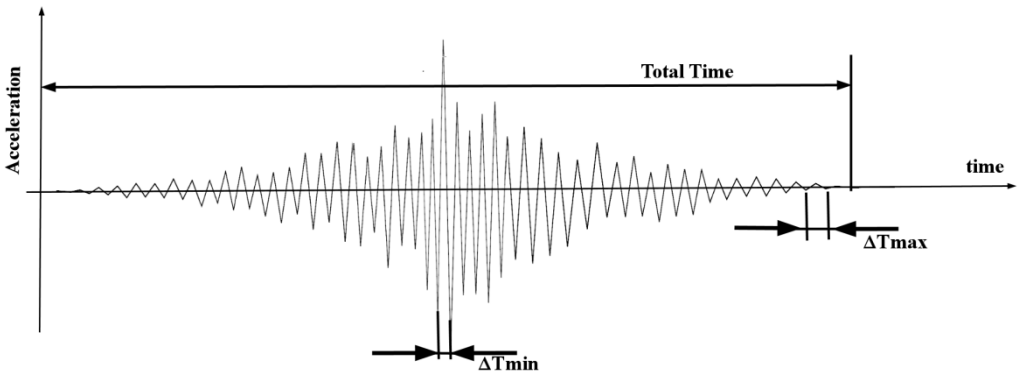

Figure 6 Main characteristics of simulated reference earthquake.

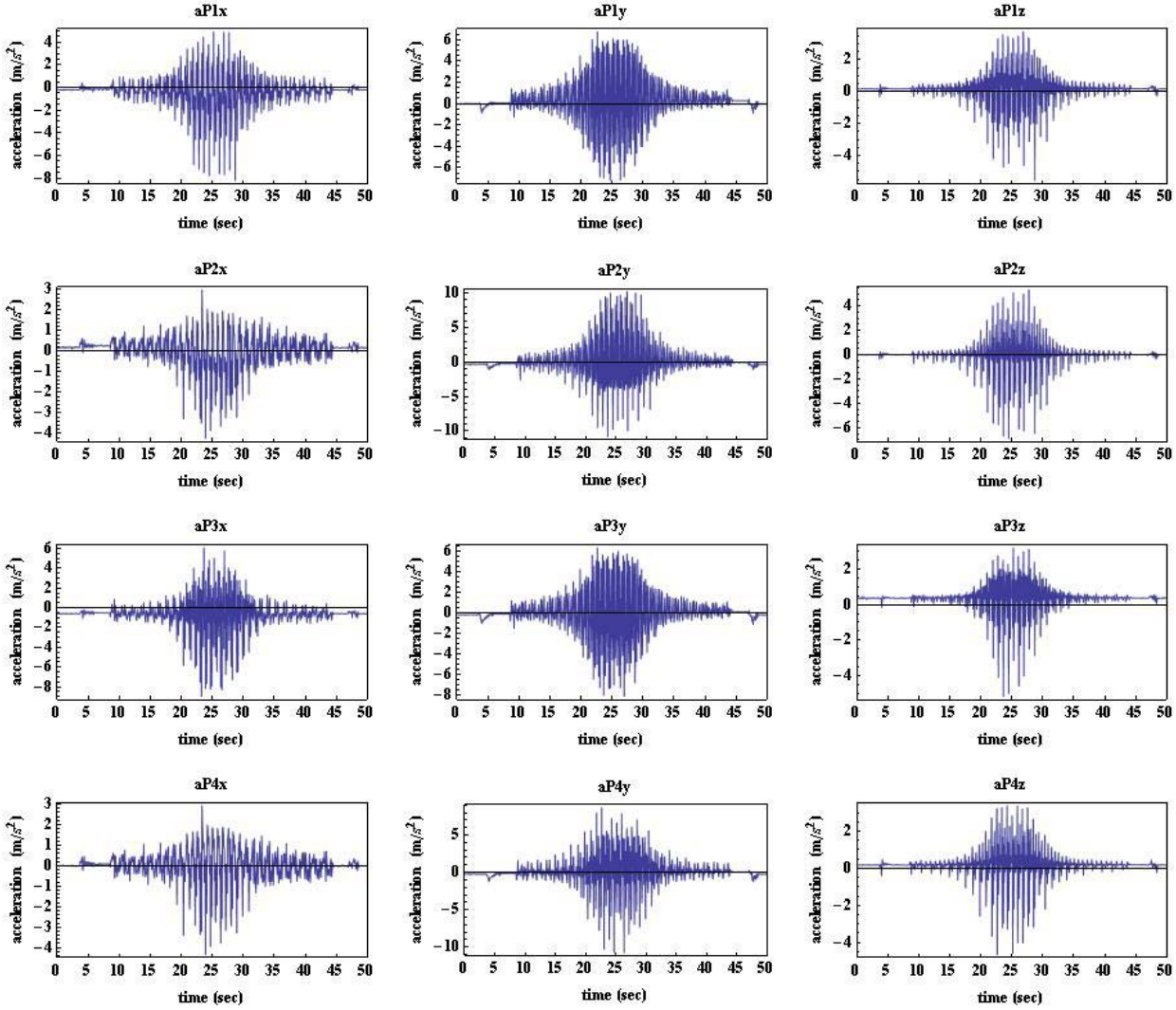

Figure 7 Measured acceleration data during an earthquake simulation as acquired from the accelerometers in the set up of Figure 4.

In order to calculate the acceleration as measured by a sensor that is attached at position $\mathbf{r}$ in the body frame O_B the sensitivity axis $\mathbf{s}$ and the sensors' metrological signal offset $\mathbf{a}_0$ must considered in Eq.(2) to give

$$\mathbf{a}_S = \mathbf{s}^T \left(\mathbf{a}_B + \boldsymbol{\alpha}_B \times \mathbf{r} + \boldsymbol{\omega}_B \times (\boldsymbol{\omega}_B \times \mathbf{r}) \right) + \mathbf{a}_0 \tag{3}$$

Equation (3) can be written in vector form as

$$\mathbf{a}_S = \mathbf{c}\,\mathbf{z} + \mathbf{a}_0 \tag{4}$$

where the vector can be expressed as

$$\mathbf{c} = \left[s_x, s_y, s_z, s_z r_y - s_y r_z, s_x r_z - s_z r_x, s_y r_x - s_x r_y, -(s_y r_y + s_z r_z), \right.$$
$$\left. -(s_x r_x + s_z r_z), -(s_x r_x + s_y r_y), s_x r_y + s_y r_x, s_x r_z + s_z r_x, s_y r_z + s_z r_y \right]^T$$

$$\mathbf{z} = \left[a_{B,x}, a_{B,y}, a_{B,z}, \alpha_{B,x}, \alpha_{B,y}, \alpha_{B,z}, \right.$$
$$\left. \omega_{B,x}^2, \omega_{B,y}^2, \omega_{B,z}^2, \omega_{B,x}\omega_{B,y}, \omega_{B,x}\omega_{B,z}, \omega_{B,y}\omega_{B,z} \right]^T$$

By using four sensors with twelve sensitive axes it is possible to directly compute $\boldsymbol{\alpha}_B$ as well as $\mathbf{a}_B$ and $\boldsymbol{\omega}_B$. In fact, the problem becomes as linear system that can be written in vector form as

$$\mathbf{y} = \mathrm{A}\,\mathbf{z} + \mathbf{a}_{0,S} \tag{5}$$

with $\mathbf{y} = \left[\mathbf{a}_{S1}, \mathbf{a}_{S2}, \cdots, \mathbf{a}_{S12} \right]^T$, $\mathrm{A} = \left[\mathbf{c}_{S1}, \mathbf{c}_{S2}, \cdots, \mathbf{c}_{S12} \right]^T$ and $\mathbf{a}_{0,S} = \left[\mathbf{a}_{0,S1}, \mathbf{a}_{0,S2}, \cdots, \mathbf{a}_{0,S12} \right]^T$.

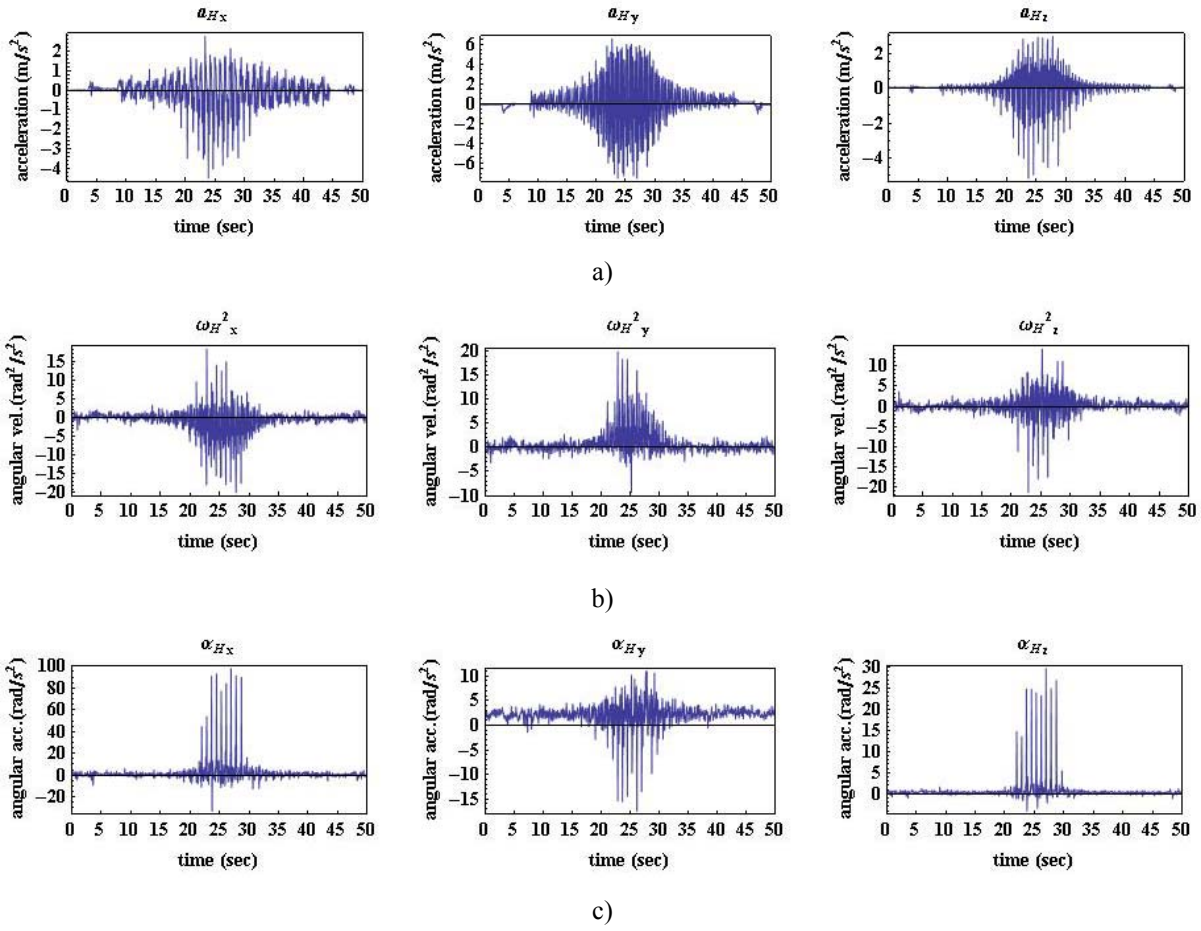

Figure 8 An example of calculated data during an earthquake simulation:
a) acceleration of the platform center H, b) square angular platform velocity, c) angular platform acceleration.

By inverting A it is possible to calculate characteristics of vector **z** of the relative body motion as function of a measured vector **y** by the expression

$$\mathbf{z} = \mathrm{A}^{-1}\left(\mathbf{y} - \mathbf{a}_{0,\mathrm{S}}\right) \tag{6}$$

By using Eq. (6) the linear acceleration $\mathbf{a}_{\mathrm{H}}$, angular acceleration $\boldsymbol{\alpha}_{\mathrm{H}}$, and angular velocity $\boldsymbol{\omega}_{\mathrm{B}}$ can straightforward calculated. An example is reported in Fig. 8 as referring to a simulated earthquake.

5 EXPERIMENTAL SET-UP WITH MECHANISM MODELS AND TEST RESULTS

Experimental tests have been carried out by using a slider-crank linkage with servo motor, a small car model, and LARM Hand as test-bed mechanisms that are sensored with acceleration or force sensors. Maximum acceleration values of the center point H can be used to summarize the earthquake disturbance of the platform motion. Maximum accelerations for the used earthquakes of type 1 and type 2 in performed tests are $a_{h1,max} = 8.4$ m/s^2 and $a_{h2,max} = 5.29$m/s^2, respectively. Experimental data from mechanism sensors during earthquake disturbance are discussed specifically in the next sub-sections for each tested mechanism.

5.1 SLIDER CRANK ACTUATED BY SERVO MOTOR

In Fig. 10a) an accelerometer is shown attached to the slider sensing axis and a torque sensor is used to monitor torque evolution during operation. In Fig. 11.a) and b) plots of torque of the motor and acceleration of the slider are shown for the case without earthquake disturbance when crank rotates at 90 rpm and 180 rpm, respectively. It can be noted that there is a noisy measurements that are very likely caused by backlash of the components assembly and manufacturing tolerances.
In Fig. 12.a) and b) experimental measures of motor torque and slider acceleration are plotted during earthquake disturbance when crank rotates at 90 rpm and 180 rpm, respectively.

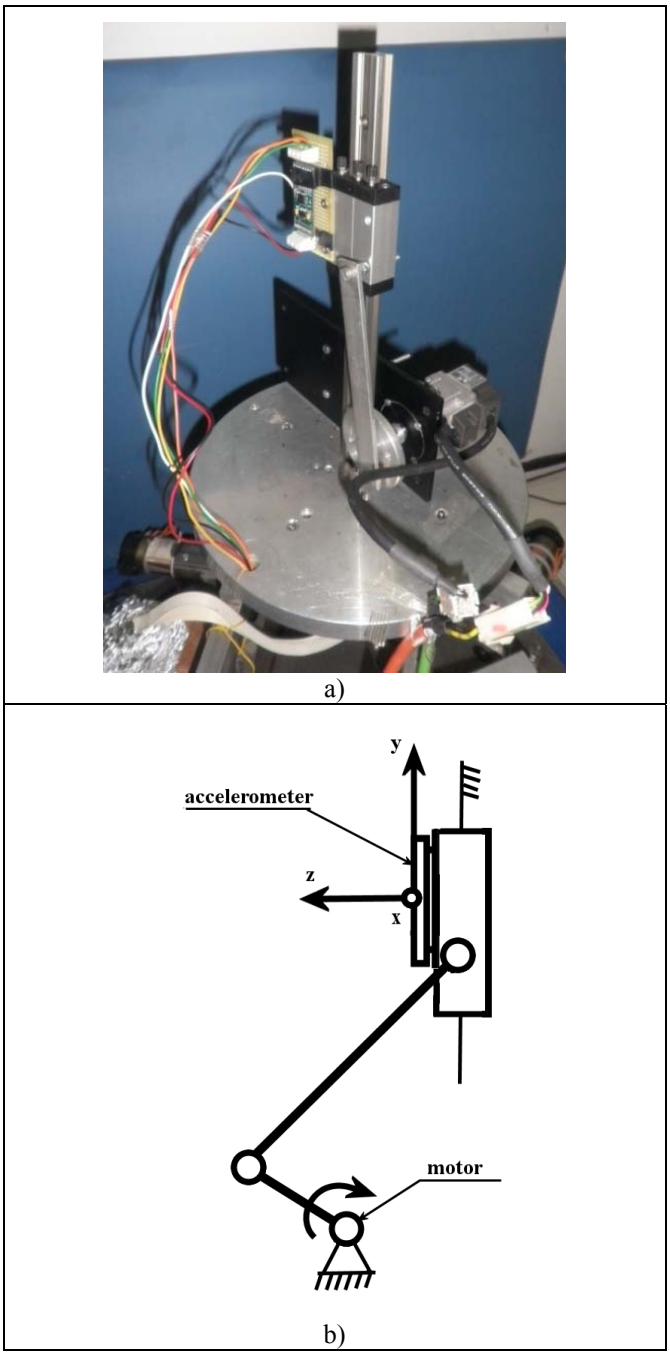

Figure 10 A test-bed slider-crank mechanism with a servo motor: a) an experimental set up with accelerometer on the slider; b) sensing axis of the accelerometer.

It can be noted from acceleration measures of slider in Fig. 12 and in Table II that not only the shape and amplitude of the acceleration of the slider is strongly modified during the simulated earthquakes are but even the oscillations of the slider are almost completely vanished. The torque of the motor shows relatively significant disturbs in amplitude and the shape and oscillation look very similar to the operation in the case of stationary frame with no earthquake.

5.2 LARM HAND

The LARM Hand prototype has been used in this work as test-bed mechanism as a case of study of robotic systems. The LARM Hand in Fig. 13 is composed of three fingers with the aim of performing a human-like grasping by each finger with one DoF motion by using a suitable mechanism [18]. The peculiarity of the finger mechanism design consists in a cross four-bar linkage that during the finger motion remains within the finger body.

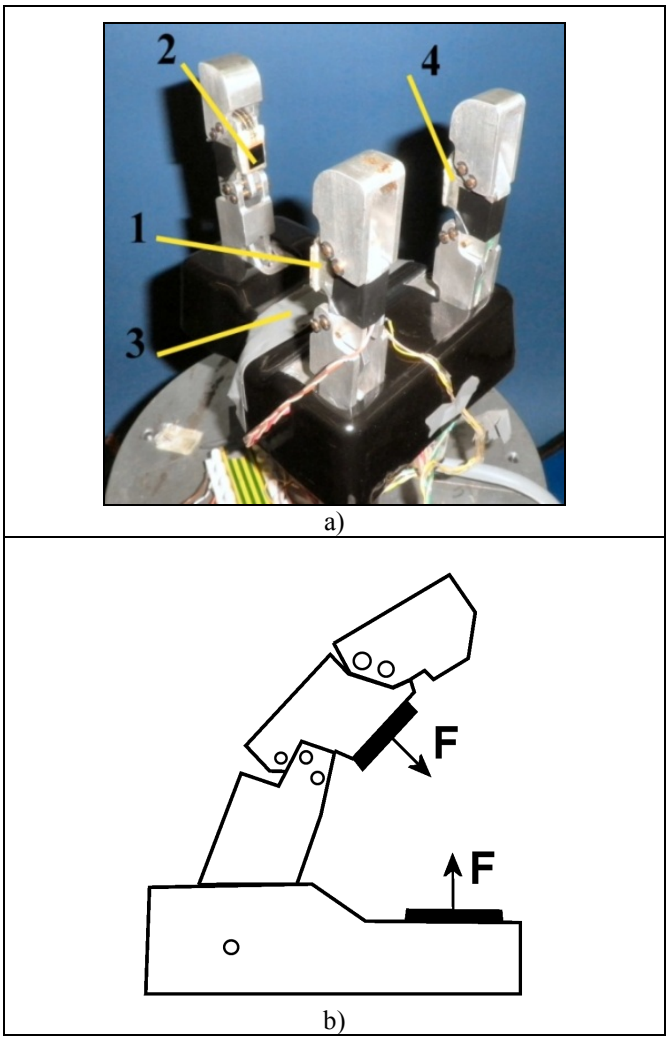

Figure 13 LARM Hand: a) a prototype, b) sensor locations.

Because the linkage design and its one DOF mobility for the finger mechanisms, a grasp can be regulated through a fairly simple control by using force sensor signals and an industrial small PLC for operation. The LARM Hand can be used as a grasping end-effector in robots and automatic systems. Each finger of LARM Hand has 3 joints and 1 actuator. The range of motion for the prototype in Fig. 13 is 40 degree for finger inputs and 140 degree for fingertip links. The used LARM Hand prototype is equipped with 4 force sensors whose range of sensitivities is from 1 to 100 N with a resolution lower than 0.5% of its full scale. The

dimensions of the finger are 1:1.2 of the human finger size and the hand has a volume of 110x240x120 mm where as the size of objects that can be grasped is between 10 to 100 mm. Both types of earthquakes have been tested with LARM Hand during grasping a cylinder block. Results are summarized in Table III for test outputs like the example in Fig. 14.

Table III lists typical forces acting on a tested object during static conditions and during earthquake disturbances. Fig. 14 show plots of forces on gripper fingers and palm with an oscillatory evolution during the earthquake disturbance with a considerable change at the end. These results show clearly that an earthquake strongly affects characteristics of robotic operation such as output force, repeatability of the operation in frequency and efficiency, and reliability of the action in term also of precision accuracy. For the LARM Hand the grasping force efficiency by the fingers can decrease during an earthquake and it can happen the slipping of a grasped object within the fingers. In addition, the applied force to the object can increase at the end of the disturbance and therefore, the object can be even damaged.

5.3 VEHICLE MODEL

Comfort and safety in transportation vehicles is felt by human users mainly in terms of acceleration of the vehicle. Motion and force characteristics describe these properties in vehicles during the run. In general, those characteristics are analyzed under any disturbance which can produce uncomfortable or unsafe operation. But even an earthquake can produce significant risk disturbance both for comfort and safety in vehicle functioning.

For this work a specific vehicle model is designed for characterizing earthquake effects on vehicle operation. The used scaled vehicle model in Fig. 15a) is equipped with a dc motor and installed on a rail. A force sensor and a three axis accelerometer are attached on the vehicle as shown in Fig. 15b). The running of the vehicle is simulated by letting the motor giving the wheel rotation. Due to friction on the wheels from the rail when voltage is applied to dc motor a force is applied on the force sensor as measure of the motion action.

Figure 17 shows plots of pushing force F for test with car model under earthquake disturbance. Comparing those plots with static data shown in Fig.16 it can be noted a relevant change in the car behaviour with significant oscillations.

Details of these changes can be appreciated in Fig. 18 with zoomed views of force data between 20 to 25 seconds of earthquake motion when the seismic accelerations are at maximum. Considering the different voltages applied to motor of the mechanism as reported in Figs. 17 and 18 with the values in Table IV earthquake disturbance seems to affect the car operation in the same way so that change in the wheel action will not help in reducing the disturbs.

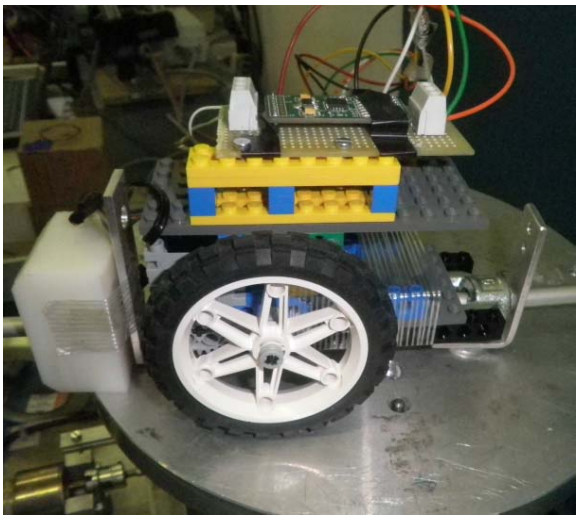

Figure 15 The used scaled car model with force and accelerometer sensors: a) an experimental setup with a LEGO prototype; b) sensors and directions.

Table II - Summary of test results with slider-crank mechanism.

Test measure - Test conditions	**Test data (earthquake frequency – crank rotation speed)**	**Earthquake type 1**	**Earthquake type 2**	**Stationary**
$ay_{max}(m/s^2)$ slider crank mechanism	15kH-90rpm	7.530	4.15	2.508
	30kH-180rpm	11.64	10.81	8.211
	60kH-360 rpm	16.90	16.03	13.97

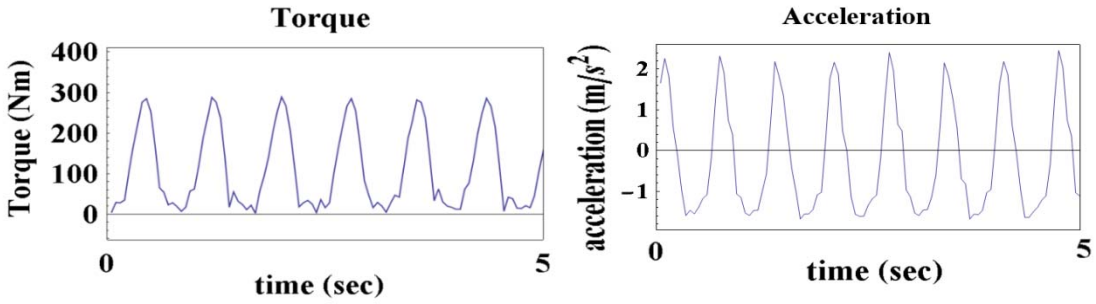

a)

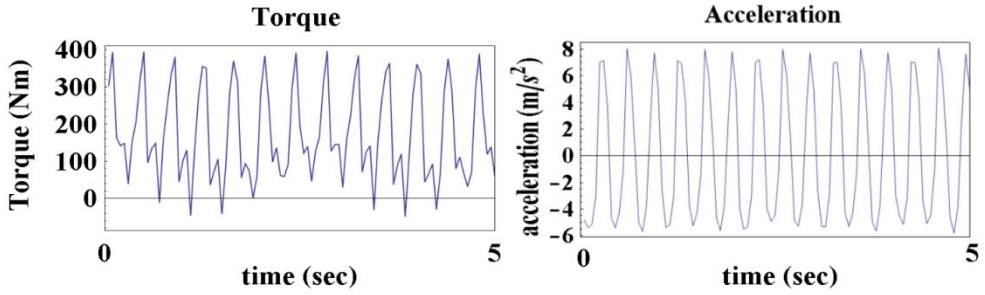

b)

Figure 11 Acquired measurements for a test with slider-crank mechanism in Fig. 10 with no earthquake disturbance: a) torque of the motor and acceleration of the slider with crank rotation 90 rpm; b) torque of the motor and acceleration of the slider with crank rotation 180 rpm.

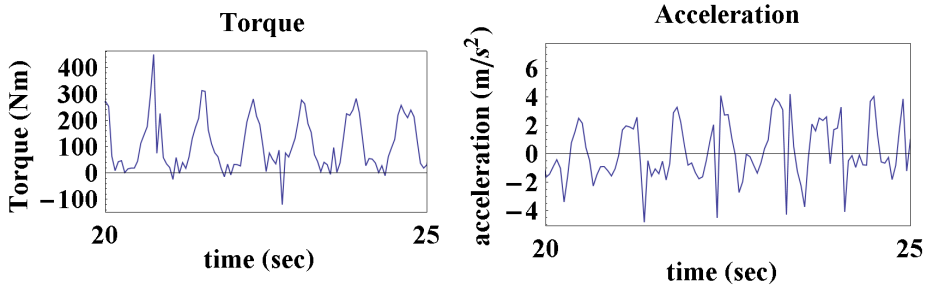

a)

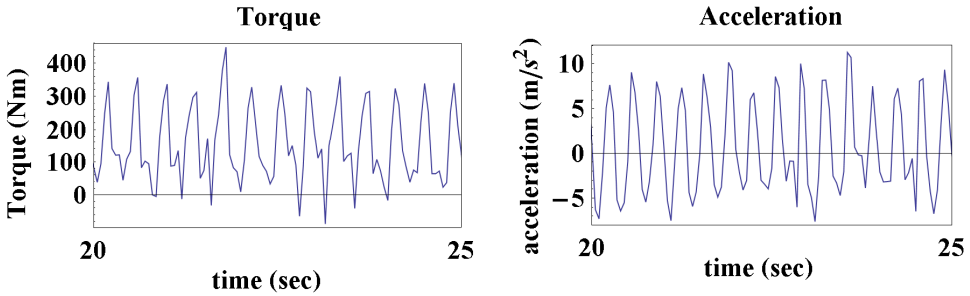

b)

Figure 12 Acquired measurements for a test with slider-crank mechanism in Fig. 10 with earthquake disturbance of type in Table I: a) torque of the motor and acceleration of the slider with crank rotating at 90 rpm, b) torque of the motor and acceleration of the slider with crank rotating at 180 rpm.

Table III - Summary of test results as grasping forces by LARM Hand.

Test measures - Test conditions	Force range	Earthquake type 1	Earthquake type 2	Stationary
Forces F1, F2, F3 and F4 in LARM Hand (N)	Max	2.65, 2.65, 2.53, 2.99	2.23, 2.30, 2.37, 3.10	2.52, 2.57, 2.47, 2.97
	Min	1.9, 1.99, 1.91, 2.25	1.64, 1.73, 1.77, 2.33	1.89, 1.94, 1.86, 2.23

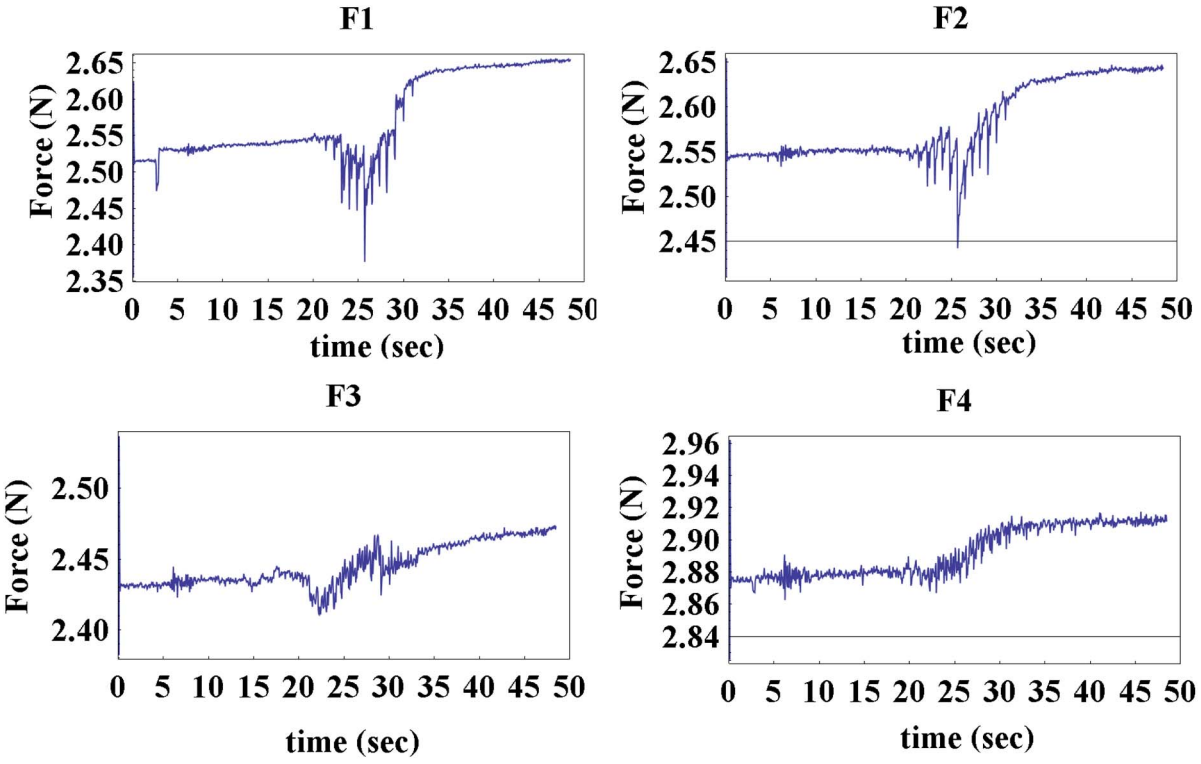

Figure 14 Acquired force measurements for a test with LARM Hand in Fig. 13 with earthquake disturbance of type 1.

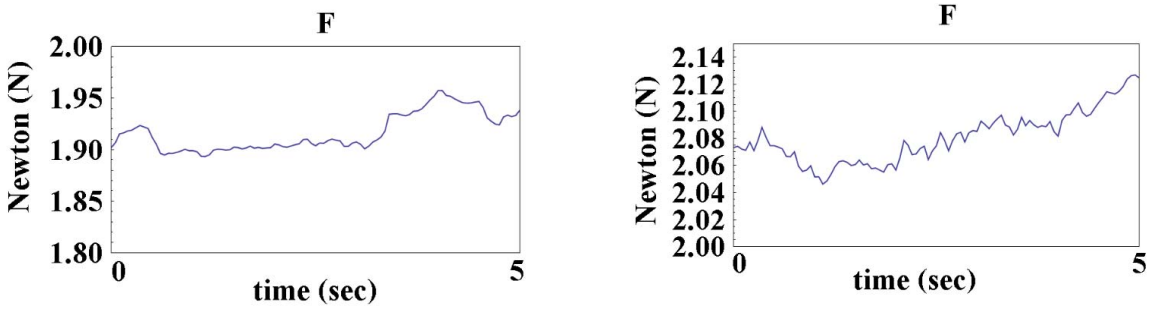

a) b)

Figure 16 Acquired measurements of pushing force F for a test with car model in Fig.15 without earthquake disturbance: a) with applied voltage of 7V; b) with applied voltage of 9V.

Table IV - Summary of test results of pushing forces by scaled car.

Test measures - Test conditions	Force range vs input voltage		Earthquake type 1	Earthquake type 2	Stationary
Pushing force (N)	7v	Max	2.086	2.121	1.980
		Min	1.189	1.604	1.839
	9v	Max	2.102	2.091	1.995
		Min	1.155	0.012	1.95

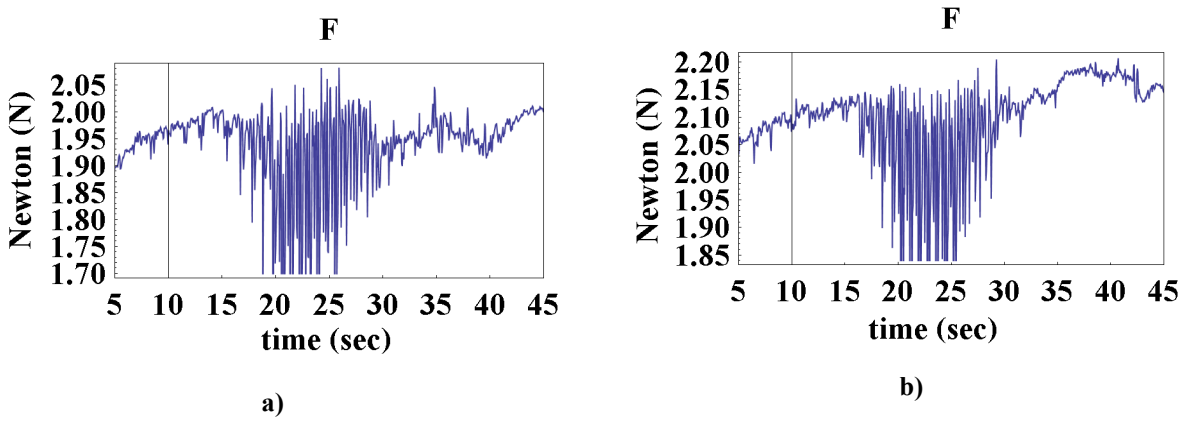

Figure 17 Acquired measurements of pushing force F for a test with car model in Fig.15 with earthquake disturbance: a) with applied voltage of 7V; b)with applied voltage of 9V.

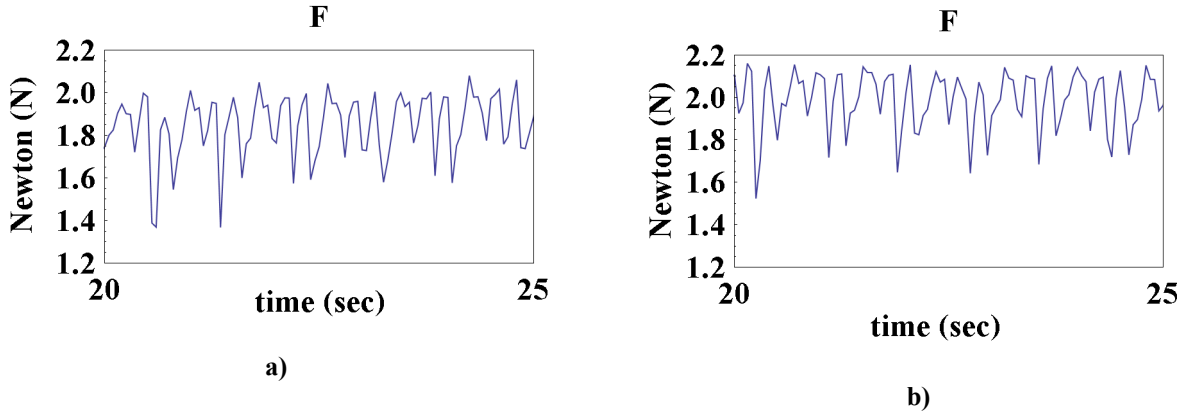

Figure 18 Zoomed views of the acquired measurements of pushing force F for a test with car model in Fig.17: a) with applied voltage of 7V; b)with applied voltage of 9V.

6 CONCLUSIONS

In this work earthquake influence on machinery operation has been investigated by an analysis and reproduction of earthquake motion with the help of CaPaMan. The sensitivity of the operation characteristics of machinery to earthquake disturbance can be characterized in terms of acceleration response and force of the output of machinery operation. Experimental tests have been carried out by using a slider-crank linkage with DC and servo motors, a scaled car model, and LARM Hand as test-bed mechanisms with proper acceleration or force sensors. The results show that an earthquake will strongly affect the acceleration of the mechanism operation both in shape and amplitude of the output motion. Task force of a mechanism affected during earthquake and it is observed that it is left increased after earthquake disturbance.

The results of laboratory experiments on a slider-crank linkage and a vehicle model shows that earthquake disturbance strongly affects the operation of a vehicle such as a train. Therefore increasing speed or force of the input of the vehicle will decrease the effects of unexpected seismic disturbance. Thus, a train operating under an earthquake disturbance should not brake but very likely it should increase the speed.

REFERENCES

[1] J.P. Conte, T.L. Trombetti, Linear dynamic modeling of a uni-axial servo-hydraulic shaking table system. Earthquake Engineering and Structural Dynamics 29 (2000) 1375-1404.

[2] J.L. Kuehn ,D.S. Epp, W.N. Patten, A high fidelity control for seismic shake tables. Proc. 12th Engineering Mechanics Conference, 17–20 May, LaJolla, CA.,1998, pp. 783–786.

[3] A.J. Crewe, R.T. Severn, The European collaborative program on evaluating the performance of shaking tables, Phil. Trans. RoyalSoc. London, Series A, 359-1786, 2001, pp. 1671-1696.

[4] N. Ogawa, K. Ohtani,T. Katayama, H. Shibata, Construction of a three-dimensional large scale shaking table and development of core technology, Phil. Trans. Royal Soc. London, Series A, 359-1786, 2001, pp. 1725-1751.

[5] J.S. Shortreed, F. Seible, A. Filiatrault, G. Benzoni, Characterization and testing of the Caltrans Seismic Response Modification Device Test System. Phil. Trans. Royal Soc. London, Series A359-1786, 2001, pp. 1829-1850.

[6] W.F. Chen, C. Scawthorn, Earthquake engineering hand book, CRC Press, Boca Raton, 2003.

[7] M. Bruneau, A. Reinhorn, M. Constantinou, S.T. Thevanayagam, A. Whittaker, S.Y. Chu, M. Pitman, K. Winter, Versatile shake tables and large-scale high-performance testing facility towards real-time hybrid seismic testing, Proceedings of ASCE Structures Congress, Denver April, 2002.

[8] M. Ceccarelli, F. Pugliese, C. Lanni, J.C.M. Carvalho, CaPaMan (Cassino Parallel Manipulator) as sensored earthquake simulator. Proceedings of the 1999 IEEE/RSJ International Conference on Intelligent Robots and Systems, Kyongiu, 1999, pp. 1501-1506.

[9] E. Ottaviano, M. Ceccarelli, Application of a 3- DOF parallel manipulator for earthquake simulations, IEEE Transactions on Mechatronics 11-2, 2006, pp. 140-146.

[10] J.C.M. Carvalho, M. Ceccarelli. Seismic motion simulation based on CaPaMan simulation, Journal of the Brazilian Society of Mechanical Sciences, 25-3, 2002, pp. 213-219.

[11] M. Ceccarelli., E. Ottaviano, C. Florea, T.P. Itul, A. Pisla, An experimental characterization of earthquake effects on mechanism operation, IEEE-TTTC International Conference on Automation, Quality and testing, Robotics, AQTR 2008,Cluj-Napoca, 2008.

[12] O. Selvi, M. Ceccarelli, Interpretation of Earthquake Effects on Mechanism Operation: An Experimental Approach, Journal of Naval Science and Engineering, 8-2, 2012, pp. 31-45.

[13] W.F. Chen, C. Scawthorn, Earthquake Engineering Handbook, CRC Press, Boca Raton, 2003.

[14] IFToMM 2003, special issue 'Standardization and Terminology', Mechanism and Machine Theory, Vol.38, n.7-10.

[15] J.J. Uicker, G.R. Pennock, J.E. Shigley, Theory of Machines and Mechanisms, Oxford University Press, Oxford, 2003.

[16] Lopez-Cajùn C.S., Ceccarelli M., Mecanismos: Fundamentos cinematicos para el diseno y la optimizacion de la maquinaria, Trillas, Ciudad de Mexico, 2008 (ISBN 978-968-24-8181-9); 2nd Edition 2014.

[17] B. Zappa, G. Legnani, A. J. van den Bogert, R. Adamin, On the Number and Placement of Accelerometers for Angular Velocity and Acceleration Determination, Journal of Dynamic Systems, Measurement, and Control, September 2001, Vol. 123, pp. 552-554

[18] G. Carbone, M. Ceccarelli, Design of LARM Hand: problems and solutions, Journal of Control Engineering and Applied Informatics, 10-2, 2008, pp. 39-46.

ISSN 1590-8844
International Journal of Mechanics and Control, Vol. 16, No. 02, 2015

RFID SYSTEMS FOR RISK REDUCTION IN BLOOD BAGS: A COST-BENEFIT ANALYSIS

Paolo Erminio Maria Teresa Pilloni

Department of Mechanical, Chemical and Material Engineering
University of Cagliari, Via Marengo, 3 – 09123 Cagliari, Italy

ABSTRACT

RFID (Radio Frequency Identification) technology has gained increasing popularity in recent years, both in the field of industrial application and in the services sector. In the latter field, in particular, many applications in the area of hospital logistics have been recently developed. This paper concerns the application of RFID systems to the control of blood bags in hospitals. The work, focused on the economic aspects of the problem, is based on a model for the economic evaluation of RFID systems based on cost / benefit analysis.
Both cases of application of HF and UHF frequencies, and different application scenarios were taken into account, based on the use of RFID in the entire transfusion loop or only to the part of it relative to the end user. The model was then tested and applied to an actual hospital reality of considerable importance from the point of view of blood transfusion. The results obtained in the different test cases were then further analysed through a sensitivity analysis in order to assess the model's response to changes in input parameters.

Keywords: Cost / benefit analysis; RFID systems; Logistic chain; Blood bags; Transfusion medicine

1 INTRODUCTION

Systems based on RFID technology (Radio Frequency IDentification) have gained in recent years a growing diffusion and importance. Their increasing success is largely due to the great number of advantages they present with respect to traditional systems such as, for example, a standard barcode (more memory capacity, read range and device robustness, possibility of more simultaneous and multidirectional readings, etc.).
These advantages have promoted its spreading in various fields of application: control of production lines (for the identification of the piece during production), industrial logistics (for goods tracking and identification), use in libraries (for managing the loans and volumes), etc.

Contact author: Maria Teresa Piloni

Dept. of Mechanical, Chemical and Material Engineering
University of Cagliari
Via Marengo, 3 – 09123 Cagliari, Italy
E-mail: mteresa.pilloni@dimcm.unica.it

Systems based on RFID technology are also used for the origin certification of food products, identification and tracking of paper documents, sensors technology and geolocation (in the field of environmental control, for instance).
Finally, several studies are being recently developed on applications of RFID systems in the health sector: tracing (locating objects in hospitals), tracking of patients and carers and their identification (to reduce errors in identification or administration of therapies, to speed up procedures in intensive care, etc.), collection and management of computer data (with a significant reduction in process time), logistics and drug management, location of patients in the emergency department, managing the process of chemotherapy etc.
In recent years several studies are being carried out, in particular, on the possibility of applying RFID systems to the logistic chain of blood bags in hospitals. Their use would allow to significantly lowering the number of risks in the transfusion chain, bringing considerable advantages in all the stages of the process: donation, transportation of blood bags, validation, storage of blood bags, patient identification, testing, and bag-patient association.

The different technical studies conducted so far have clearly demonstrated the wide possibilities of the application of RFID systems to the transfusion chain and the significant benefits that this would entail, especially in terms of reduction of clinical risk and of processing times.
From the point of view of economic evaluation linked to the introduction of RFID, the classic cost - revenue analysis is clearly not sufficient to completely take into account the potential of the technology in question, which brings into play a number of advantages not easily quantifiable in monetary terms, mainly related to the lowering of clinical risk.
In this sense, it is considered appropriate to use, for this specific application, the typical technical analysis C / B, through which even the non-monetary quantities are taken into account in the economic analysis. For this purpose an economic model based on the cost / benefit analysis for the economic evaluation of RFID systems applied to the case of transfusion medicine was developed, adjusted and validated. The model, based on some average statistic data referred to the European case for the quantification of benefits, was applied to the case of the Transfusion Department of the Hospital Brotzu of Cagliari.
This model and its application are described in this paper.

2 LITERATURE ON THE TOPIC

In agreement with the increasing deployment of RFID systems, the literature on the subject has greatly developed and enhanced too, in recent years. The fields of research are manifold, including both theoretical analysis and applications of a more markedly technical-practical character. The spectrum of topics covered is very wide as well as the number of papers produced: therefore, given the limitations of space, only the most recent and significant works are reported in this paper.
Both the theoretical speculations and the practical applications concern studies on the application of RFID in various fields of application (for which we list only a few quotes for space reasons): green product design [17], pharmaceutical supply chain [67], healthcare service for tracking medical assets [41], hospitals for data treatment [49], monitoring system for ships passenger evacuation [59], apparel retail industry [27], food supply chain [22, 68], warehouse management [9, 33], pallet management [25], traceability in food industry and in general [5, 23], supply chain logistics [22, 13, 61], document management [6, 66, 37], aircraft production processes [36, 40], fashion retailing (especially in recent years) [20, 62, 31], just to name a few.
A large part of this bibliography covers case studies demonstrating both the technical and economic viability and the application potential of RFID systems in specific applications, and how these systems are able to significantly improve the efficiency of the overall system.
To these, many works must be added focused on the development of the technique, often oriented towards the problems of the safety of operation: these are articles of a more close to electronics matrix, which often propose and develop protocols for communication between tag and reader, or innovative algorithms [51, 57].
Part of the reviewed literature focuses on the economic aspects of the application of RFID, and on the attempt to take into account in the economic evaluations also several benefits determined by the introduction of RFID systems, benefits which the traditional economic analysis do not directly consider.
In particular, the bibliography concerning the economic aspects associated with the RFID technology is based on the application of various techniques, among which: AHP (Analytic Hierarchic Process) methods [17], fuzzy logic [50], Monte-Carlo method [50], analysis to draw [18] assessment and analysis of the costs and benefits [67, 27, 9, 32, 60] and cost / effectiveness [59], ABC (Activity Based Costing) methods [25], System Dynamics [19, 39, 20], simulative approaches [47, 56, 3], Markov chains [44, 64].
Coming to applications closer to the case under investigation, and then to the use of RFID in the health field, many articles can be found on the subject, dealing with general aspects; among them deserve to be mentioned: [58], which contains a framework for evaluating the performance of an RFID system in various applications in the field of health, [30], which reports a work aimed at identifying the hospital supply chain in which RFID can obtain the greater efficacy, [45] which shows how RFID can improve patient care supply chain, [54], which shows several case studies, always in the field of health care, in order to highlight and explain the benefits obtainable from the use of RFID; in addition, among the papers focusing on general aspects of RFID applications in healthcare can be included: [29, 24, 65 and 52], all of which consist of a review of RFID in the health field, highlighting problems, benefits and applications, [46, 30 and 45], which explore the limits and possible implementations using RFID in various fields of health (authentication, medication safety, patient tracking, blood transfusion medicine).

We also find [4, 64, 38 and 1] concerning the traceability with RFID systems, [58], which shows the development of an approach for evaluating RFID systems in the field of health; then there are some papers which, always in the health field, focuses on the development of protocols for the problem of security of data stored in the tag ([63, 55 and 43]), then in [12] and [34] the use of RFID for the management of physicians, patients and small clinics is illustrated; still: [44], which describes the traceability of equipment in hospitals, [41], which regards healthcare service for tracking medical assets, [26], concerning the comparison RFID - Bar-code and [42], which focuses on RFID-based systems developed to reduce the risk of incorrect administration of drugs, and then in the field of security: the application in this case covers all phases of the process of drug administration.
Particular attention should finally deserve several articles focusing on the problems arising in the transfusion supply chain: [48, 2, 16, and 53] regarding the issue of risk, [28], which focuses on the proposal of an alternative approach to

decision making, [11] and [15] concerning the application of RFID systems aimed at reducing clinical risk.

From all this vast literature on the theme of the application of RFID to the health sector, it is clear that it is well established without any doubt that RFID can improve the efficiency of all processes, the quality of the health service as a whole and improve the overall security for the patient.
Although numerous articles, as shown, are aimed at healthcare applications and at least as many are dedicated to the economic evaluation of RFID applications through various methods, including the cost / benefit analysis, however, up to our knowledge, no studies have been carried out on the economic evaluation of an implementation of RFID in the supply chain of blood, using systems based on the cost / benefits analysis.
This gap comforted us in the development of this work, together with the consideration that the chain of blood is an application which, from an economic point of view, is particularly suitable to be examined via models based on the C / B and C / E analysis, because of the numerous advantages well-illustrated in [11], many concern not directly quantifiable aspects, therefore not directly quantifiable in an economic analysis with traditional methods, such as, for example, the reduced risk of death for incorrect transfusion, or the risk of contracting diseases, etc.
Based on these considerations, the work described in this article was carried on with a dual purpose: on the one hand to analyse, in general, the possibility of using the C/B method for the economic evaluation of the entire RFID system applied to the blood logistics chain; on the other hand, to evaluate, in particular, in strictly economic terms, the relative economic weight of the various benefits of implementing this technology, with the aim to evaluate which, among other positive aspects, was of greater importance, and so what better justifies its investment.

3 THE BROTZU HOSPITAL AND THE BLOOD SUPPLY CHAIN

The Brotzu Hospital (AOB), located in Cagliari, is the main hospital in Sardinia and admits annually more than thirty thousand patients in its 630 beds.
More than 400 physicians and a little more than a thousand nurses are working in the seven departments of AOB. The Blood Transfusion Centre of AOB is composed of two distinct but closely interlinked structures, the Service of Immunohematology within the Hospital and the Hall of Takings which is located in a separate building. The Service annually manages approximately 50.000 units of blood, of which about 60% comes from imports from other Italian Regions, necessary to cover the high demand of blood for patients suffering from beta thalassemia.
The logistic chain of blood from the donor phase to the final transfusion can be briefly described as follows.
The blood is donated in the taking room, and then it is transported to the collection centre where are also collected the bags from other centres in the province of Cagliari and imported from the rest of Italy and Europe.
Then the separation of the various emo-components takes place through squeezing and centrifugation and interim storage. Tests are conducted in parallel on blood samples associated with each bag; if the result is positive then the bags are validated, otherwise they are eliminated. The bags ready for donation are stored permanently in the blood bank according to the division into RBC (Red Blood Cells), platelets (PT) and plasma (FP), with different storage times depending on the hemoderivate.
In the wards of the hospital the patient identification and the demand for blood components takes place, which requires the performance of at least two tests to determine blood group, AB0 test. Once the request has correctly been made, the communication is sent to the Blood Transfusion Centre for the blood to be sent to the ward. The Chain of Blood final procedure is the transfusion, or administration at the patient's bedside, which requires the correct identification of the patient and the correct association with the requested bag.
The complete transfusion process just described (Blood supply chain), from donation to transfusion to the patient, can be subdivided into two lines, which will be henceforth referred to as "first level" and "second level":

- First Level (Transfusion Loop) includes the steps of the transfusion process in the strict sense, from the request of the blood products in the ward to the end of the transfusion (patient area);
- Second Level: it includes all the steps from the stage of blood donation to the sending of the bag to AOB departments (donor area).

The Figure 1 shows, in a nutshell, the block diagram that illustrates the two levels described above.

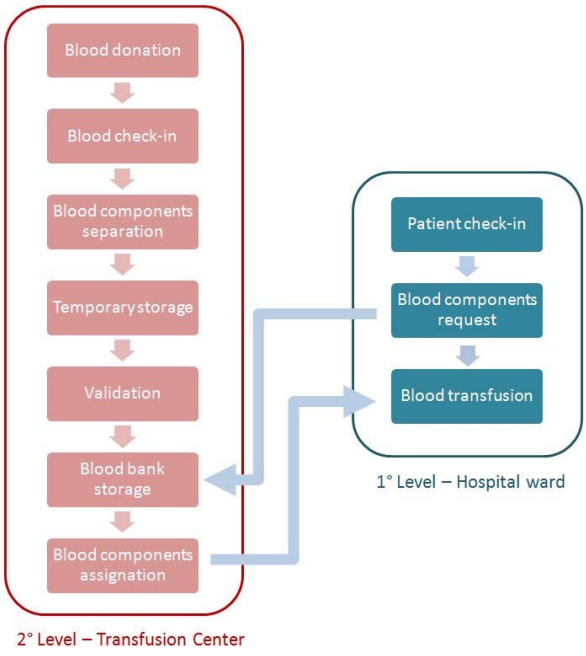

Figure 1 Scheme of the full transfusion process and its subdivision in two levels.

The use of RFID in the transfusion chain could reduce transcription errors and shorten the time of the procedure in the identification phase of the patient in the donations ward. The subsequent transmission to the Collection Centre for the identification and the validation test can be carried out with remarkable speed and a substantial reduction of the risk of human errors, thus obtaining a real-time process control until the storage in the blood bank.
From the point of view of the hospital ward, the RFID allows to quickly identify with virtually zero errors, both the patient and the associated AB0 test tube. With the integration of RFID in a hospital information system, it is possible to significantly reduce the communication time of the request to the Blood Transfusion Centre.
In the blood bank it is therefore possible to manage the inventory in real-time, to select and identify the bag to be sent to the ward, performing the delivery in reduced times, also in this case with a substantial reduction of potential human errors.

The real key point of RFID use is the correct association between the bag and the patient in the ward, reducing the risk of blood group incompatibility, which can also lead to potentially deadly haemolytic reactions.
Several studies have already been carried out at the AOB Haematology Department in order to analyse the possibility of introducing an RFID system for blood bags monitoring (see, e.g. [7]). The results of these studies have been highly encouraging, and such studies should be consulted for any technical details.
In the present study, as already mentioned, the economic aspects of the use of this technology are examined, through a comparison between the costs and the benefits obtained.
Starting from the studies already carried out at AOB, 8 possible scenarios of RFID implementation were developed, characterized by different degrees of RFID application (only in the 1st level or in the 1st and 2nd level), by different types of treated blood (RBC only or all blood types) and frequency band (HF or UHF) (chosen, respectively, the HF for its extensive dissemination and UHF for its promising employment prospects).

Table I – List of the solutions considered in the model.

Solution	Implementation levels	Blood Products	RFID frequency
1	As is	ABP	-
2	1°	RBC	HF
3	1°	RBC	UHF
4	1°	ABP	HF
5	1°	ABP	UHF
6	1° & 2°	RBC	HF
7	1° & 2°	RBC	UHF
8	1° & 2°	ABP	HF
9	1° & 2°	ABP	UHF

In Table I are presented in a concise form the conditions which characterize the 8 scenarios considered (solution 2 to 9). "Solution 1" indicates the current situation, which will then be used only as a term of comparison.
As can be seen from the Table I, the solutions 2 to 5 have a re-engineering only of the 1st level, while solutions from 6 to 9 have both levels 1 and 2 renovated with the use of RFID, and therefore an integrated redesign of the entire hospital transfusion process.

4 QUANTIFICATION OF COSTS AND BENEFITS

For each of the 8 scenarios costs and benefits were evaluated.
The costs were divided in installation costs, incurred at time 0, for the implementation of the RFID system, and in operating costs, which are necessary for the normal system operation once steady-state conditions are achieved.
As far as the benefits are concerned, the three main positive aspects resulting from the use of RFID technology were taken into consideration: clinical risk reduction, blood bags wasting reduction and process time reduction.
For all the scenarios a discount rate of 5% has been selected, a value commonly accepted for the economic analysis in the health care sector.
A time horizon of 15 years was also considered in the analyses carried out, chosen as a compromise between short-term scenarios (under 10 years), fully meeting the rapid evolutionary characteristics of RFID but difficult to achieve in the field of Public Health in Italy, and projects with a duration of more than 20 years, in which the level of obsolescence of the system would be fully evident.

Some parameters of the analysis were considered variable in time. Among these, in particular, the number of blood bags and the number of patients. As regards the former, the initial data were taken from both the 2008 Regional Blood Plan (PRS), based specifically on data retrieved from AOB and AVIS (National Blood Donors Organization), allowing to get the full picture on the basis of the types of blood products employed. On the basis of the data from the 2008 PRS, possible variations in the number of plasma, platelets, regional and imported RBC bags were then conservatively estimated, with a reduction of the latter component. Concerning the type of blood from donations carried out in the Region, annual growth rates were considered resulting in an absolute increase of 20% at the end of the 15 years of the project. For RBC bags imported extra-region, the absolute change was assumed equal to 15%.
The number of AOB patients which may be involved in the transfusion system, was based on the value provided by the AOB itself and reported in [7]. It was assumed, for this parameter, an annual increase of 10% of the patients for the AOB structure at the end of 15 years.

4.1 COST EVALUATION IN THE DIFFERENT SCENARIOS

Installation costs include the costs of hardware, software, infrastructure and development costs. The operating costs include the costs for buying tags, bracelets and barcodes (in solutions of the 2nd level), the hardware, software and infrastructure maintenance costs, and those to be incurred for the annual training of a small number of new operators ("training at tertiary level").

4.1.1 Investment costs

The initial investment costs include the initial hardware: PC, PDA (Personal Digital Assistant), portable RFID reader, massive tunnel readers (devices used for the simultaneous reading of multiple blood bags, required only in the solutions with bank blood), and finally RFID labels printers.

The cost of the software includes: PDA readers software and management software of the blood bank and of the process (related to the 2nd level of implementation).

The infrastructure costs considered include buying the Wi-Fi network and other equipment necessary for the operation of the system.

Development costs consider the costs incurred for the installation and setup of the communication network between the mobile readers and the computer network and of all the fixed devices (routers, antennas, etc.). In the development costs also those incurred for the training of personnel at various levels, differentiated between training costs for management level and for medical department operators, are included.

Table II – Detailed list of initial costs for HF frequency RFID solutions.

		HF							
		2		4		6		8	
		1° Level, RBC only		1° Level, ABP		1° & 2° Level, RBC only		1° & 2° Level, ABP	
	UNIT COST	QUANTITY	COST [€]	QUANTITY	COST [€]	QUANTITY	COST [€]	QUANTITY	COST [€]
HARDWARE									
PC	1.500	15	22.500	15	22.500	18	27.000	18	27.000
PDA	1.800	70	126.000	70	126.000	90	162.000	90	162.000
TUNNEL	8.000	0	0	0	0	1	8.000	1	8.000
PRINTER	2.500	25	62.500	25	62.500	28	70.000	28	70.000
TOTAL			211.000		211.000		267.000		267.000
SOFTWARE									
PDA SOFTWARE	1.000	70	70.000	70	70.000	90	90.000	90	90.000
BLOOD BANK MANAG.	15.000	0	0	0	0	1	15.000	1	15.000
MANAGEMENT SW	2.000	70	140.000	70	140.000	90	180.000	90	180.000
TOTAL			210.000		210.000		285.000		285.000
INFRASTRUCTURE									
Wi-Fi NETWORK	2.500	25	62.500	25	62.500	28	70.000	28	70.000
OTHER COSTS	1.500	0	0	25	37.500	28	42.000	28	42.000
TOTAL			62.500		100.000		112.000		112.000
DEVELOPMENT COSTS									
INSTALLATION	2.000	25	50.000	25	50.000	28	56.000	28	56.000
TRAINING 1	10.000	3	30.000	3	30.000	4	40.000	4	40.000
TRAINING 2	120	120	14.400	120	14.400	150	18.000	150	18.000
TRAINING 3	120	5	600	5	600	7	840	7	840
TOTAL			94.400		94.400		114.000		114.000
TOTAL INVESTMENT COST			**577.900**		**615.400**		**778.000**		**778.000**

Table III - Detailed list of initial costs for UHF frequency RFID solutions.

		UHF							
		3		5		7		9	
		1° Level, RBC only		1° Level, ABP		1° & 2° Level, RBC only		1° & 2° Level, ABP	
	UNIT COST	QUANTITY [IT]	COST [€]	QUANTITY [IT]	COST [€]	QUANTITY [IT]	COST [€]	QUANTITY [IT]	COST [€]
HARDWARE									
PC	1.500	15	22.500	15	22.500	18	27.000	18	27.000
PDA	1.800	70	126.000	70	126.000	90	162.000	90	162.000
TUNNEL	8.000	0	0	0	0	1	8.000	1	8.000
PRINTER 1	5.000	2	10.000	2	10.000	4	20.000	4	20.000
PRINTER 2	3.300	23	75.900	23	75.900	28	92.400	28	92.400
TOTAL			234.400		234.400		309.400		309.400
SOFTWARE									
PDA SOFTWARE	1.000	70	70.000	70	70.000	90	90.000	90	90.000
BLOOD BANK MANAG.	15.000	0	0	0	0	1	15.000	1	15.000
MANAGEMENT SW	2.000	70	140.000	70	140.000	90	180.000	90	180.000
TOTAL			210.000		210.000		285.000		285.000
INFRASTRUCTURE									
Wi-Fi NETWORK DEPLOP.	1.500	25	37.500	25	37.500	32	48.000	32	48.000
OTHER-COSTS	1.500	25	37.500	25	37.500	32	48.000	32	48.000
TOTAL			75.000		75.000		96.000		96.000
DEVELOPMENT COSTS									
INSTALLATION	2.000	25	50.000	25	50.000	32	64.000	32	64.000
TRAINING 1	10.000	3	30.000	3	30.000	4	40.000	4	40.000
TRAINING 2	120	120	14.400	120	14.400	150	18.000	150	18.000
TRAINING 3	120	5	600	5	600	7	840	7	840
TOTAL			94.400		94.400		122.000		122.000
TOTAL INVESTMENT COST			**613.800**		**613.800**		**812.400**		**812.400**

All of these costs have been quantified as reported in Table II and Table III, based respectively on HF and UHF frequency. The costs considered were taken from market values or estimated in a conservative manner.
As for the quantities of the individual elements, they are referred to estimates based on hospital size (specifically, for example, for the PDA, it was based on the number of wards concerned by the implementation), on the size of the processes considered and on information from operators working in the existing structure.
The solutions with full implementation (6,7,8 and 9) have a higher cost compared to those of the 1st level only. In addition, of the two frequencies, the UHF has a higher investment cost, mainly due to the higher cost of the Hardware which exceeds, in solutions 7 and 9, the threshold of € 300.000.
As can be seen from Table II and Table III, in the solutions of 1st and 2nd level, costs are higher because the entire transfusion process is managed, i.e. including also the donation centre and the blood bank, which require additional components, such as the reading tunnels. The larger size of the process to be re-engineered in the second level involves a greater number of materials to be used and of operators to form. The total cost to be incurred in the various alternatives, however, does not differ greatly between solutions of 1st and of 1st and 2nd level when operating costs are considered, as they directly reflect the difference in bags volume between the two levels.

4.1.2 Operating costs

Operating costs basically concern the costs incurred for the purchase of tags, wristbands and, for some solutions, barcodes too. These cost items vary each year as they are directly linked to the number of bags and to the unit cost of the tags, both supposed to change annually.
As for the cost of barcodes, tags, bracelets, etc., reference was made to the values reported in [8].
Also the cost of RFID tags and bracelets has been hypothesized to change annually, considering a progressive reduction of the purchase price, because of an expected spread of tags diffusion and a consolidation of the technology.
The magnitude of these changes was conservatively estimated in a value of 1,5% per annum, with an absolute variation of the purchase price equal to approximately 20% in 15 years of the project. For the two types of tags, HF and UHF, the same purchase price variation are considered.
The difference in cost of a single tag for the two frequencies is not very marked (there was no desire to overestimate the benefits in the use of UHF); however, due to the number of tags used and the time horizon of the project, the total cost differences between the two technologies are substantial.
The following table shows the unit costs considered for the tags, bracelets and barcodes, the estimated annual rates of variation for different purchase prices and finally the fields of variation assumed in the sensitivity analysis.

Table IV – Unit costs [€/u] assumed for tags, wristbands and barcodes for HF and UHF technologies.

		Initial cost	Annual cost ratio
HF	Wristbands	2	-1,5%
	Tag	0,2	-1,5%
	Barcode	0,01	0,0%
UHF	Wristbands	1,8	-1,5%
	Tag	0,18	-1,5%
	Barcode	0,01	0,0%

The purchase price of the UHF tags has been estimated to be less than that of the HF frequency transponder.
For labels and barcodes, used in limited cases of the project, no annual variations were assumed, both because their influence in the analysis is decidedly limited, and for the high diffusion of this technology, which ensures a substantial stability in the purchase cost. The use of barcodes was limited to the identification of the tubes to be used in the TC (Transfusion Centre) laboratory analysis.
The costs of tags, bracelets and barcode must be increased of the costs incurred for the maintenance of hardware and software (conservatively estimated as equal to 2% of the initial investment cost and constant in the 15-year estimated life of the project), as well as the network and its devices, for fixed and mobile communications.
It must also be added the costs for the regular annually training of personnel required to integrate operators coming from other structures; in the model this item was indicated as 3rd level training.
Ultimately, the operating costs of maintenance and annual training are constant in the 15 years of the life of the project.
The following two tables (one referred to the solutions employing HF frequency, Table V, and the other to the solutions based on UHF technology, Table VI) show in detail all the constant items in operating costs, independent of the number of bags or patients.
The number of tags required for each solution was calculated considering the number of bags handled, in particular taking into account that, from a single donation bag (bag mother), satellite bags are also obtained as a result of the separation of blood components. As the distribution of mother and satellite bags varies according to demand, a subdivision of the totality of the bags mothers was assumed, thus obtaining a higher and conservative operating cost.
The number of wristbands required depends on the statistics on the number of patients and donors that refer to AOB. The total number of both categories was supposed variable over time, with an annual growth rate of 0,6%, therefore the cost to purchase the bracelets varies annually.

Table V – Constant items of operating costs for HF frequency solutions.

	HF			
	2 1° Level, RBC only COST [€]	4 1° Level, ABP COST [€]	6 1° & 2° Level, RBC only COST [€]	8 1° & 2° Level, ABP COST [€]
HARDWARE				
TOTAL HARDWARE COST	211.000	211.000	267.000	267.000
HARDWARE MAINTENANCE (2% TOTAL COST)	4.220	4.220	5.340	5.340
SOFTWARE				
TOTAL SOFTWARE COST	210.000	210.000	285.000	285.000
SOFTWARE MAINTENANCE (2% TOTAL COST)	4.200	4.200	5.700	5.700
INFRASTRUCTURE				
TOTAL INFRASTRUCTURE COST	62.500	100.000	112.000	112.000
INFRASTRUCTURE MAINTENANCE (2% TOTAL COST)	1.250	2.000	2.240	2.240
TRAINING COSTS				
3° LEVEL TRAINING	600	600	840	840
MAINTENANCE & 3° LEVEL TRAINING COSTS	**10.270**	**11.020**	**14.120**	**14.120**

Table VI – Constant items of operating costs for UHF frequency solutions.

	UHF			
	3 1° Level, RBC only COST [€]	5 1° Level, ABP COST [€]	7 1° & 2° Level, RBC only COST [€]	9 1° & 2° Level, ABP COST [€]
HARDWARE				
TOTAL HARDWARE COST	234.400	234.400	309.400	309.400
HARDWARE MAINTENANCE (2% TOTAL COST)	4.688	4.688	6.188	6.188
SOFTWARE				
TOTAL	210.000	210.000	285.000	285.000
SOFTWARE MAINTENANCE (2% TOTAL COST)	4.200	4.200	5.700	5.700
INFRASTRUCTURE				
TOTAL	75.000	75.000	96.000	96.000
INFRASTRUCTURE MAINTENANCE (2% TOTAL COST)	1.500	1.500	1.920	1.920
TRAINING COSTS				
3° LEVEL TRAINING	600	600	840	840
MAINTENANCE & 3° LEVEL TRAINING COSTS	**10.988**	**10.988**	**14.648**	**14.648**

4.1.3 Total costs analysis

The total discounted costs, divided into the two components of investment costs and operating costs, are shown in Figure 2 for the 8 projected scenarios.

It can be seen that the solutions for a total use of RFID in the process (solutions 6-9 1st and 2nd level) have a much higher cost than those of corresponding level 1 only, with increases in the range 67 ÷ 77%, with the maximum value for the pair of solutions 4-8. It therefore appears significant the difference in total cost for solutions which also manage the 2nd level because of the significant impact of the operating costs, mainly for the purchase of bracelets and tags. On the contrary, the increase of the initial investment costs, in the passage from solutions of 1st to 1st and 2nd level, is decidedly limited when compared with the operating costs.

4.2 BENEFITS QUANTIFICATION

As already mentioned, the main benefits considered in this first phase were the reduction of clinical risk for mortality from AB0 incompatibility, waste reduction and savings of time in the process, leaving more positive items, such as, for example, the quality perceived, to a next level of detail of the project.

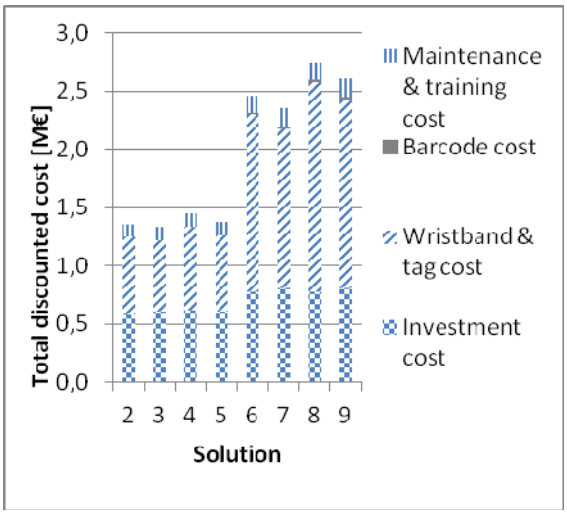

Figure 2 Division of total cost in initial investment cost and operating costs.

4.2.1 Reduction of clinical risk

One of the benefits expected from the use of RFID in the transfusion sector is a reduction of the clinical risk, in particular that of an incorrect association patient-bag of blood, whose main effect is the haemolytic reaction AB0 which, in approximately 10 % of cases, can be lethal [21].
The statistics on the risk of AB0 incompatibility reported very different values depending on the health care system to which they relate, on the technologies employed and methods used to assess the clinical risk. It was decided therefore to use a mean value between the two extremes that can be found in Europe [2]: maximum risk value: Germany, 1/36.000, minimal risk value: France, 1/135.207.
The coefficient 0,1 was added in order to consider the incidence of mortality from acute haemolytic reaction. The value chosen for the calculation, 1/85.603,5, was obtained as an average between the two values above.
In the present study benefits for temporary or permanent damage in transfused patients were not considered. In the first case due to lack of reliable data on compensation, in the second case because the work was concentrated on AB0 incompatibility, the main problem related to the exchange of bags.

In the absence of reliable data about the risk reduction with RFID in transfusion monitoring structures, studies of massive and intensive application of the barcode system or in systems similar to RFID were considered (in particular, the studies [16] and [53]), according to which an advanced system for the identification and management of the entire supply chain of the blood bags can lead to an increase in the safety of blood transfusions of the order of 90% or greater; it is then possible to attain a risk reduction of up to an order of magnitude, that is, with a procedure 10 times less risky for the patient subjected to transfusion. This result is achievable with analogous association of bag-patient-donor systems, or with extensive use of process information technology and barcode technology.

Although RFID allows to obtain and overcome these results obtainable with analogous systems and barcode, for the calculation a precautionary value of the security increase equal to 90% was chosen in the case of implementation in the whole blood chain, that is, for both levels 1 and 2.
Concerning the estimate of the risk reduction in the solutions of level 1only, reference is made to the study of Linden [35]. It shows that the total number of handling errors for the RBC type, not due to the blood bank, amounts to approximately 56%. As in the solutions of the first level, the use of RFID from the blood bank is not foreseen, it was therefore assumed a 50% reduction of the effectiveness from the maximum value obtained in the 1st and 2nd level.
Therefore, having chosen a 90%, increase of security for the 1st and 2nd levels, a value equal to half, 45%, for the solutions of the first level is found.
In both cases were therefore chosen two conservative values of the reduction of the risk compared to the possible performance obtainable from RFID systems.

For the CBA this lower risk determines an avoided cost for the structure and for the NHS (National Health System) which should pay the compensation to the families.
The extreme values of the compensation were taken from the data of the Milan court, assuming the average value between € 130.000 and € 1.6 million, the highest value reported for these cases in 2012. These compensations applies only to the case of mortality occurred as a result of a transfusion.
Not all of the claims, however, arrive at a positive judgment for the patient, usually after 10 years of proceedings. In the Region of Tuscany, for example, only 14,72% of the claims against the NHS was paid in 2003-2008, a value similar to those reported in 2002 by CINEAS (University Consortium for engineering in insurance) [14]. For this reason the benefit of compensation is conservatively underestimated, considering only 15% of the value of compensation. The result is a hypothetical value of the compensation amounting to € 129.750.

In Figure 3 the number of avoidable deaths in the various solutions are shown.
The security increase of the process is present both in the transition from RBC to ABP, and in the transition to solutions also including the implementation of RFID in the hospital CT (1st and 2nd level). The increase in security achieved exceeds the "psychological" threshold of a mortality averted during the 15 years of the project only in the solutions 8 and 9 (all blood types, 1st and 2nd level), with an efficacy approximately 3 times higher than that obtainable in solutions 2 and 3 (only RBC, 1st level).

4.2.2 Waste reduction

The reduction of waste is considered as a benefit in the solutions of levels 1 and 2 only, because only in level 2 a blood bank computerized with RFID systems is set up to manage the bags in order to reduce waste. The benefits are also due to the reduction of false negatives, to the fewest bags past its use-by date and to a better management of the existing stock on the basis of the donations occurred.

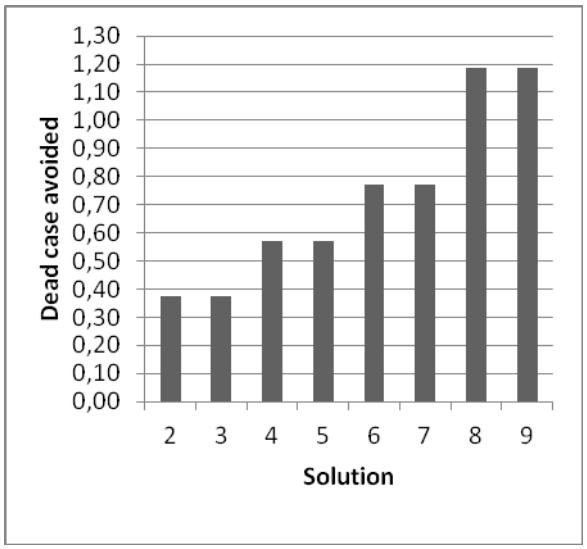

Figure 3 Number of deaths avoided over 15 years in various solutions.

The quantification of the benefit is based on the current efficiency percentage, assuming a process efficiency increase, due to the RFID introduction, equal to 3,5% according to information obtained by direct discussions with the sector operators and according to [7].
As a calculation choice, not being known specific sources on platelets and plasma bags, the value of increase in efficiency was assumed identical for all three types of blood.
The main benefit from the smaller number of expected waste is due to the cost avoided by the elimination of the bag before it has carried out the function for which it is intended. The cost of the bag refers to the infrastructure, personnel and all entries that have created added value, following the voluntary personal donation. The value of the bags was calculated starting from the value reported in [7], and updating it with the value 1,205 (ISTAT coefficient for December 2013).
As shown in the Table VII, also other medical assets bearing a cost related to the process were also included in the calculation, therefore a reduction of waste would involve directly their associated savings.

Table VII – Actual and estimated economic values of the bags and other associated assets.

		Sicilian Region, 2004		Estimated, 2013	
		Regional	Extra regional	Regional	Extra regional
Blood products	RBC	€ 129,76	€ 153,00	€ 156,36	€ 184,37
	FP	€ 20,00	€ 20,00	€ 24,10	€ 24,10
	PL	€ 115,00	€ 115,00	€ 138,58	€ 138,58
Assets	Consumables	-	-	€ 0,10	€ 0,10
	Medical disposables	-	-	€ 3,00	€ 3,00

Each not discarded bag can be considered as a not wasted value of the structure, a saving which, in the differential analysis with respect to the current situation, can be considered as a revenue in the CBA. The total value of revenues is then obtained by multiplying the waste avoided each year by the value of the bags considered constant in the 15 years.

As the reduction of waste was assumed only for the 1st and 2nd level solutions, in the Figure 4 only the solutions from 6 to 9 are shown, i.e. those in which the re-engineering of the blood bank is included in the process.

In this case there are no differences in efficiency in the use of tags with HF or UHF frequency, therefore the only variable that changes the result of the expected deviation is the amount of bags handled, which varies greatly between ABP and RBC only.

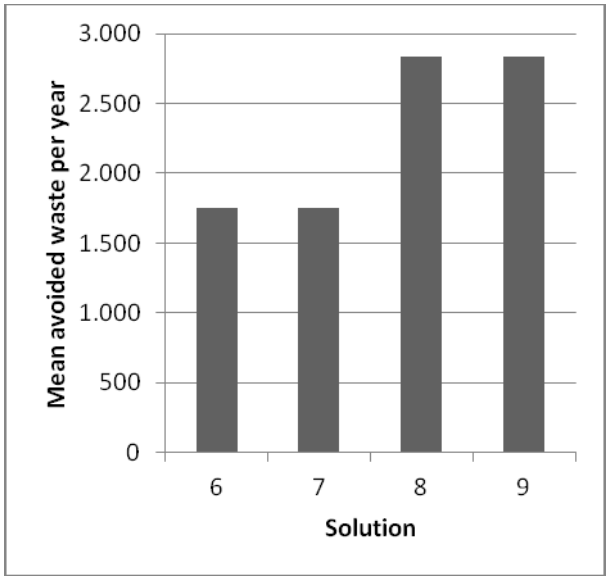

Figure 4 Average number of not discarded bags per year in the 1st and 2ndlevel solutions.

4.2.3 Time savings

In order to perform a more complete analysis, the quantification of the benefits arising from time savings obtainable in various stages of the process has been introduced (see [7]), considering the operations carried out by doctors, nurses, laboratory technicians and auxiliary workers (for the transportation). The average wages for each category, as indicated in the National Collective Work Labourcontracts (CCNL) was reported in €/min, and then multiplied by the number of bags produced in the process.

The Table VIII shows changes in the cycle timing considered.
The hemocomponents separation phase was considered as not affected by the use of RFID as they are not included in such operations. As can be seen from the table 8, not all of the operations have reduced process times and some were assessed as slightly pejorative (negative values) compared to the current situation (in terms of time).

The values of time for each phase have been assumed on the basis of the information provided by the operators of the hospital [8]; all estimates have been made in conservative terms.
By multiplying the time savings and the delays by the corresponding operator salary, the economic benefit (or loss) can be obtained, then all the various contributions can be added to find the overall result in the two hypothesized levels.
In the last two columns to the right it is possible to see how in the first level the cases involving the blood bank (blood donation and acceptance) were not considered, while they are fully covered in the second level of implementation.

Table VIII – Cycle time modifications considered for the different operator categories and process phase.

Process phase	Operator	Cycle time [min/cycle]	Salary [€/min]	Economic benefit [€/cycle] 1° level	2° level
Blood request	Physician	0,5	0,4	0,2	-
	Nurses	1,5	0,25	0,375	-
	Lab Technicians	0	0,25	0	-
	Auxiliaries	0	0,12	0	-
Blood transfusion	Physician	0	0,4	0	-
	Nurses	-1	0,25	-0,25	-
	Lab Technicians	0	0,25	0	-
	Auxiliaries	0	0,12	0	-
Whole blood donation	Physician	0	0,4	-	0
	Nurses	-2	0,25	-	-0,5
	Lab Technicians	0	0,25	-	0
	Auxiliaries	0	0,12	-	0
Whole blood check-in	Physician	0	0,4	-	0
	Nurses	0	0,25	-	0
	Lab Technicians	2,5	0,25	-	0,625
	Auxiliaries	0	0,12		0
Blood components assignation	Physician	0,05	0,4	0,02	-
	Nurses	0,25	0,25	0,0625	-
	Lab Technicians	0,2	0,25	0,05	-
	Auxiliaries	0	0,12	0	-
Blood components check-out	Physician	0	0,4	0	-
	Nurses	-0,5	0,25	-0,125	-
	Lab Technicians	0	0,25	0	-
	Auxiliaries	0	0,12	0	-
Total economic benefit				0,3325	0,125

In order to obtain the economic benefit the number of bags in the first and second level was multiplied for a coefficient respectively equal to € 0,3325 and € 0,125 (coefficient obtained as a product of time per cycle multiplied for the salary per minute).
In the 2nd level the RBC bags from outside the region are not considered because they are not attributable to savings being blood samplings made outside the hospital structure.
Although the time reduction may be at first sight regarded as not very significant, as the saving in the case of the first level is of only 1 minute and 1.5 minutes for the complete implementation, it assumes a great importance when it is multiplied by the number of bags managed with RFID in the various solutions.
As far as the productivity increase calculation is concerned, it was performed separately for the levels 1 and 2, subsequently adding up the two in order to obtain the total value. In solutions of level 1 (solutions 2-5) the value of the benefit for the part relating to the 2nd level is zero.

4.2.4 Total quantification of cba benefits

As illustrated, all benefits have been converted on a common monetary basis for each year of the project. The three benefits were calculated separately, by calculating the total economic value for each period and discounting the cash flows.
The calculation was performed both for the three types of blood (RBC, plasma, and platelets), and for the other elements of consumables and medical devices associated with individual bags.
Figure 5 summarizes the results obtained from the benefits calculation.

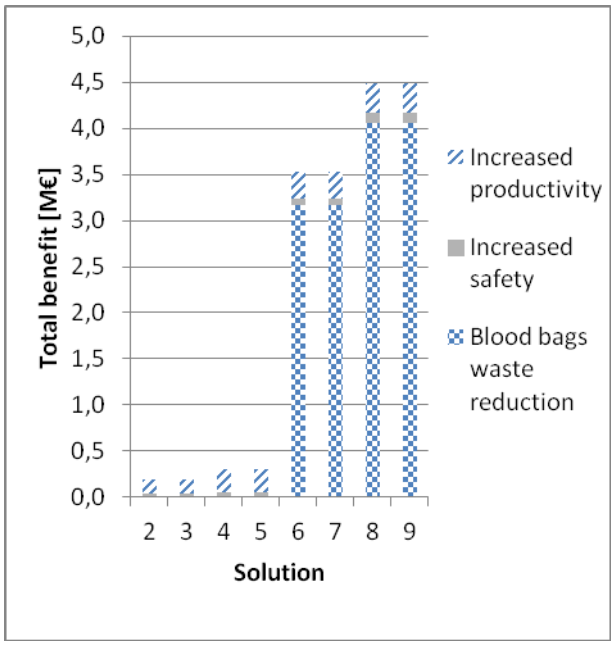

Figure 5 Total economic benefits subdivided in the 8 different solutions.

It is possible to observe that there exists a considerable disproportion between the economic benefit of reducing waste compared to the other two benefits considered: the gap is of an order of magnitude compared to the increase of productivity, and even of two orders in the case of the safety increase of clinical risk.
It also appears clearly that there is a strong imbalance in the economic benefits derived from the solutions of the first level and those with full implementation of RFID. In fact, although the bags have a very low and even insignificant value compared to the scale of compensation for mortality, their number is several orders of magnitude greater than the number of adverse events avoided. Instead, we can appreciate how in the solutions of the first level, the magnitude of the benefit of increased productivity prevails over the reduction in mortality.

After the quantification of all the benefits in monetary terms and of the costs of the various solutions, several indicators were calculated in order to assess the economic quality of the various investments.

5 RESULTS

On the basis of the benefits and costs calculated as described in the previous paragraphs, the calculation of the cash flows was performed, over the 15 years of life expected for the project and for the different solutions considered, thus forming the basis for the calculation of the economic indicators used in the economic analysis: NPV, ROR, Pay-Back Time (PBT) and benefit/cost ratio (B/C), all calculated at i=5%.
The results of the economic calculation are shown in the following summary Table IX, where for each year and for the different scenarios are reported the values of progressive discounted NPV. Table IX also shows the values of all the calculated economic indicators.

Table IX – Results of the economic analysis.

Economic Indicator	Year	Solution							
		2	3	4	5	6	7	8	9
NPV	0	-577.900	-613.800	-615.400	-613.800	-778.000	-812.400	-778.000	-812.400
	1	-620.695	-652.183	-652.876	-645.873	-579.378	-603.537	-513.345	-535.525
	2	-660.994	-688.325	-687.999	-675.895	-389.411	-403.908	-259.690	-270.339
	3	-698.940	-722.355	-720.909	-703.992	-207.703	-213.084	-16.565	-16.332
	4	-734.668	-754.394	-751.739	-730.279	-33.878	-30.658	216.479	226.982
	5	-768.307	-784.558	-780.614	-754.866	132.422	143.757	439.873	460.067
	6	-799.976	-812.953	-807.651	-777.856	291.538	310.530	654.027	683.369
	7	-829.789	-839.682	-832.962	-799.346	443.796	470.014	859.335	897.311
	8	-857.853	-864.841	-856.650	-819.428	589.505	622.542	1.056.174	1.102.300
	9	-884.269	-888.520	-878.813	-838.188	728.962	768.434	1.244.902	1.298.722
	10	-909.132	-910.804	-899.544	-855.707	862.448	907.992	1.425.864	1.486.947
	11	-932.531	-931.775	-918.930	-872.060	990.231	1.041.506	1.599.389	1.667.329
	12	-954.552	-951.507	-937.053	-887.320	1.112.567	1.169.251	1.765.793	1.840.207
	13	-975.273	-970.073	-953.989	-901.554	1.229.700	1.291.489	1.925.377	2.005.903
	14	-994.770	-987.539	-969.810	-914.825	1.341.862	1.408.469	2.078.428	2.164.726
	15	**-1.013.114**	**-1.003.970**	**-984.586**	**-927.192**	**1.449.276**	**1.520.431**	**2.225.223**	**2.316.971**
PBT		**> 15**	**> 15**	**> 15**	**> 15**	**4,19**	**4,17**	**3,07**	**3,06**
ROR		**-**	**-**	**-**	**-**	**26,41%**	**26,55%**	**35,98%**	**35,98%**
B/C		**0,16**	**0,16**	**0,23**	**0,24**	**1,70**	**1,76**	**1,98**	**2,07**

As can be noticed, positive values of the cash flows are obtained only for the solutions that implement RFID also in the 2nd level of the Blood Chain; vice versa the solutions that operate only on the 1st level result, from the economic point of view, are not advantageous.
This result is confirmed by the ROR indicator, which is defined only for the solutions 6-9, with higher values in the last two alternatives. The order of magnitude of the indicator ROR may appear high when compared with the classical values for the economic analyses of other investments; however, it is fully within the range of the CBA analysis of service companies. (see [10]).

Concerning the PBT, the solutions achieving the best performances are the 8 and 9; however, even 6 and 7, both with full RFID implementation, attain similar overall results. All solutions of 1st level instead are not able to guarantee a return on investment within the 15 years of the project life.
Finally, the most important indicator for the CBA, the B / C ratio, confirms what was above said and indicates solutions 8 and 9 as the most attractive, followed by the solutions 6 and 7, both valid in allowing B / C ratio higher than unit. All 1st level solutions instead fail to get B / C higher than unit, therefore no economically valid solutions result from the CBA analysis.
A better view of what has been said can be obtained from the Figure 6, in which the evolution of the various progressive VAN computed for the 8 solutions is represented.

The difference of economic attractiveness between the solutions of 1st and of 1st and 2nd level appears clearly; the main reason for this may be sought in the weight which the waste reduction has played in the calculation of benefits.
The Figure 6 also highlights significant differences between the RBC and ABP solutions in the case 1st+2nd level, and how the differences between the solutions of the first level are decidedly small.
Concerning the frequency of the RFID systems used, only for applications of 1st+2nd level there are, for the indicators calculated, appreciable differences between HF and UHF, with a slight (<10%) economic benefit to the latter frequency.

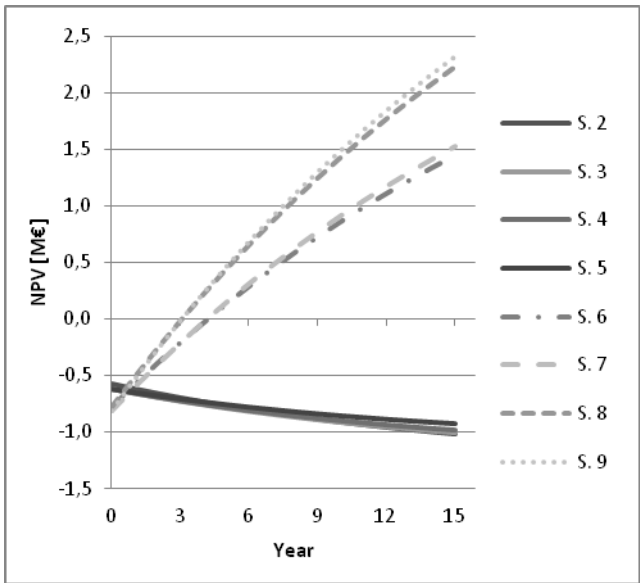

Figure 6 Progressive NPV trend.

In conclusion, the more attractive solutions are the 8 and 9 (both ABP), followed by 6 and 7 (RBC, always 1st and 2nd level); they give a cost-benefit result considerably greater than those of the first level, therefore a health investment should be focused towards complete implementations of RFID.

6 SENSITIVITY ANALYSIS

A sensitivity analysis was therefore carried out in order to test the robustness of the model; the parameters on which the analysis is based and their values are shown in table 10.

Table X – Summary of parameters considered in the sensitivity analysis.

				Standard value	Sensitivity analysis range
Discount rate				5%	0 - 7%
Blood bags waste reduction	1° & 2° level			3,50%	2,5 - 4,5%
Clinical risk reduction	1° level			45%	42,5 - 47,5%
	1° & 2° level			90%	85 - 95%
Tags cost	HF	Wristband	Initial cost	2 €	1,6 - 2,4 €
		Tag	Initial cost	0,20 €	0,16 - 0,24 €
		Barcode		0,01 €	-
	UHF	Wristband	Initial cost	1,80 €	1,44 - 2,16 €
		Tag	Initial cost	0,18 €	0,144 - 0,216 €
		Barcode		0,01 €	-

No variation range was selected for the barcode cost of acquisition, as this technology is now mature and settled.
In order to limit the number of graphs concerning the progressive NPV, only the results for the solutions 4 and 8, both HF solutions and ABP will be exposed, as representative of the alternatives 1st and 1st + 2nd level.

6.1 DISCOUNT RATE

The discount rate trend is shown in Figures from 7 to 11, which show as it significantly modifies the economic output of the solutions. In particular, it remarkably alters the NPV which, as seen in the figure below, is reduced by more than half in solutions 6 and 7, while it is slightly lower in the solutions 8 and 9. The first level solutions results are less influenced; however, they have an opposite trend compared to the other four, as they increasingly reduce their negative economic result.

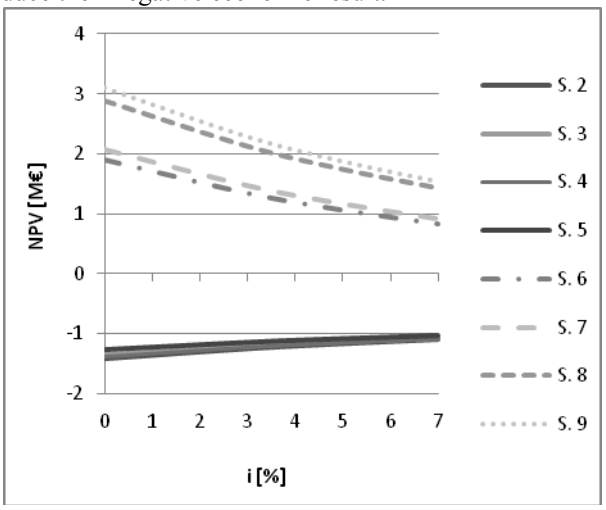

Figure 7 NPV vs. discount rate.

Concerning the PBT (Figure 8) it is possible to make reference only to solutions with a positive NPV; the time of return on investment grows of about one year in the case of solutions 6 and 7, and of about half a year for the other two. Therefore in the latter there is a strong NPV reduction, with a variation greater than that of the solutions 6 and 7 but for the PBT there is an increase slightly more limited (16% against about 23% of the 6 and 7).

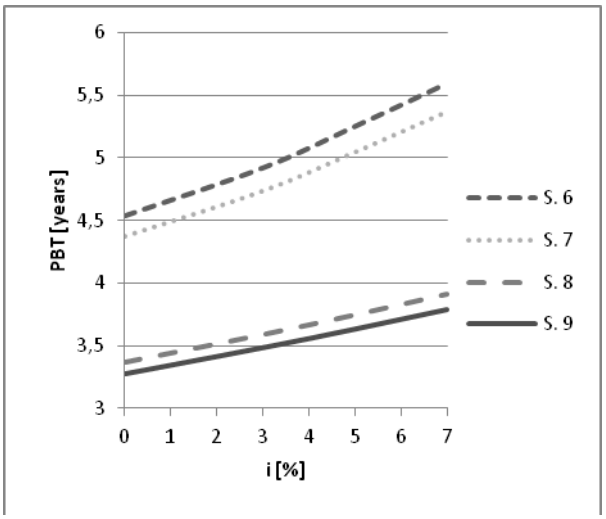

Figure 8 PBT vs. discount rate.

The benefit/cost ratio shown in

Figure shows a trend similar to the NPV, although this indicator is almost linear; there is a reduction of the B/C ratio with the growth of the discount rate. The reduction is almost null for the 1st level solutions.
Figures 10 and 11 show, respectively, the progressive NPV trend for solutions 4 and 8. The findings found in previous diagrams are confirmed. It can be noted how, in the case of solution 4, the increase of i results in a shift of the curves above the straight line corresponding to the case i = 0; vice versa, in the solution 8, the increase of i determines a progressive worsening of the economic result, as can be noted by the progressive distancing of the curves from linear solution below the straight line characterized by i = 0.

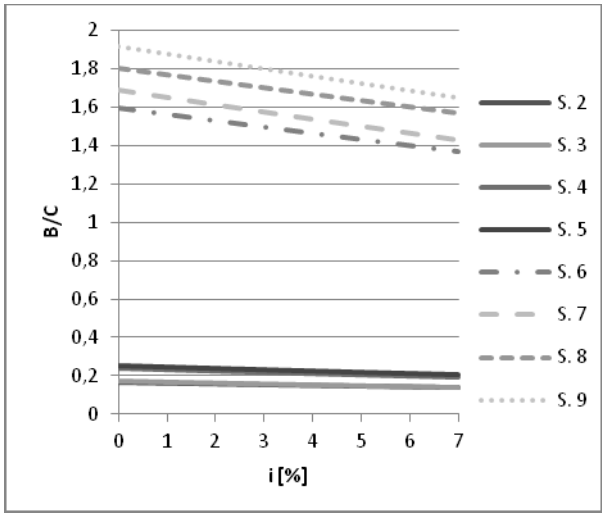

Figure 9 Costs/benefit ratio vs. discount rate.

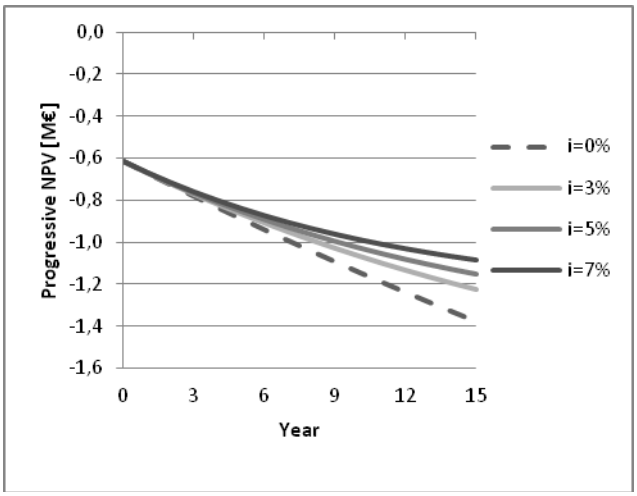

Figure 10 Progressive NPV trend vs. discount rate, solution 4.

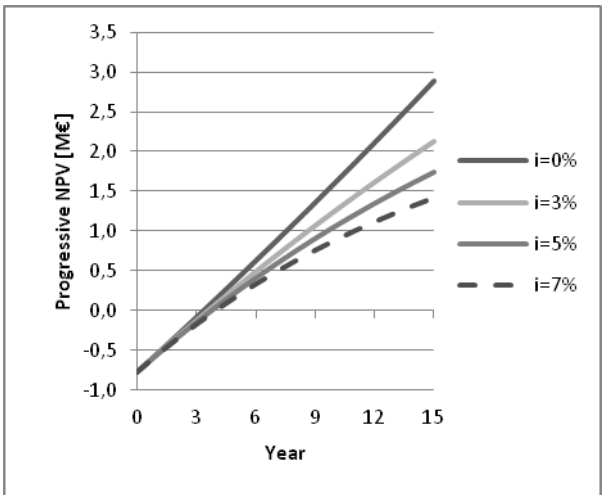

Figure 11 Progressive NPV trend vs. discount rate, solution 8.

6.2 WASTE REDUCTION

The variation of the coefficient employed for the waste reduction calculation has a significant effect on the economic results of the process model, as shown in
Figure 12; In fact, its increase greatly amplifies the NPV, with a divergence rewarding ABP solutions; obviously the sensitivity with this parameter affects only the alternatives providing for the reduction of waste (solutions from 6 to 9).
The PBT graph (Figure 13) shows, however, that there is a transition interval in which the economic result changes rapidly: progressing from low values to higher levels of waste reduction, it appears that at around 3% PBT starts to decrease less quickly, in particular for RBC solutions. Operating in the 2,5% to 3% range or even lower, the investment could show capital recovery times too high, with the solutions 6 and 7 quickly above the threshold of 15 years of the life of the project. However, it is in this range that the major variations in the economic performance in terms of PBP determined by the new technology occur.
It can also be noted that for values of waste reduction close to or above 4% the two types of frequencies, HF and UHF, lead to identical PBT results, while for the B/C indicator the UHF is still advantageous (see Figure 14).
In the field 3% ÷ 3,5%, both in the RBC and ABP case, the HF solutions show a slight advantage compared to UHF.
The ROR trend (Figure 15) leads to conclusions similar to what we saw in the PBT; there is a substantial equality of economic appeal between HF and UHF solutions, identifiable in the field over the threshold of 4% of waste reduction.
The B/C indicator confirms what related above for NPV.
The curves of progressive NPV as a function of the change in percentage of waste reduction (Figure 16) does not show changes in the shape of the curve, as was the case with the variation in the discount rate. The final NPV, however, grows significantly with the increase of waste reduction.

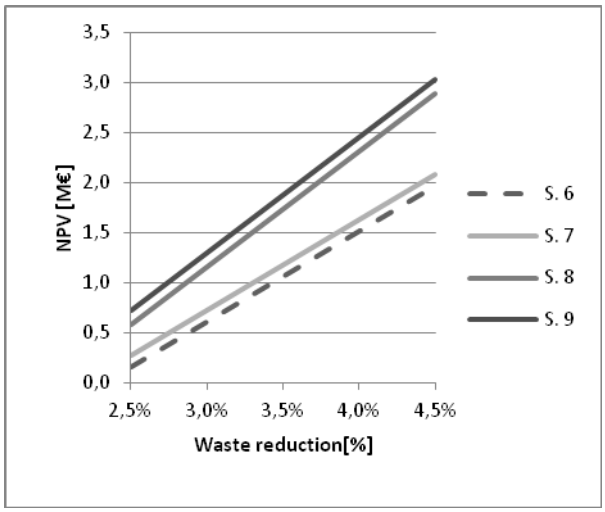

Figure 12 NPV vs. waste reduction.

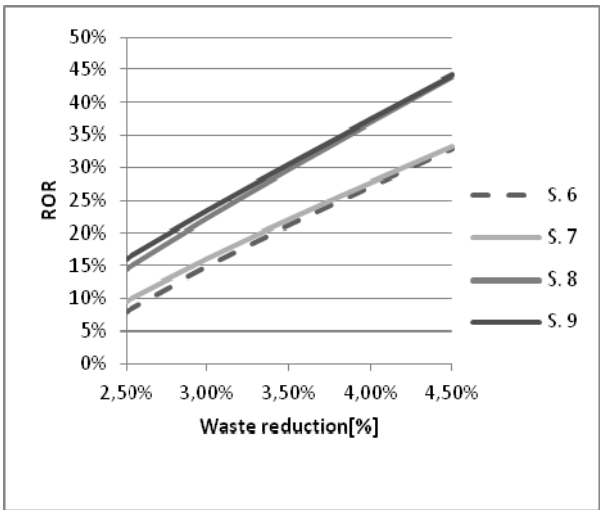

Figure 15 ROR vs. waste reduction.

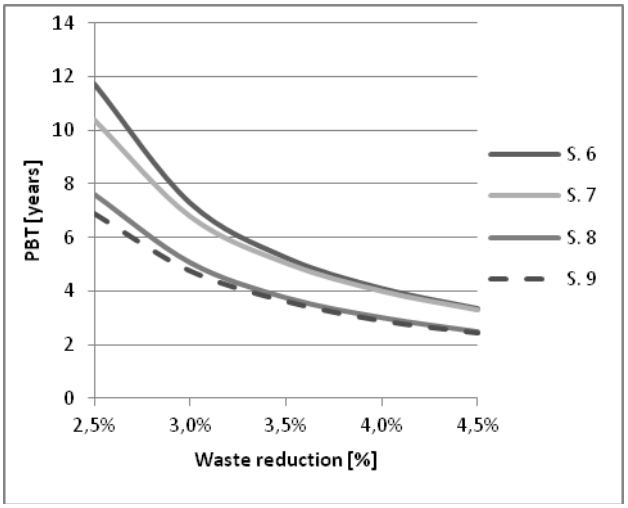

Figure 13 PBP vs. waste reduction.

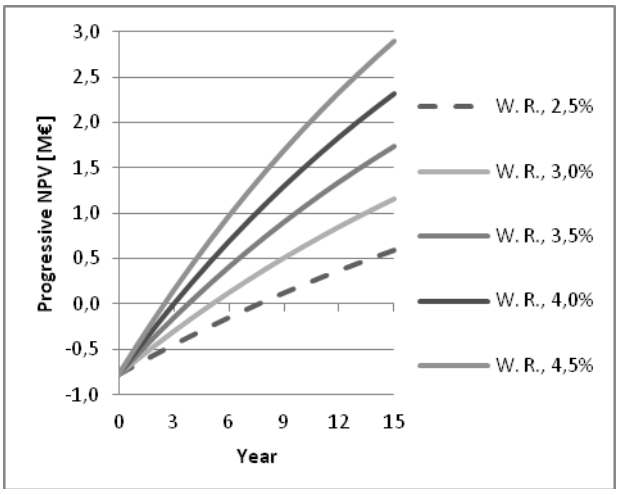

Figure 16 Progressive NPV vs. waste reduction (solution 8).

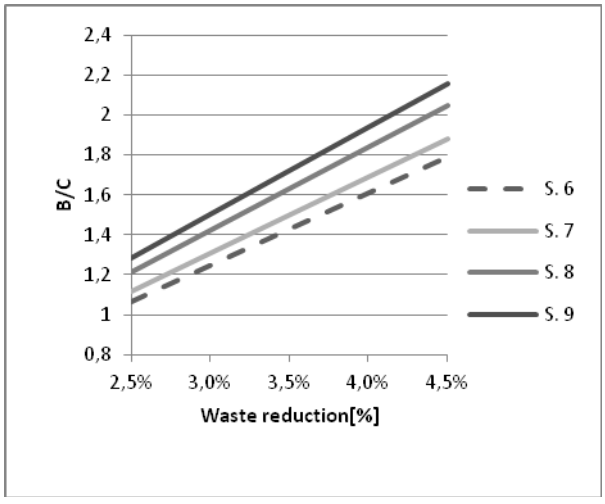

Figure 14 B/C Ratio vs. waste reduction.

It can be concluded that the monitored parameter influences decisively the economic result. This is immediately verifiable in the same Figure 16, from which it is clear that both the PBT and the NPV go, respectively, from 8 to 2,5 years and from € 500.000 to almost € 3 million.

6.3 CLINICAL RISK REDUCTION

A variation in the efficacy of the clinical risk reduction, according to the model developed, determines very small and substantially constant changes in the economic results for the various solutions, as shown by the curves of Figures 17 and 18 (for this reason the results concerning ROR and B/C ratio were not reported).

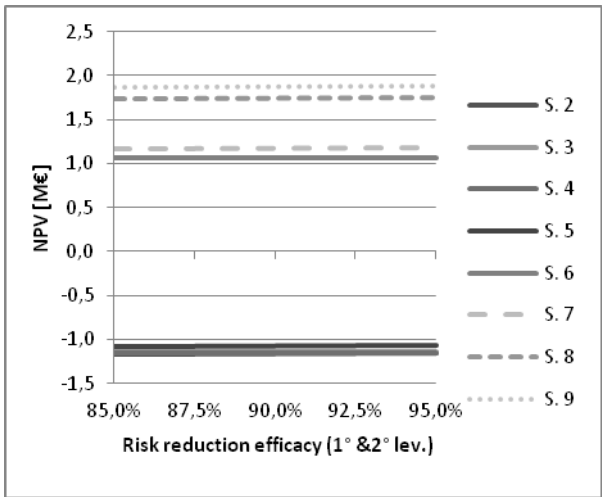

Figure 17 NPV vs. clinical risk reduction efficacy.

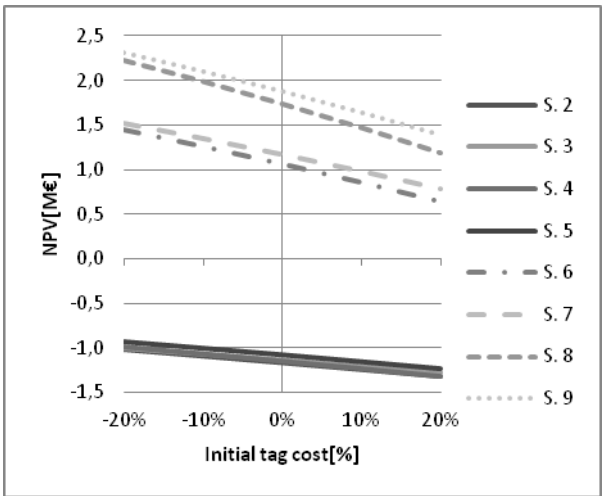

Figure 19 NPV vs. tag differential initial cost.

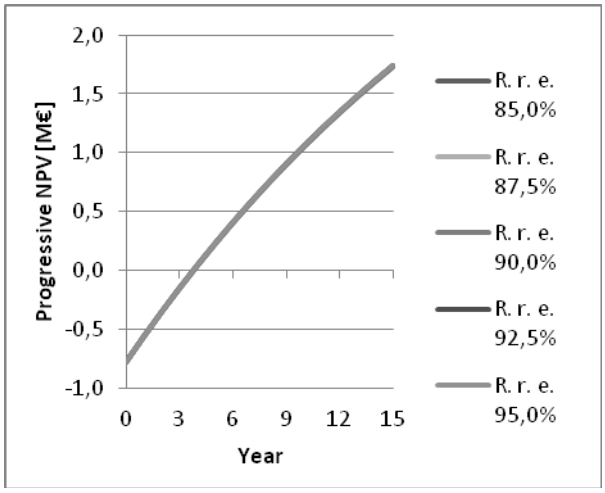

Figure 18 Progressive NPV vs. clinical risk reduction efficacy (solution 8).

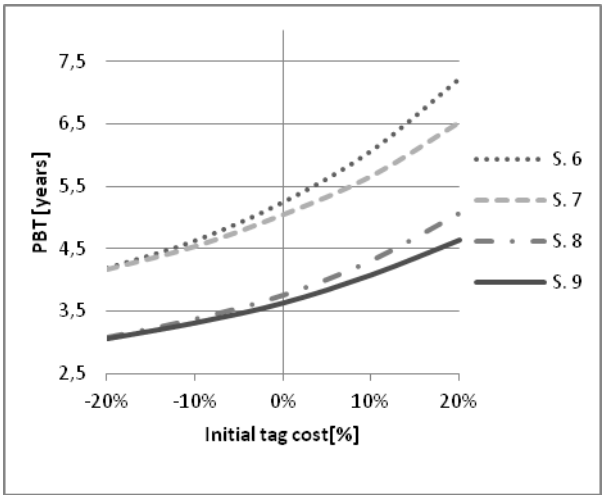

Figure 20 PBT vs. tag differential initial cost.

In particular, as progressive NPV is concerned (Figure 18), it does not allow to appreciate minimum variations in the trend of the various curves, which result substantially superimposed; therefore there are no changes in the solution PBT. As already shown in Figure 9 and related comments, this is substantially due to the fact that the benefit resulting from a reduction of clinical risk is, in strictly economic terms, about two orders of magnitude lower than the benefit of waste reduction of blood bags.

6.4 TAGS DIFFERENTIAL INITIAL COST

The fourth and final parameter considered in the sensitivity analysis was the tag differential initial cost compared to the "standard" case, analysed in Figure 19.

In this picture it is possible to see the trend of the NPV for each solution: it can be noticed that the cost of tags is crucial for the economic result in those alternatives requiring a large number of tags; the variation is in fact significant between the two extremes of -20% to 20% for the 1st and 2nd level.

For solutions with positive economic result it is interesting to note (Figure 20) the performance of the PBT; it can be noticed that the return time grows more for HF than for UHF frequency tags with increasing purchase price.

Concerning the B/C ratio (Figure 21), it was noted that the cost of the tag has a very limited influence over the economic output of the solutions of the 1st level, while appreciable changes occurs in those of 1st and 2nd level.

The convenience of UHF is also evident from the results obtained in the calculation of the ROR, as shown in Figure 22.

The cost of the tag also greatly influences all progressive VAN trends (Figures 23 and 24); therefore if they were readily available at a lower cost, the economic result will have a substantial improvement in all the alternatives.

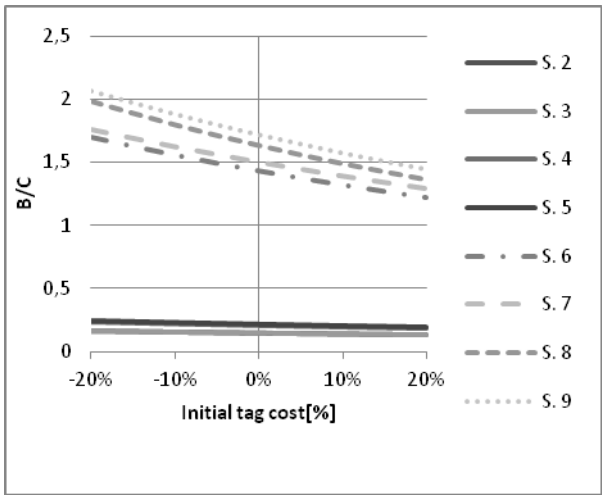

Figure 21 B/C Ratio vs. tag differential initial cost.

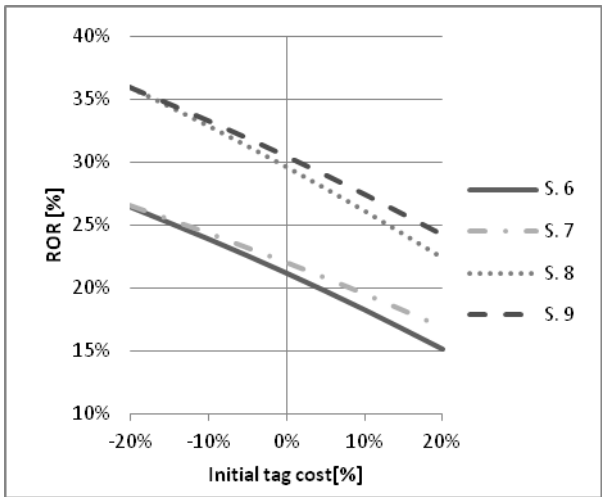

Figure 22 ROR vs. tag differential initial cost.

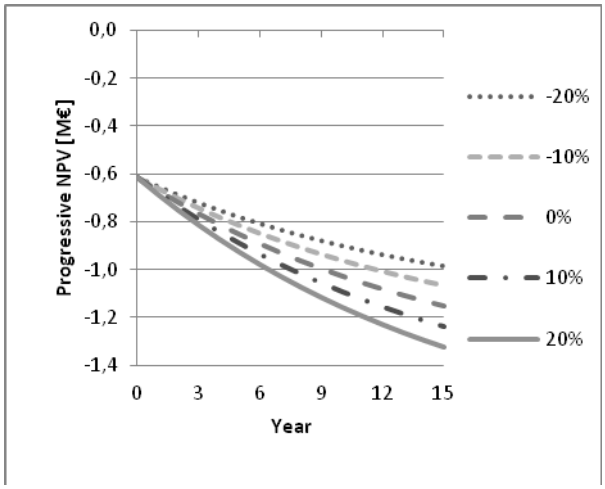

Figure 23 Progressive NPV vs. tag differential initial cost (solution 4).

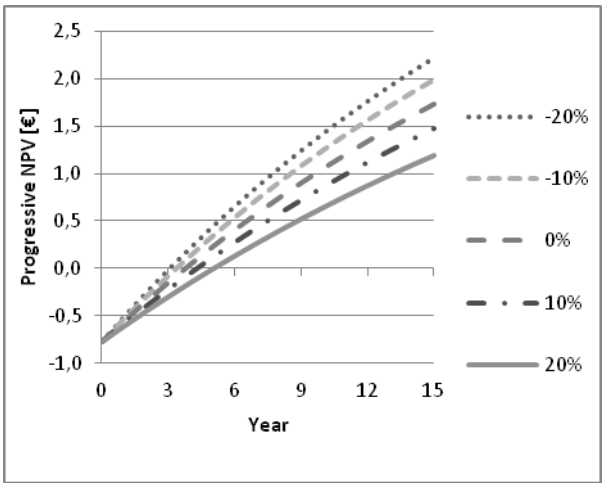

Figure 24 Progressive NPV vs. tag differential initial cost (solution 8).

7 CONCLUSIONS

The study performed has allowed to quantify the extent of the benefits that RFID technology is able to produce in the transfusion sector, from the point of view both of the patient safety and of the improvement of the process.

The cost-effective solutions have been identified in the solutions of 1st and 2nd level, with a fair margin for the solutions 8 and 9 compared to the only RBC solutions, which however are also fully acceptable for the economic sustainability.

The sensitivity analysis did not alter significantly the results obtained; it nevertheless allowed to show how the economic result is very sensitive to the variation of the bags waste reduction in the process and to the initial differential cost of the tag. In this sense, the choice between HF and UHF may fall on the latter frequency up to the limit case in which the cost of the tag is 15% higher than that assumed in this calculation as standard, and when the waste reduction is close to 2,5%.

A limited sensitivity of the model to clinical risk reduction was also noticed, the true primary objective in the use of RFID; as mentioned earlier, the reason may be sought in the limited impact that this benefit has in the global economy of the solutions addressed with the CBA method concerned.

From the results of the analysis it can be concluded that the most interesting solutions for RFID implementation, among these discussed in this study, are those requiring the extension of the RFID systems to the entire transfusion process, with management of all types of blood products used.

Although the benefit of the clinical risk reduction does not result economically viable in the CBA, the extension of the use of RFID for the management of the whole blood chain allows to fully compensate for this disadvantage. It is important to remember, however, that some RFID technology implementation risks, to be evaluated in an advanced stage of design were not considered in the analysis; they refer to organizational risks, related to public

opinion or operational difficulties, or due to unforeseen circumstances, etc.. A correct management set up is able to evaluate case by case the extent of these risks and operate accordingly.

From the point of view of the technology to be used, it has been finally highlighted, for some ranges of values of input parameters, a slight advance of the UHF frequency band over the HF; however, only a more detailed analysis on the particular case of use may indicate whether such convenience is able to compensate for the various additional difficulties that presently characterize such technology.

REFERENCES

[1] Abu Rrub, J., Al-Jabi, J., El-Khatib, K., Security model for real time tracking system (RTLS) in the healthcare sector. 2012 *International Conference on Communications and Information Technology (ICCIT)*, pp.369-73, 2012.

[2] Ahrens, N., Pruss, A., Kiesewetter, H., &Salama, A., Failure of bedside ABO testing is still the most common cause of incorrect blood transfusion in the Barcode era. *Transfusion and Apheresis Science* 33, N.1, pp.25-29, 2005.

[3] Becker, J., Vilkov, L., Weiβ, B., Winkelmann, A., A model based approach for calculating the process driven business value of RFID investments. *International Journal of Production Economics*, Vol.127, N.2, pp.358-371, 2010.

[4] Bendavid, Y., Boeck, H., Philippe, R., RFID-enabled traceability system for consignment and high value products: a case study in the healthcare sector. *Journal of Medical Systems*, Vol.36, N.6, pp.3473-89, 2012.

[5] Bertolini, M., Bottani, E., Rizzi, A., Volpi, A., Renzi, P., Shrinkage reduction in perishable food supply chain by means of an RFID-based FIFO management policy. *International Journal of RF Technologies: Research and Applications*, Vol.5, N.3-4, pp.123-136, 2013.

[6] Bodhuin, T., Preziosi, R., Tortorella, M., Using RFID technology for supporting document management. Proceedings of the *1st International Workshop on RFID Technology* - Concepts, Applications, Challenges, pp.14-24, 2007.

[7] Borelli G., Orrù P.F., Pilloni M.T., Zedda F., Riduction of clinical risk in Blood Transfusion Center with an RFID system. *WAMS International Workshop on Applied Modeling& Simulation*, Rio de Janeiro, pp.218-223, 2010.

[8] Borelli G., Orrù P.F., Zedda F., Performance analysis of a healthcare supply chain for RFID-enabled process reengineering. *International Journal of Procurement Management*, Special Issue on: Smart and Sustainable Healthcare Supply Chain, Vol. 8, N.1/2, pp.169 - 181, 2015.

[9] Bottani, E., Montanari, R., RFID and real time localization systems for warehouse management: A model for technical and economic evaluation. *International Journal of RF Technologies: Research and Applications*, Vol.4, N.3-4, pp.209-245, 2013.

[10] Bottani, E., Rizzi, A., Economical assessment of the impact of RFID technology and EPC system on the fast-moving consumer goods supply chain. *International Journal of Production Economics*, Vol.112, pp.548-569, 2008.

[11] Briggs L., Davis R., Gutierrez A., Kopetsky M., Young K., Veeramani R., RFID in the blood supply chain – increasing productivity, quality and patient safety. *Journal of Healthcare information Management*, Vol.23, N.4, pp.54-63, 2009.

[12] Chen, J. C., Collins, T. J., Creation of a RFID based real time tracking (R-RTT) system for small healthcare clinics. *Journal of Medical Systems*, Vol.36, N.6, pp.3851-60, 2012.

[13] Chuu, S., J., An investment evaluation of supply chain RFID technologies: A group decision-making model with multiple information sources. *Knowledge-Based Systems*, Vol.66, pp.210-220, 2014.

[14] *CINEAS*, Quando l'errore entra in ospedale, 2002.

[15] Davis, R., Geiger, B., Gutierrez, A., Heaser, J., Veeramani, D., Tracking blood products in blood centres using radio frequency identification: a comprehensive assessment. *VoxSanguinis*, Vol.97, N.1, pp.50-60, 2009.

[16] Davies, A., Staves, J., Kay, J., Casbard, A. C. and Murphy, M. F., End-to-end electronic control of the hospital transfusion process to increase the safety of blood transfusion: strengths and weaknesses, *Transfusion*, Vol.46, N.3, pp.352-364, 2006.

[17] De Felice, F., Petrillo, A., RFID in green supply chain: Proposal of a multicriteria decision model based on AHP. Proceedings - 2013 IEEE 10th *International Conference on e-Business Engineering*, ICEBE, pp.364-369, 2013.

[18] De Kok, A.G., Van Donselaar, K.H., Van Woensel, T., A break even analysis of RFID technology for inventory sensitive to shrinkage, *International Journal of Production Economics*, Vol.112, N.2, pp.521-531, 2008.

[19] De Marco, A., Cagliano, A., Nervo, M., Rafele, C., Using System Dynamics to assess the impact of RFID technology on retail operations, *International Journal of Production Economics*, Vol.135, No.1, pp.333-344, 2012.

[20] De Marco, A., Cagliano, A.C., Nervo, M.L., Rafele, C., Modeling the effectiveness of radio frequency identification (RFID) technologies in improving sales performance in fashion retail outlets', *Fashion Supply Chain Management Using Radio Frequency Identification (Rfid) Technologies*, pp.203-229, 2014.

[21] De Sanctis Lucentini, E., Marconi, M., Bevilacqua, L., Bonini, P., Ciampalini, S., Colicchia, A., et al., Risk Management in Sanità. Il problema degli errori. Roma: Ministero della Salute, Commissione tecnica sul rischio clinico, pp.1-105, 2004.

[22] Dimakopoulou, A. G., Pramatari, K. C., Tsekrekos, A. E., Applying real Options to IT investment evaluation: The case of radio frequency identification (RFID) technology in the supply chain'. *International Journal of Production Economics*, Vol.156, pp.191-207, 2014.

[23] Feng J., Zetian Fu, Zaiqiong Wang, Mark Xu, Xiaoshuan Zhang, Development and evaluation on a RFID-based traceability system for cattle/beef quality safety in China. *Food Control*, Vol.31, N.2, pp.314-325, 2013.

[24] FossoWamba, S, RFID-enabled healthcare applications, issues and benefits: an archival analysis (1997-2011). *Journal of Medical Systems*, Vol.36, N.6, pp.3393-3398, 2012.

[25] Gnoni, M.G.; Rollo, A., A scenario analysis for evaluating RFID investments in pallet management. *International Journal of RF Technologies: Research and Applications*, Vol.2, N.1, pp.1-21, 2010.

[26] Hau-Ling, C., Tsan-Ming, C., Chi-Leung, H., RFID versus bar-coding systems: Transactions errors in health care apparel inventory control. *Decision Support Systems*, Vol.54, N.1, pp.803-811, 2012.

[27] Jasser, A. K., Nezar, M., Frédéric, T., Fleisch, E., A cost-benefit calculator for RFID implementations in the apparel retail industry. *15th Americas Conference on Information Systems* 2009, pp.4323-4333, 2009.

[28] Katsaliaki, K., Mustafee, N., Kumar, S., A game-based approach towards facilitating decision making for perishable products: An example of blood supply chain. *Expert Systems with Applications*, Vol.41, N.9, pp.4043-4059, 2014.

[29] Kolokathi, A., Rallis, P., Radio Frequency Identification (RFID) in healthcare: a literature review. *Studies in health technology and informatics*, Vol.190, pp.157-159, 2013.

[30] Kumar, S., Swanson, E., Tran, T., RFID in the healthcare supply chain: usage and application. *International Journal of Health Care Quality Assurance*, Vol. 22, N.1, pp.67-81, 2009.

[31] Lee C.K.H., K.L. Choy, G.T.S. Ho, K.M.Y. Law, K.M.Y., A RFID-based Resource Allocation System for garment manufacturing. *Expert Systems with Applications*, Vol.40, N.2, pp.784-799, 2013.

[32] Lee, I., Lee, B. C., An investment evaluation of supply chain RFID technologies: A normative modeling approach. *International Journal of Production Economics*, Vol.125, N.2, pp.313-323, 2010.

[33] Lim, M.K., Bahr, W., Leung, S.C.H., RFID in the warehouse: A literature analysis (1995–2010) of its applications, benefits, challenges and future trends. *International Journal of Production Economics*, Vol.145, n.1, pp.409-430, 2013.

[34] Lin, S. S, Hung, M. H., Tsai, C. L., Chou, L. P., Development of an ease-of-use remote healthcare system architecture using RFID and networking technologies. *Journal of Medical Systems*, Vol.36, N.6, pp.3605-19, 2012.

[35] Linden, J. V., Wagner, K., Voytovich, A. E., Transfusion errors in New York State: An analysis of 10 years' experience. *Transfusion*, Vol.40, pp.1207–1213, 2000.

[36] Mancini, V., Pasquali, M., Schiraldi, M., Opportunities for using RFID in the aircraft production process. *International Journal of RF Technologies: Research and Applications*, Vol.3, N.4, pp.243-255, 2012.

[37] Mazzenga, F., Simonetta, A., Giuliano, R., Vari, M., Applications of smart tagged RFID tapes for localization services in historical and cultural heritage environments. Proceedings of the *Workshop on Enabling Technologies: Infrastructure for Collaborative Enterprises*, pp.186-191, 2010.

[38] Meiller, Y., Bureau, S., Wei, Z., Piramuthu, S., RFID-embedded Decision Support for Tracking Surgical Equipment. Proceedings of the *44th Hawaii International Conference on System Sciences* (HICSS 2011), pp.1-6, 2011.

[39] Narges, K., Ramesh, S., Real options and system dynamics for information technology investment decisions: Application to RFID adoption in retail. *ACM Transactions on Management Information Systems*, Vol.4, N.3, pp.1-25, 2013.

[40] Ngai E.W.T., Cheung, B.K.S,. Lam S.S, Ng C.T, RFID value in aircraft parts supply chains: A case study. *International Journal of Production Economics*, Vol. 147, Part B, pp.330-339, 2014.

[41] Oztekin, A., Mahdavi, F., Erande, K., Kong, Z., Swim, L.,Bukkapatnam, S. T. S., Criticality index analysis based optimal RFID reader placement models for asset tracking. *International Journal of Production Research*, Vol.48, N.9, pp.2679-2698, 2010.

[42] Peris-Lopez, P., Orfila, A., Mitrokotsa, A., Van der Lubbe, J. C. A., A comprehensive RFID solution to enhance inpatient medication safety. *International Journal of Medical Informatics*, Vol. 80, pp.13-24, 2011.

[43] Picazo-Sanchez, P., Bagheri, N., Peris-Lopez, P., Tapiador, J. E., Two RFID Standard-based Security Protocols for Healthcare Environments. *Journal of Medical Systems*, Vol.37, N.5, pp.9962, 2013.

[44] Qu, X., Simpson, L.T., Stanfield, P., A model for quantifying the value of RFID-enabled equipment tracking in hospitals, *Advanced Engineering Informatics*, Vol.25, pp.23-31, 2011.

[45] Revere L. Black K. Zalila F., RFIDs can improve the patient care supply chain, *Hospital Topics*, Vol. 88, N.1, pp.26-31, 2010.

[46] Rosenbaum, B. P., Radio Frequency Identification (RFID) in Health Care: Privacy and Security Concerns Limiting Adoption. *Journal of Medical Systems*, Vol.38, N.3, pp.1-6, 2014.

[47] Sarac, A., Absi, N., Dauzére-Pérés, S., A simulation approach to evaluate the impact of introducing rfid technologies in a threelevel supply chain. Proceedings

of the *2008 Winter Simulation Conference*, WSC 2008, pp.2741-2749, 2008.

[48] Slonim, A., D., Bish, E. K., Xie, R. S., Red Blood Cell Transfusion Safety: Probabilistic Risk Assessment and Cost/ Benefits of Risk Reduction Strategies. *Annals of Operation Research*, Vol.221, N.1, pp.377-406, 2014.

[49] Taneva, S., Law, E., In and out of the hospital: The hidden interface of high fidelity research via RFID. *Lecture Notes in Computer Science*, 4662 LNCS, pp.624-627, 2007.

[50] Thipparate, T., Economic analysis of RFID investments for construction project management using ANFIS. *International Journal of Information Technology and Management*, Vol.12, N.1-2, pp.129-142, 2013

[51] Tian, F., Zhen, W., Pan Deng, Y., A kind of effective protection of privacy and low cost RFID security authentication protocol, *Applied Mechanics and Materials*, Vol. 336-338, pp.1882-1886, 2013.

[52] Ting, SL., Kwok, S. K., Tsang, A. H., Lee, W. B., Critical elements and lessons learnt from the implementation of an RFID-enabled healthcare management system in a medical organization. *Journal of Medical Systems*, Vol. 35, N.4, pp.657-69, 2011.

[53] Turner, C. L, Casbard, A. C, Murphy, M. F., Barcode technology: its role in increasing the safety of blood transfusion. *Transfusion*, Vol.43, pp.1200-1209, 2003.

[54] Tzeng, S. F., Chen, W. H., Pai, F. Y., Evaluating the business value of RFID: Evidence from five case studies, *International Journal of Production Economics*, Vol.112, pp.601-613, 2008.

[55] Ullah S., Alamri A., A Secure RFID-based WBAN for Healthcare Applications, *Journal of Medical Systems,* Vol.37, N.5, pp. 1-9, 2013.

[56] Ustundag A., Tanyas M., The impact of Radio Frequency Identification (RFID) technology on supply chain costs. *Transportation Research Part E*, Vol.45, pp.29-38, 2009.

[57] Vahedi, E., Shah-Mansouri, V., Wong, V. W. S., Blake, I. F., Ward, R. K., Probabilistic analysis of blocking attack in RFID systems. *IEEE Transactions on Information Forensics and Security*, pp.803-817, 2011.

[58] Van der Togt, R., Bakker, P. J. M., Jaspers, M. W. M., A framework for performance and data quality assessment of Radio Frequency IDentification (RFID) systems in health care settings. *Journal of Biomedical Informatics*, Vol. 44, N.2, pp.372-383, 2011.

[59] Vanem, E., Ellis, J., Evaluating the cost-effectiveness of a monitoring system for improved evacuation from passenger ships, *Safety Science*, Vol.48, N.6, pp.788-802, 2010.

[60] Veronneau, S., Roy, J., RFID benefits, costs and possibilities: the economical analysis of RFID deployment in a cruise corporation global service supply chain. *International Journal of Production Economics*, Vol.122, pp.692-702, 2009.

[61] Vlachos, I., P., A hierarchical model of the impact of RFID practices on retail supply chain performance. *Expert Systems with Applications*, Vol.41, N.1, pp.5-15, 2014.

[62] Wong, W.K., Leung, S.Y.S., Guo, Z.X., Zeng, Z.H., Mok, P.Y., Intelligent apparel product cross-selling using radio frequency identification (RFID) technology for fashion retailing. *Fashion Supply Chain Management Using Radio Frequency Identification (Rfid) Technologies*, Woodhead Publishing, pp.159-186, 2014.

[63] Wu, Z. Y., Chen, L., Wu, J. C., A reliable RFID mutual authentication scheme for healthcare environments. *Journal of Medical Systems*, Vol.37, N.2, pp.9917, 2013.

[64] Xiuli, Q., Simpson, L. T., Stanfield, P., A model for quantifying the value of RFID-enabled equipment tracking in hospitals. *Advanced Engineering Informatics*, Vol.25, N.1, pp.23-31, 2011.

[65] Yao, W., Chu, C., Li, Z., The adoption and implementation of RFID technologies in healthcare: a literature review. *Journal of Medical Systems*, Vol.36, N.6, pp.3507-3525, 2012.

[66] Yu, S. C., RFID implementation and benefits in libraries. *Electronic Library,* Vol. 25, N.1, pp.54-64, 2007.

[67] Yue, D., Wu, X., Hao, M., Bai, J., A cost-benefit analysis for applying RFID to pharmaceutical supply chain. 8th International *Conference on Service Systems and Service Management*, pp. 1-5, 2011.

[68] Zhang M., Li, P, RFID Application Strategy in Agri-Food Supply Chain Based on Safety and Benefit Analysis. *Physics Procedia*, Vol.25, pp.636-642, 2012.

ISSN 1590-8844
International Journal of Mechanics and Control, Vol. 16, No. 02, 2015

TEMPLATE FOR PREPARING PAPERS FOR PUBLISHING IN INTERNATIONAL JOURNAL OF MECHANICS AND CONTROL

Author1* Author2**

* affiliation Author1

** affiliation Author2

ABSTRACT

This is a brief guide to prepare papers in a better style for publishing in International Journal of Mechanics and Control (JoMaC). It gives details of the preferred style in a template format to ease paper presentation. The abstract must be able to indicate the principal authors' contribution to the argument containing the chosen method and the obtained results. (max 200 words)

Keywords: keywords list (max 5 words)

1 TITLE OF SECTION (E.G. INTRODUCTION)

This sample article is to show you how to prepare papers in a standard style for publishing in International Journal of Mechanics and Control.
It offers you a template for paper layout, and describes points you should notice before you submit your papers.

2 PREPARATION OF PAPERS

2.1 SUBMISSION OF PAPERS

The papers should be submitted in the form of an electronic document, either in Microsoft Word format (Word'97 version or earlier).
In addition to the electronic version a hardcopy of the complete paper including diagrams with annotations must be supplied. The final format of the papers will be A4 page size with a two column layout. The text will be Times New Roman font size 10.

Contact author: author1[1], author2[2]

[1]Address of author1.
[2]Address of author2 if different from author1's address
E-mail: author1@univ1.com , author2@univ2.com

2.2 DETAILS OF PAPER LAYOUT

2.2.1 Style of Writing

The language is English and with UK/European spelling. The papers should be written in the third person. Related work conducted elsewhere may be criticised but not the individuals conducting the work. The paper should be comprehensible both to specialists in the appropriate field and to those with a general understanding of the subject.
Company names or advertising, direct or indirect, is not permitted and product names will only be included at the discretion of the editor. Abbreviations should be spelt out in full the first time they appear and their abbreviated form included in brackets immediately after. Words used in a special context should appear in inverted single quotation mark the first time they appear. Papers are accepted also on the basis that they may be edited for style and language.

2.2.2 Paper length

Paper length is free, but should normally not exceed 10000 words and twenty illustrations.

2.2.3 Diagrams and figures

Figures and Tables will either be entered in one column or two columns and should be 80 mm or 160 mm wide respectively. A minimum line width of 1 point is required at actual size. Captions and annotations should be in 10 point with the first letter only capitalised *at actual size* (see Figure 1 and Table VII).

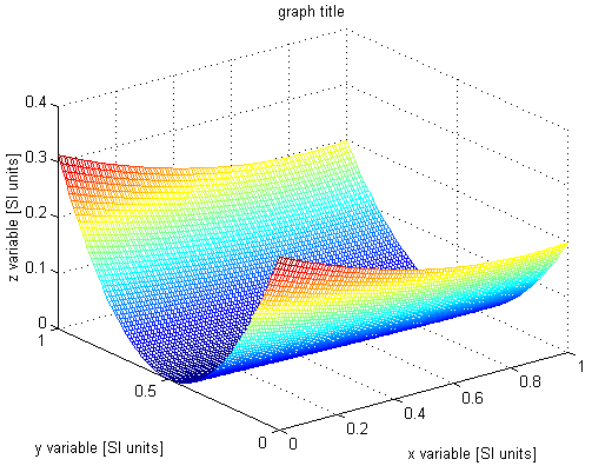

Figure 1 Simple chart.

Table VII - Experimental values

Robot Arm Velocity (rad/s)	Motor Torque (Nm)
0.123	10.123
1.456	20.234
2.789	30.345
3.012	40.456

2.2.4 Photographs and illustrations

Authors could wish to publish in full colour photographs and illustrations. Photographs and illustrations should be included in the electronic document and a copy of their original sent. Illustrations in full colour …

2.2.5 Equations

Each equation should occur on a new line with uniform spacing from adjacent text as indicated in this template. The equations, where they are referred to in the text, should be numbered sequentially and their identifier enclosed in parenthesis, right justified. The symbols, where referred to in the text, should be italicised.

- point 1
  - point 2
    - point 3

1. numbered point 1
   2. numbered point 2
      3. numbered point 3

$$W(d) = G(A_0, \sigma, d) = \frac{1}{T}\int_0^{+\infty} A_0 \cdot e^{-\frac{d^2}{2\sigma^2}} dt \qquad (1)$$

3 COPYRIGHT

Authors will be asked to sign a copyright transfer form prior to JoMaC publishing of their paper. Reproduction of any part of the publication is not allowed elsewhere without permission from JoMaC whose prior publication must be cited. The understanding is that they have been neither previously published nor submitted concurrently to any other publisher.

4 PEER REVIEW

Papers for publication in JoMaC will first undergo review by anonymous, impartial specialists in the appropriate field. Based on the comments of the referees the Editor will decide on acceptance, revision or rejection. The authors will be provided with copies of the reviewers' remarks to aid in revision and improvement where appropriate.

5 REFERENCES (DESCRIPTION)

The papers in the reference list must be cited in the text. In the text the citation should appear in square brackets [ ], as in, for example, "the red fox has been shown to jump the black cat [3] but not when...". In the Reference list the font should be Times New Roman with 10 point size. Author's first names should be terminated by a 'full stop'. The reference number should be enclosed in brackets.

The book titles should be in *italics*, followed by a 'full stop'. Proceedings or journal titles should be in *italics.* For instance:

REFERENCES (EXAMPLE)

[1] Smith J., Jones A.B. and Brown J., *The title of the book*. 1st edition, Publisher, 2001.

[2] Smith J., Jones A.B. and Brown J., The title of the paper. *Proc. of* C*onference Name*, where it took place, Vol. 1, paper number, pp. 1-11, 2001.

[3] Smith J., Jones A.B. and Brown J., The title of the paper. *Journal Name*, Vol. 1, No. 1, pp. 1-11, 2001.

[4] Smith J., Jones A.B. and Brown J., *Patent title*, U.S. Patent number, 2001.

International Journal of Mechanics and Control – JoMaC
Published by Levrotto&Bella
TRANSFER OF COPYRIGHT AGREEMENT

NOTE: Authors/copyright holders are asked to complete this form signing section A, B or C and mail it to the editor office with the manuscript or as soon afterwards as possible.	*Editor's office address:* Andrea Manuello Bertetto Elvio Bonisoli *Dept. of Mechanics* *Technical University – Politecnico di Torino* *C.so Duca degli Abruzzi, 24 – 10129 Torino – Italy* *e_mail: jomac@polito.it* *fax n.: +39.011.564.6999*

The article title:

By:_____

To be Published in ***International Journal of Mechanics and Control JoMaC***
Official legal Turin court registration Number 5320 (5 May 2000) - reg. Tribunale di Torino N. 5390 del 5 maggio 2000

A Copyright to the above article is hereby transferred to the JoMaC, effective upon acceptance for publication. However the following rights are reserved by the author(s)/copyright holder(s):
1. All proprietary rights other than copyright, such as patent rights;
2. The right to use, free or charge, all or part of this article in future works of their own, such as books and lectures;
3. The right to reproduce the article for their own purposes provided the copies are not offered for sale.

To be signed below by all authors or, if signed by only one author on behalf of all co-authors, the statement A2 below must be signed.

A1. All authors:

SIGNATURE_____DATE_____ SIGNATURE_____DATE_____

PRINTED NAME_____ PRINTED NAME_____

SIGNATURE_____DATE_____ SIGNATURE_____DATE_____

PRINTED NAME_____ PRINTED NAME_____

A2. One author on behalf of all co-authors:
"I represent and warrant that I am authorised to execute this transfer of copyright on behalf of all the authors of the article referred to above"

PRINTED NAME_____

SIGNATURE_____ TITLE_____ DATE_____

B. The above article was written as part of duties as an employee or otherwise as a work made for hire. As an authorised representative of the employer or other proprietor. I hereby transfer copyright to the above article to *International Journal of Mechanics and Control* effective upon publication. However, the following rights are reserved:
1. All proprietary rights other than copyright, such as patent rights;
2. The right to use, free or charge, all or part of this article in future works of their own, such as books and lectures;
3. The right to reproduce the article for their own purposes provided the copies are not offered for sale.

PRINTED NAME_____

SIGNATURE_____ TITLE_____ DATE_____

C. I certify that the above article has been written in the course of employment by the United States Government so that no copyright exists, or by the United Kingdom Government (Crown Copyright), thus there is no transfer of copyright.

PRINTED NAME_____

SIGNATURE_____ TITLE_____ DATE_____

CONTENTS

next issue titles will be from the papers of:

RAAD 2015

24th International Conference on Robotics in Alpe-Adria-Danube Region

Bucharest, Romania
27 – 29 May 2015

Scopus Indexed Journal

Reference Journal of IFToMM Italy
International Federation for the Promotion of Mechanism and Machine Science